

**THE BEHAVIOR OF ANCHORED SHEET PILE
WALLS CONSTRUCTED BY EXCAVATION
AND BACKFILLING**

By

OMER BILGIN

Bachelor of Science

Middle East Technical University


Ankara, Turkey

1991

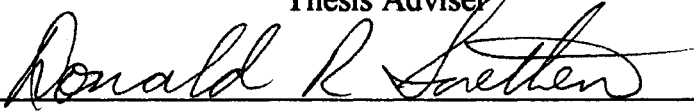
**Submitted to the Faculty of the
Graduate College of the
Oklahoma State University
in partial fulfillment of
the requirements for
the Degree of
MASTER OF SCIENCE
December, 1994**

THE BEHAVIOR OF ANCHORED SHEET PILE
WALLS CONSTRUCTED BY EXCAVATION
AND BACKFILLING

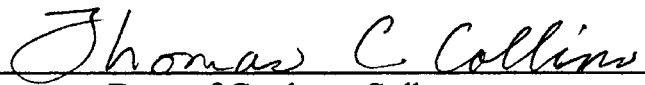
Thesis Approved:



Thesis Adviser







Dean of Graduate College

ACKNOWLEDGMENTS

I wish to express my sincere appreciation to Dr. Mete Oner, my academic advisor, for his encouragement, advice, and the many hours of guidance throughout my graduate program. Many thanks also go to Dr. Donald R. Snethen and Dr. Vernon A. Mast for serving on my graduate committee.

It is with sincere appreciation that I acknowledge the assistance of all the special people in my life that helped me accomplish my goal.

I would like to dedicate this work to my parents Müşerref and Sefer Bilgin and to other family members Hülya, Mustafa and T. Murat Gülşen for their love, understanding, and encouragement over the years.

TABLE OF CONTENTS

Chapter	Page
I. INTRODUCTION	1
II. METHODOLOGY.....	3
General.....	3
Non-Linear Model Used in FEM: <i>f</i> -Model.....	4
Soil Parameters Required.....	8
Construction Simulation.....	8
Pre-Processing and Post-Processing for FEM.....	10
III. SHEET PILE WALLS AND SOIL PROFILES STUDIED	13
Selection of Typical Wall Cases.....	13
Basic Geometry	13
Soil Types	15
Shear Strength of Sands in the Profiles.....	17
Shear Strength of Clays in the Profiles	17
Selection of the Stress-Strain Model Parameters	18
Soil-Structure Interface Properties.....	20
Conventional Design Calculations	21
Selection of Finite Element Grids and Other Analysis Parameters	22
Selection of Grid Size	23
Selection of the Number of Substeps.....	26
The Anchor Stiffnesses	34
IV. RESULTS OF ANALYSES AND COMPARISONS	37
General	37
Behavior of the Soil	37
Soil Deformations.....	37
Soil Stresses	41
Degree of Mobilization	51
Stress Paths	57
Behavior of the Structure	66
Wall Deflections	66
Bending Moments in The Wall.....	78
Anchor Forces	85

Chapter	Page
The Effects of the Anchor Installation Time.....	89
Anchor Placement Time Effect on Deflection of The Wall.....	90
Anchor Placement Time Effect on Bending Moments.....	91
Anchor Placement Time Effect on Anchor Forces.....	96
 V. CONCLUSIONS.....	 101
 BIBLIOGRAPHY	 104
 APPENDIXES	 106
APPENDIX-A INPUT AND OUTPUT FILES USED IN THE FINITE ELEMENT ANALYSES.....	 107
 APPENDIX-B POST-PROCESSING PLOTS	 114

LIST OF TABLES

Table	Page
3.1. Soil Properties Defining the Soil Types Considered.....	16
3.2. All Combinations of the Soil Types Considered.....	16
3.3. Used Model Parameters For Soil Stress-Strain Relationship	20
3.4. Results of Free Earth Support Calculations (after Oner, 1992)	22
3.5. Results of Analysis For Different Grid Sizes.....	25
3.6. Results of Analysis For Different Substeps	33
4.1. Comparison of Wall Top Deflections for Excavation and Backfill Cases.....	76
4.2. Comparison of Maximum Wall Deflections for Excavation and Backfill Cases.....	77
4.3. Comparison of Bending Moments in the Wall for Excavation and Backfill Cases.....	85
4.4. Comparison of Anchor Forces for Excavation and Backfill Cases.....	88
4.5. Results of Analysis for Putting the Anchor at Different Fill Levels.....	90

LIST OF FIGURES

Figure	Page
2.1. Representation of the Degree of Mobilization in Mohr Diagram	7
2.2. Soil Section Analyzed in The Excavation Cases.....	9
2.3. Soil Section Analyzed in The Backfill Cases.....	11
3.1. Typical Anchored Sheet Pile Wall Section Analyzed in This Study	14
3.2. Undrained Shear Strength Profile Used in the Analysis	19
3.3. Grid Sizes Used to Analyze Grid Size Effect	24
3.4. Maximum Deflections Obtained Using Different Grid Sizes.....	27
3.5. Maximum Bending Moments Obtained Using Different Grid Sizes.....	28
3.6. Anchor Forces Obtained Using Different Grid Sizes.....	29
3.7. Maximum Deflections Obtained Using Different Substeps.....	30
3.8. Maximum Bending Moments Obtained Using Different Substeps	31
3.9. Anchor Forces Obtained Using Different Substeps	32
3.10. Determination of a Safe Location For the Anchor Block	35
3.11. Determination of the Anchor Stiffness For LL40 Case.....	36
4.1. DD40 Case - Excavation: Deformed Shape (x30).....	38
4.2. DD40 Case - Backfill: Deformed Shape (x 30).....	39
4.3. DD40 Case - Excavation: Displacement Vectors (x 50).....	42

Figure	Page
4.4. DD40 Case - Backfill: Displacement Vectors (x 50).....	43
4.5. DD40 Case - Excavation: Horizontal Stress - σ_x (psf).....	44
4.6. DD40 Case - Backfill: Horizontal Stress - σ_x (psf).....	45
4.7(a). Passive Pressure in Front of the Wall (DD40 Case).....	47
4.7(b). Passive Pressure in Front of the Wall (LM40 Case).....	48
4.8. DD40 Case - Excavation: Vertical Stress - σ_y (psf).....	49
4.9. DD40 Case - Backfill: Vertical Stress - σ_y (psf).....	50
4.10. DD40 Case - Excavation: Shear Stress - τ_{xy} (psf).....	52
4.11. DD40 Case - Backfill: Shear Stress - τ_{xy} (psf).....	53
4.12. DD40 Case - Excavation: Degree of Mobilization - f (%).....	54
4.13. DD40 Case - Backfill: Degree of Mobilization - f (%).....	55
4.14. Stress Paths For Point 1 - DD40 Case.....	58
4.15. Stress Paths For Point 2 - DD40 Case.....	60
4.16. Stress Paths For Point 3 - DD40 Case.....	61
4.17. Stress Paths For Point A - LM40 Case.....	62
4.18. Stress Paths For Point B - LM40 Case.....	63
4.19. Stress Paths For Point C - LM40 Case.....	64
4.20. Stress Paths For Point D - LM40 Case.....	65
4.21. Wall Deformed Shape At The End Of Each Step (DD40 Excavation Case).....	67
4.22. Wall Deformed Shape At The End Of Each Step (DD40 Backfill Case).....	68
4.23. Wall Deformed Shape At The End Of Each Step (LM40 Excavation Case).....	71

Figure	Page
4.24. Wall Deformed Shape At The End Of Each Step (LM40 Backfill Case)	72
4.25. Wall Deformed Shape At The End Of Each Step (DT40 Excavation Case).....	74
4.26. Wall Deformed Shape At The End Of Each Step (DT40 Backfill Case).....	75
4.27. Comparison of Maximum Wall Deflections (in.) for Excavation and Backfill	79
4.28. Bending Moment Diagram of the Wall at the End of Each Step (DD40 Excavation Case).....	80
4.29. Bending Moment Diagram of the Wall at the End of Each Step (DD40 Backfill Case).....	81
4.30. Bending Moment Diagram of the Wall at the End of Each Step (LM40 Excavation Case)	83
4.31. Bending Moment Diagram of the Wall at the End of Each Step (LM40 Backfill Case).....	84
4.32. Comparison of Maximum Bending Moments (k-ft) for Exc. and Backfill.....	86
4.33. Comparison of Anchor Forces (kips) for Excavation and Backfill.....	87
4.34. Maximum Wall Deflections Obtained When the Anchor Is Placed at Different Fill Levels.....	92
4.35. Wall Deformed Shapes for DD40 Case When the Anchor Is Placed at Different Fill Levels.....	93
4.36. Wall Deformed Shapes for LM40 Case When the Anchor Is Placed at Different Fill Levels.....	94
4.37. Maximum Bending Moments Obtained When the Anchor Is Placed at Different Fill Levels.....	95
4.38. Bending Moments for DD40 Case When the Anchor Is Placed at Different Fill Levels.....	97
4.39. Bending Moments for LM40 Case When the Anchor Is Placed at Different Fill Levels.....	98

Figure	Page
4.40. Anchor Forces Obtained When the Anchor Is Placed at Different Fill Levels.....	99
B.1. LM40 Case - Excavation: Deformed Shape (x50).....	115
B.2. LM40 Case - Backfill: Deformed Shape (x50).....	116
B.3. LM40 Case - Excavation: Displacement Vectors (x50).....	117
B.4. LM40 Case - Backfill: Displacement Vectors (x50).....	118
B.5. LM40 Case - Excavation: Horizontal Stress - σ_x (psf).....	119
B.6. LM40 Case - Backfill: Horizontal Stress - σ_x (psf).....	120
B.7. LM40 Case - Excavation: Vertical Stress - σ_y (psf).....	121
B.8. LM40 Case - Backfill: Vertical Stress - σ_y (psf).....	122
B.9. LM40 Case - Excavation: Shear Stress - τ_{xy} (psf).....	123
B.10. LM40 Case - Backfill: Shear Stress - τ_{xy} (psf).....	124
B.11. LM40 Case - Excavation: Degree of Mobilization - f (%).....	125
B.12. LM40 Case - Backfill: Degree of Mobilization - f (%).....	126
B.13. DN40 Case - Excavation: Degree of Mobilization - f (%).....	127
B.14. DN40 Case - Backfill: Degree of Mobilization - f (%).....	128
B.15. DT40 Case - Excavation: Degree of Mobilization - f (%).....	129
B.16. DT40 Case - Backfill: Degree of Mobilization - f (%).....	130
B.17. LT40 Case - Excavation: Degree of Mobilization - f (%).....	131
B.18. LT40 Case - Backfill: Degree of Mobilization - f (%).....	132

CHAPTER I

INTRODUCTION

The conventional methods for the design of anchored sheet pile walls are the Free Earth Support (FES) Method and Fixed Earth Support Method. These two methods have been used for a long time in the design of anchored sheet pile walls. The former, FES, is especially popular because of its simplicity.

In practice, anchored sheet pile walls are constructed either by excavating the “front” or filling the “back” side of the wall. In the excavation case, first the sheet piles are driven into the ground and then the front side is excavated to the desired elevation. In the filling case, the wall is partly driven into the soil, to the required penetration depth, and then the back side is filled. The construction may also involve a combination of these two basic methods. These different construction procedures will undoubtedly create different stress paths in the soil. Therefore one would expect a different soil behavior in each case. If the soil behaves differently, clearly the wall will not behave the same way in the two distinctly different ways of construction.

Conventional design methods do not consider the method of construction used. They are based on active and passive earth pressures that are concerned with the failure condition based on Coulomb-Mohr failure criterion. This criterion does not depend on the stress path followed to reach the failure condition; therefore, active and passive pressures

have no relevance to the method of construction. Because of this, engineers have come to believe that there is no difference in the method used for the construction of a wall. The fact is this belief has no theoretical nor experimental basis.

The objective of this thesis is to analyze the behavior of anchored sheet pile walls constructed by excavation and backfilling. Through these analyses, information will be obtained on the soil-structure interaction mechanisms involved in these systems. The results will be used to compare the two construction methods from an engineering point of view.

Twelve different soil profiles that contain a wide variety of soil types were selected for the purposes of this study. Twelve different sheet pile walls, designed by conventional methods in each soil profile were considered. For each one of these walls both types of construction, excavation and backfilling, were analyzed. The analysis method employed here was the Finite Element Method (FEM) equipped with suitable models of the soil-structure interface, nonlinear soil behavior and loading sequence. By using the FEM, it is possible to obtain the complete distribution of stresses and deformations everywhere in the soil and in the wall. Therefore this approach is suitable for the purposes of this study.

The details of the methodology employed are presented in Chapter II.

The characteristics of the soil profiles and the sheet pile walls studied are explained in Chapter III. The results obtained and comparisons are presented in Chapter IV. Significant differences were found between the walls constructed by excavation and backfilling.

CHAPTER II

METHODOLOGY

General

The Finite Element Method (FEM) is a powerful tool for analyzing soil-structure interaction problems. It is possible to perform a non-linear analysis and to obtain stresses and deformations everywhere in the entire system. The other alternatives to perform a study such as this one is either full-scale physical modeling or smaller-scale centrifuge modeling, both of which are very expensive and time consuming.

The finite element computer program, FEMSSI, Finite Element Method for Soil Structure Analysis, Version *HW* (Version *H* for Windows; Oner, 1993) was employed in this study. This program uses a simple, yet realistic stress-strain or “constitutive” model, and allows the simulation of any construction sequence. The program FEMSSI incorporates the following features (Hallal, 1988):

1. Beam-column elements - for a sheet pile wall sections,
2. Soil elements - for the soil around a sheet pile wall,
3. Frictional and/or adhesive soil-structure interface elements - for connection of the wall to the soil next to it,
4. Simulation of sequential construction and stepwise loading,

5. Consideration of soil drainage conditions,
6. A nonlinear constitutive model for the soil.

Simulation of sequential construction is an important feature since it allows calculation of stresses and deformations in the soil in each step during the construction process. This is also a requirement for performing a nonlinear analysis. Therefore the changes in the geometry, fill or excavation, are imposed step by step. Nonlinear soil stress-strain model is one of the most crucial aspects of a geotechnical finite element analysis.

Non-Linear Model Used in FEM: *f*-Model

It is well known that there is a vast variety of constitutive models available today for use in predicting soil behavior. Some of these models have been incorporated into finite element codes with varying degrees of success; others are too complicated or require the determination of a lot of parameters which renders them impractical.

The *f*-model used in this study is simple, nonlinear elastic soil constitutive model such as the Hyperbolic (Duncan and Chang, 1970), and Parabolic models. The *f*-model is based on the following principles (Oner, 1988):

1. The model should capture the essential characteristics of the soil behavior,
2. The model should be as simple as possible,
3. There should be a minimum of soil parameters describing the model, and
4. The soil model parameters should have simple and clear physical meaning.

The essential characteristics of soil behavior that should be represented in a nonlinear soil model are,

1. Strain softening as the material approaches failure,
2. Increase in rigidity parallel to an increase in confining pressure,
3. Returning to a high rigidity upon load reversal (unloading),
4. Failure due to an extended load reversal (as in passive failure).

These essential soil characteristics are represented in most soil models. For both unloading and reloading, the f -model utilizes nonlinear curves. The generalized form of the f -model is described below.

The current implementation of the f -model uses the following form of the stress-strain matrix;

$$\begin{Bmatrix} \sigma_x \\ \sigma_y \\ \tau_{xy} \end{Bmatrix} = \begin{bmatrix} M & M-2G & 0 \\ M-2G & M & 0 \\ 0 & 0 & 2G \end{bmatrix} \begin{Bmatrix} \varepsilon_x \\ \varepsilon_y \\ \varepsilon_{xy} \end{Bmatrix} \quad (1)$$

where the constrained modulus, M , and shear modulus, G , are related to Young's modulus, E , and Poisson's ratio, ν , as follows:

$$M = \frac{E(1-\nu)}{(1-2\nu)(1+\nu)} \quad (2)$$

$$G = \frac{E}{2(1+\nu)} \quad (3)$$

The constrained modulus at the earth pressure at rest, K_0 , condition, M_0 , is given by the empirical relationship (Janbu, 1963):

$$M_0 = mp_a \left(\frac{\sigma_1}{p_a} \right)^n \quad (4)$$

where p_a is atmospheric pressure (approximately 1 tsf, 1kg/cm², or 100 kPa), σ_1 is the major principal stress and m and n are dimensionless empirical soil parameters.

The degree of mobilization, f , is defined as the inverse of shear strength factor of safety:

$$f = \frac{\tan \phi_d}{\tan \phi} \quad \text{for } \phi > 0 \quad (5)$$

$$f = \frac{\tau_{\max}}{c_u} \quad \text{for } \phi = 0 \quad (6)$$

where ϕ_d is the angle of a line tangent to the Mohr circle of stresses, ϕ is the same angle for the failure condition, τ_{\max} is the maximum shear stress, and c_u is the undrained shear strength of the soil.

Failure in the f -model ($f = 1$) is based on Mohr-Coulomb failure criteria; f is the ratio of slopes as shown in Figure 2.1.

At any stress level, shear modulus, G , is given by:

$$G = G_0 \frac{(1-f)}{(1-f_0)} \quad (7)$$

where, f_0 is the degree of mobilization at K_0 condition and G_0 is the shear modulus at K_0 condition. f_0 value can be determined from the Equations (5) and (6). The Equation (7) can also be written as:

$$G = G_i(1-f) \quad (8)$$

where, G_i is the initial modulus, shear modulus value at $f = 0$.

As the soil approaches failure the shear modulus decreases to zero whereas the constrained modulus, M , is kept constant at its initial value in a drained situation. However, in an undrained condition Poisson's ratio, ν , is kept constant; consequently, M varies along with G as indicated in Equations (2) and (3).

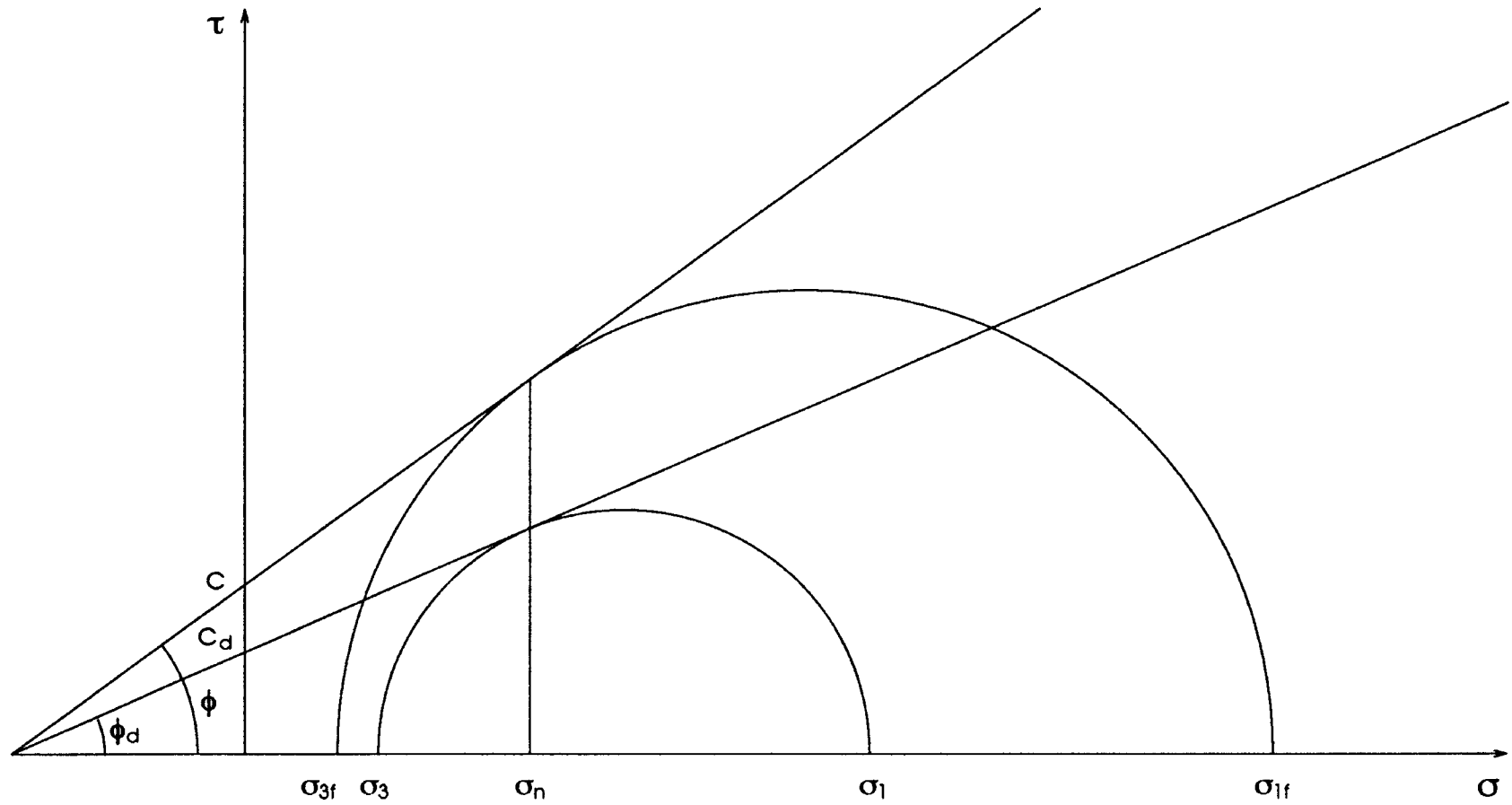


Figure 2.1. Representation of the Degree of Mobilization in Mohr Diagram

For the drained clayey soils, m is related to the compression index C_c as:

$$m = \frac{1+e}{C_c \log 2} \quad (9)$$

This equation predicts m values in the range 10 to 50 for the C_c range of 0.1 to 0.6 and void ratio range of 0.7 to 1.2. Janbu (1985) gives an m range of 10 to 30 for the drained clayey soils.

For the undrained condition of clayey soils ($\phi = 0$ condition) $n = 0$ and m is given as:

$$m = \frac{E_u}{c_u} \quad (10)$$

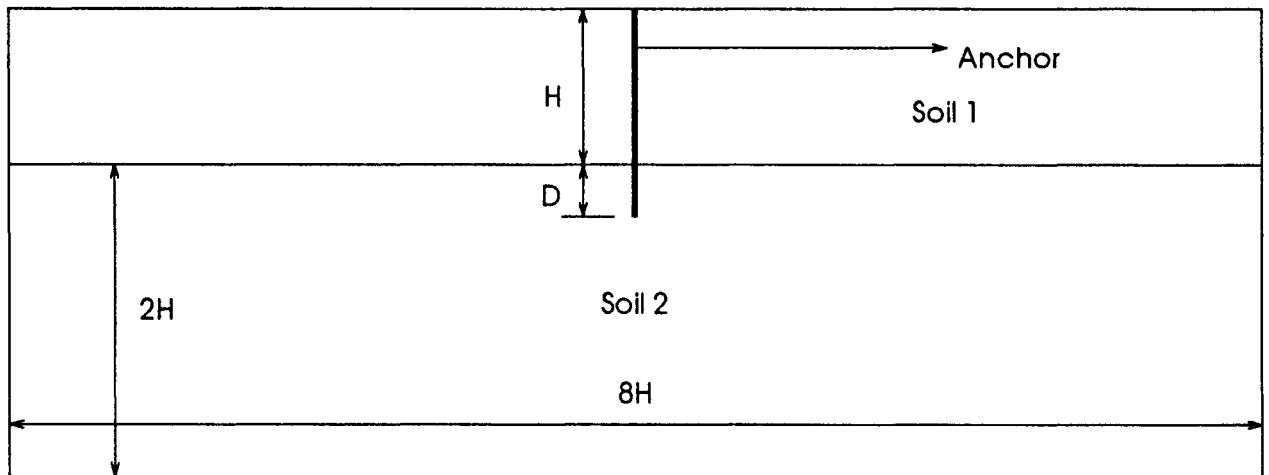
where E_u is the undrained secant Young's modulus at a stress level of about 50% of the failure value, and c_u is the undrained shear strength of the soil. Since the modulus has the stress unit, m is again dimensionless.

Soil Parameters Required

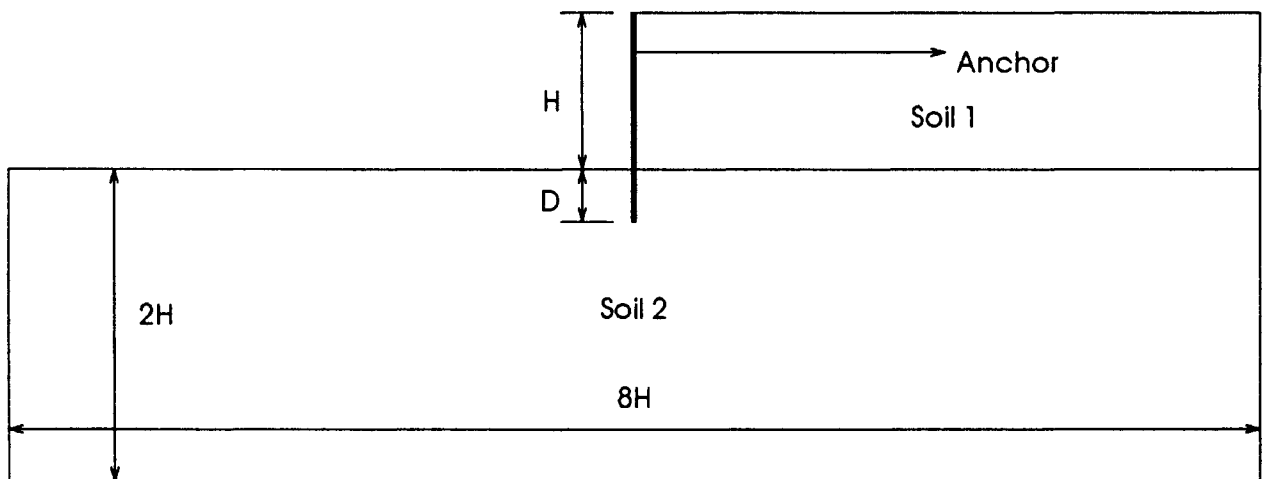
The parameters required for the f model explained above are ordinary soil properties such as earth pressure at rest, K_0 , cohesion, c , internal friction angle, ϕ , and f -model parameters m and n .

Construction Simulation

The grid section used in the finite element analyses of excavation cases is shown in Figure 2.2. At the beginning of the analysis the ground surface is horizontal and the sheet pile wall is inserted as the first step right after the "gravity-turn-on" step. Therefore the



(a) At the beginning of construction



(b) At the end of construction

Figure 2.2. Soil Section Analyzed in the Excavation Cases

finite element grid covers the front of the wall as well as the back. To simulate excavation, layers of finite elements were removed, step by step, until the dredge line level is reached.

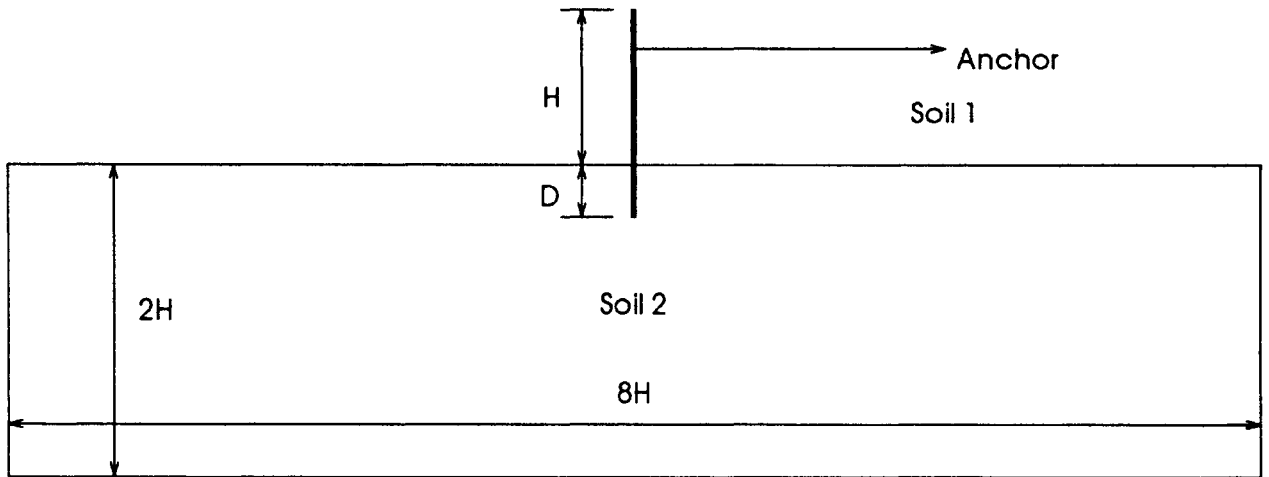
In the backfill cases, the ground surface was at the “dredge line” level at the beginning (Figure 2.3). To simulate backfilling, horizontal layers of finite elements were laid on the back of the wall until the top of the wall was reached. Ten to fifteen layers of finite elements were used in this process.

The removal and addition of finite elements are done automatically by the FEM program once the user specifies the numbers of the elements affected in an analysis step.

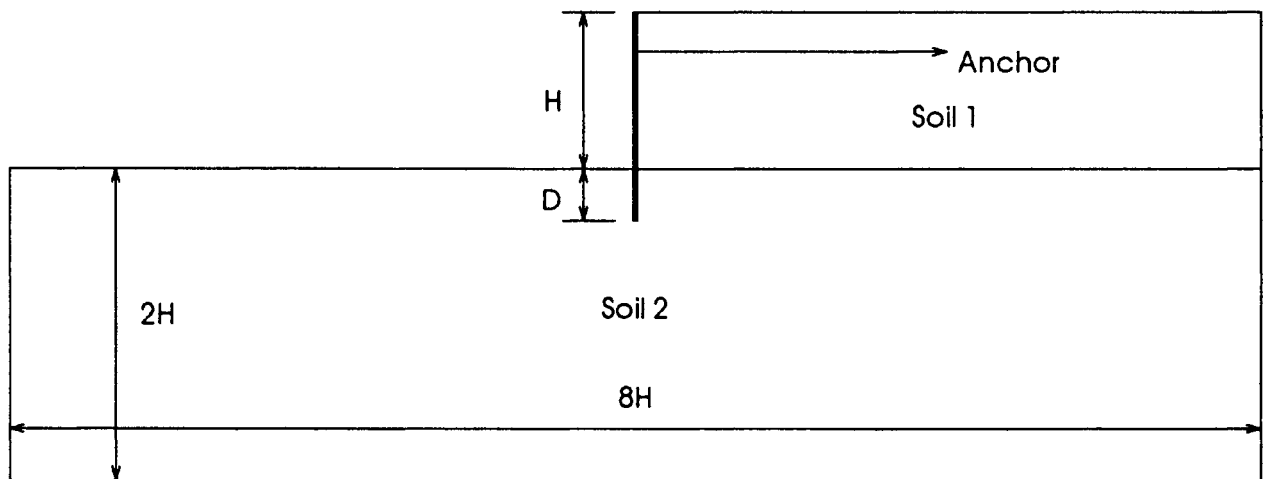
Pre-Processing and Post-Processing for FEM

In an application of the finite element method a problem is described for the FEM program using an “input data file.” An input data file contains the geometry data, material properties, boundary conditions and the description of the steps of construction. The geometry data consists of two main sections: (1) a table of the x and y coordinates of each node, or *the coordinate array*, and (2) the numbers of the corner nodes for each element, or *the connectivity matrix*. For each analysis step, the elements which will be excavated or backfilled are specified.

Since the input data file can become very long and complicated, the preparation of this file is time consuming and error prone. Because of this the input data files for finite element analyses are frequently prepared by using special computer programs. Such programs are called *pre-processors*. In this study, two preprocessors were used. For the excavation cases the program called GENEREX was used. For fill cases a new program,



(a) At the beginning of construction



(b) At the end of construction

Figure 2.3. Soil Section Analyzed in the Backfill Cases

called GENEREF, was developed during the course of this study (Bilgin and Oner, 1993).

GENEREX and GENEREF programs generate rectangular grid data for the FEMSSI (Oner, 1993) computer program. They generate a symmetric grid with a sheet pile wall in the middle. These programs get the information about the grid required from a very small data file (about 2% of the FEMSSI input data file), called the GEN file. Using this information they form the rectangular grid, generate node coordinates and element corner nodes. The output file obtained from the execution of a preprocessor is directly used as an input data file for the finite element program.

A GEN file used by the preprocessors contains the following basic data: (1) the number of divisions wanted in vertical and horizontal directions, (2) the number of layers to excavate or backfill, (3) the boundary conditions, (4) the material properties, (5) the pile section name (such as "PZ27"), (6) the anchor stiffness and where to attach the anchor, and (7) the height of the wall.

A typical finite element analysis generates literally millions of numbers; the output files can easily be several megabytes long. Therefore the interpretation of the results are done by using another special-purpose computer program, a *post-processor*. The post-processor used in this study, POSTFEM, reads the FEM output file as data and produces several plots: (1) Deformed shape of the grid, (2) Displacement vectors, and (3) Contours of stresses and degree of mobilization.

Samples of the GEN file, the input data file and the output file, are given in Appendix A for a typical analysis case.

CHAPTER III

SHEET PILE WALLS AND SOIL PROFILES STUDIED

The implementation details, such as the characteristics of the anchored sheet pile walls studied, the selection of the soil profiles and parameters, and the finite element grid generation procedures are presented in this Chapter.

The data related to geometry and soil properties were selected by a joint research team of OSU and WES (Waterways Experiment Station, US Army Corps of Engineers). These are presented in the following sections.

Selection of Typical Wall Cases

Basic Geometry

The free height of a typical sheet pile wall designed by the Corps engineers is 40 feet, although shorter heights such as 30 feet are also common. In the majority of the cases studied, the free wall height was set at 40 ft. For the profiles that involved soft clays, this height was unreasonably high, so in these cases the free wall height was selected as 30 ft. Ground water table elevation was assumed to be at the anchor level on both sides. The typical wall section is shown in Figure 3.1.

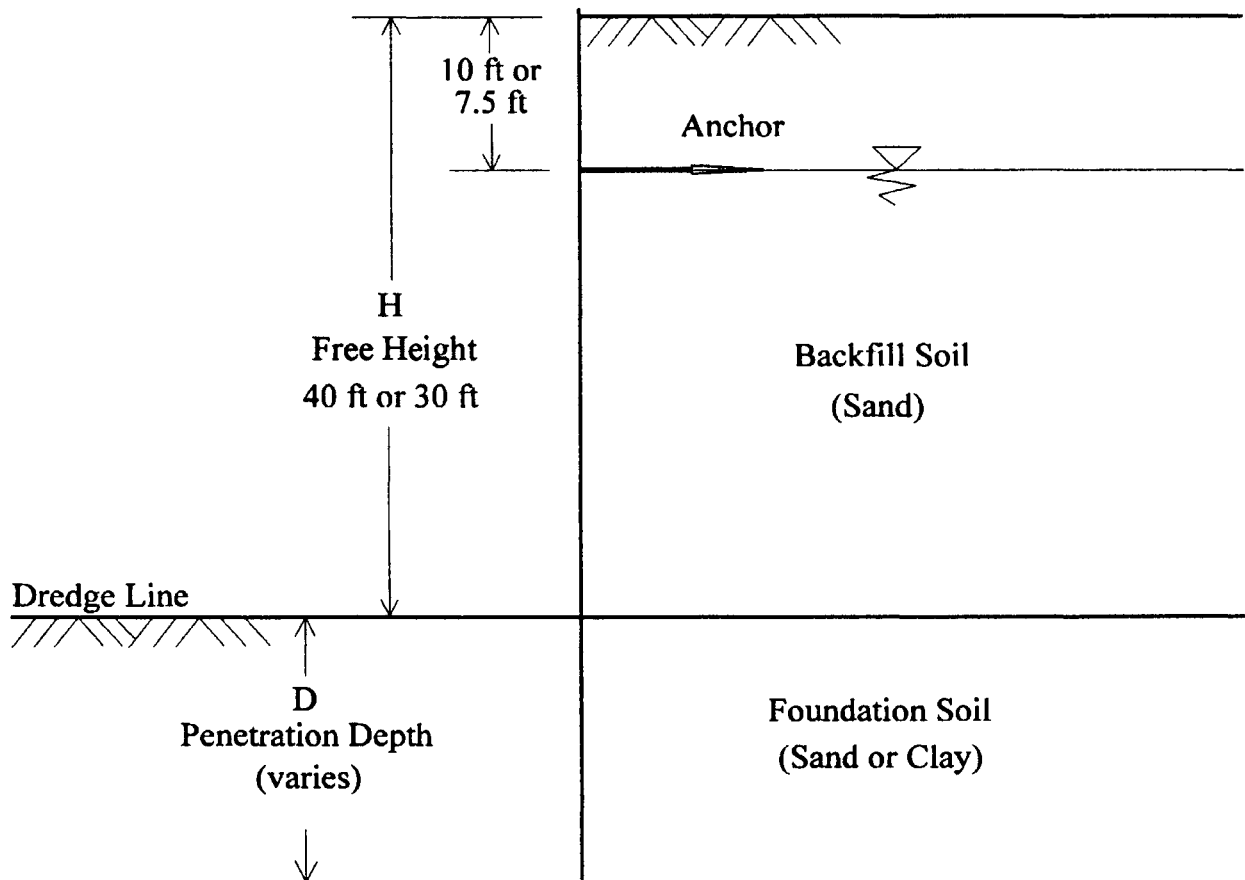


Figure 3.1. Typical Anchored Sheet Pile Wall Section Analyzed in This Study

Soil Types

Considering the soil types encountered at sheet pile wall sites, the following six soil types were selected:

1. Medium-dense sand (D)
2. Loose sand (L)
3. Medium-stiff clay, undrained (M)
4. Soft clay, undrained (S)
5. Medium-stiff clay, drained (N)
6. Soft clay, drained (T)

The codes given in the parentheses for the soil types are used to designate the cases. In utilizing various empirical correlations available, the “medium-dense sand” is taken as one with a relative density in the range of 50 to 70%, and the “loose sand” is taken as one with a relative density of 0 to 40%. The “medium-stiff clay” is slightly overconsolidated, with a low to medium plasticity index (30 to 40) while the “soft clay” is considered to be normally consolidated with medium to high plasticity index (50+).

The properties selected for these soil types are given in Table 3.1. The unit weights are based on the void ratio, e , and specific gravity, G_s , values listed in the last column of the table.

Considering the preferred practice of using only granular backfills, only sand was considered (D and L) for the soil above the dredge line. For the soil below the dredge line, *the foundation soil*, all six soil types were considered (D , L , M , S , N , T). So the total number of combinations possible with two soil types above the dredge line and six soil

types below the dredge line is twelve (Table 3.2). Each case is given a two-letter identification code using the soil types' one-letter code names. The first letter in a two-letter code indicates the soil above the dredge line and the second letter shows the soil type below the dredge line. For example case *DL* means medium-dense sand above dredge line and loose sand below dredge line.

TABLE 3.1
SOIL PROPERTIES DEFINING THE SOIL TYPES CONSIDERED

Soil Type	c	ϕ	γ_{wet}	γ'	γ' based on
Medium-Dense Sand, <i>D</i>	0	36	110	68.5	$e = 0.5, G_s = 2.65$
Loose Sand, <i>L</i>	0	30	97	60.5	$e = 0.7, G_s = 2.65$
Medium-Stiff Clay, Undrained, <i>M</i>	varies*	0	110	58	$e = 0.8, G_s = 2.70$
Soft Clay, Undrained, <i>S</i>	varies**	0	95	48	$e = 1.2, G_s = 2.70$
Medium-Stiff Clay, Drained, <i>N</i>	0	30	110	58	$e = 0.8, G_s = 2.70$
Soft Clay, Drained, <i>T</i>	0	25	95	48	$e = 1.2, G_s = 2.70$

(*) Varies as $c_u = 0.40\sigma'_v$ from current surface, or $c_u = 0.35\sigma'_v$ with 20' erosion

(**) Varies as $c_u = 0.25\sigma'_v$

TABLE 3.2
ALL COMBINATIONS OF THE SOIL TYPES CONSIDERED

Backfill Soil →	Medium-Dense Sand	Loose Sand
Foundation Soil ↓		
Medium-Dense Sand	<i>DD</i>	<i>LD</i>
Loose Sand	<i>DL</i>	<i>LL</i>
Medium-Stiff Clay, Undrained	<i>DM</i>	<i>LM</i>
Soft Clay, Undrained	<i>DS</i>	<i>LS</i>
Medium-Stiff Clay, Drained	<i>DN</i>	<i>LN</i>
Soft Clay, Drained	<i>DT</i>	<i>LT</i>

Shear Strength of Sands in the Profiles

The shear strength of sand is generally defined by a ϕ angle, referred to as internal friction angle, angle of shear strength or angle of shear resistance. If there is a small cohesion intercept measured, it is generally neglected in practical calculations to be on the conservative side.

Shear Strength of Clays in the Profiles

The shear strength of clays is more complicated. Because clays have lower permeability, higher void ratios, and water interaction with particles that affect the clay strength behavior. The shear strength of a clayey soil should at least be expressed in terms of drained and undrained conditions.

Undrained condition of clays is considered to correspond to a short term condition in the field. This condition occurs due to loading which causes excess pore pressures because water can not drain from the system. With time drained conditions occur because of the drainage of water from the system.

The undrained shear strength of clays is expressed by c_u and ϕ is taken as zero for normally consolidated clays. The c_u value typically increases with depth due to increasing confinement. This is generally expressed with the ratio " c_u / p ", where p is the effective vertical stress.

As far as stresses and strains are concerned, the drained shear strength of a normally consolidated clay is similar to a loose sand for which $c' = 0$. However, the friction angle ϕ' , is generally lower than that for sands. Similarly, the drained shear

strength of over-consolidated clays is similar to dense sands, again with a lower friction angle.

The c_u values for the two clay types are based on the conventional “ c_u/p ” ratio, where p is the effective vertical stress. The selection of the c_u/p values is based on data compiled by Ladd et al. (1977). The effective vertical stresses used in constructing the c_u profiles are based on the assumption that the current ground water table is at the anchor level and the soil is normally consolidated. For the medium-stiff clay, two alternatives were considered: (1) $c_u = 0.40\sigma_v'$, representative of a low-plasticity clay, and σ_v' from the current profile, and (2) $c_u = 0.35\sigma_v'$, representative of medium plasticity normally consolidated clay, and σ_v' calculated from some hypothetical “maximum past pressure” defined by a level higher than the current ground surface by 20'. This condition represents a slightly over consolidated clay due to erosion (average OCR about 1.5, decreasing with depth). An average c_u profile was selected from the values calculated from these two methods. The c_u profiles obtained in this manner are shown in Figure 3.2.

ϕ' values for drained clay cases are based on the statistics given by Kovacs (1981). The ϕ values used for sands are somewhat conservative (probably by about 2 to 4 degrees) but intended to reflect typical practice.

Selection of the Stress-Strain Model Parameters

K_0 values required for initial stress calculations were chosen using the well known Jaky's formula:

$$K_0 = 1 - \sin\phi \quad (11)$$

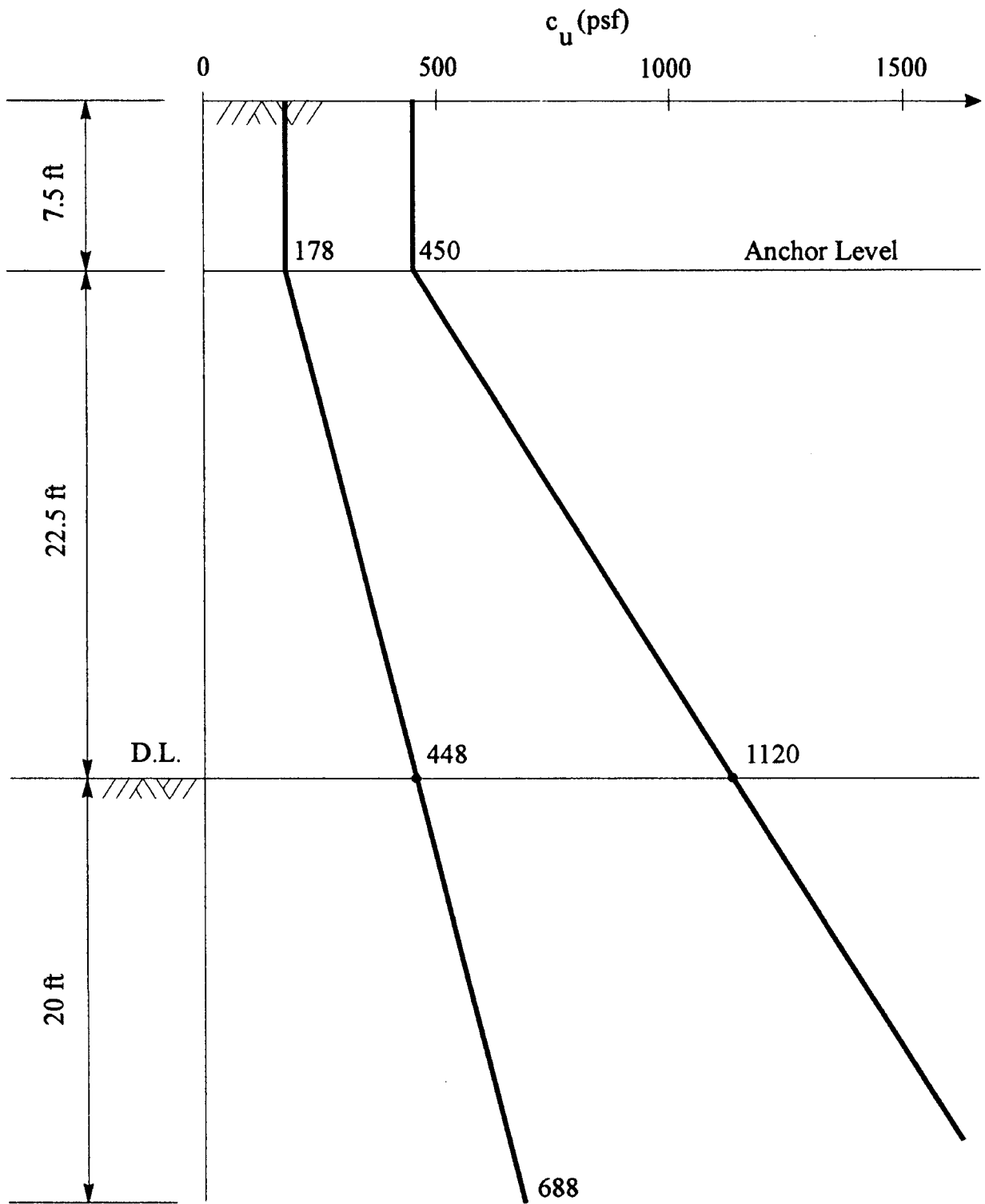


Figure 3.2. Undrained Shear Strength Profile Used in the Analysis

The values used for cohesion, c , and internal friction angle, ϕ , were given in the soil properties section (Table 3.2). The values for the parameters earth pressure at rest, K_0 , and f -model parameters m and n used in the analysis are given on Table 3.3.

TABLE 3.3
USED MODEL PARAMETERS FOR SOIL STRESS-STRAIN RELATIONSHIP

Soil Type	K_0	ν_i	m	n
Medium-Dense Sand, D	0.412	0.25	200	0.5
Loose Sand, L	0.50	0.30	120	0.5
Medium-Stiff Clay, Undrained, M	0.96	0.49	500	0.0
Soft Clay, Undrained, S	0.96	0.49	250	0.0
Medium-Stiff Clay, Drained, N	0.50	0.30	30	0.6
Soft Clay, Drained, T	0.577	0.35	15	0.9

Soil-Structure Interface Properties

For the soil-wall interface, a wall friction angle is assumed in a conventional design calculation. This angle is defined as the angle made between the shear and normal stresses at the interface. In FEM no assumption is made about the angle between the stresses. Only the maximum angle (and an adhesion value where appropriate) is specified and the stresses are allowed to develop freely to satisfy equilibrium, compatibility, and the stress-strain relationship.

The interface properties used in this study were selected as follows. For sand and drained clay cases an interface friction angle equal to $2/3\phi'$ was used. In undrained clay

cases friction was zero, but an adhesion equal to a fraction of c_u was assigned; $c_a = \alpha c_u$. The fraction α was determined as in vertically loaded pile foundations ($\alpha = 1$ for $c_u < 500$ psf, and decreasing with c_u). The interface stiffness was set as 10^6 lb/ft for normal stiffness and 10^5 lb/ft shear stiffness as in former studies with these soil profiles.

Conventional Design Calculations

The penetration depths and the sections given by free earth support method were found in previous studies (Oner, 1992). The penetration depths and wall sections obtained by using WALSH program (Dawkins, 1985) were used in this study. A summary of the results of these studies are given in the Table 3.4 for convenience in referencing them for comparisons in this work.

The case names in the table above indicate the soil types and the wall free height, H . (Note that the first letter indicates the soil above the dredge line, the second letter shows the soil type below the dredge line and the number indicates the free height of the wall). The depth of the anchor was taken as one fourth of the free wall height. The anchored sheet pile wall profile was shown in Figure 3.1.

TABLE 3.4

RESULTS OF FREE EARTH SUPPORT CALCULATIONS (after Oner, 1992)

CASE	H (ft)	D (ft)	Pile Section	I (in ⁴ /ft)	M_{\max} (k-ft/ft)	A_p (kips)
DD40	40.00	8.44	PZ35	361.20	76.06	8.52
DL40	40.00	13.23	PZ32	220.40	95.95	9.50
DM40	40.00	5.67	PLZ25	223.25	62.05	7.77
DS30	30.00	25.49	PZ32	220.40	68.99	6.95
DN40	40.00	13.66	PLZ23	203.75	98.09	9.61
DT40	40.00	22.04	PLZ23	203.75	145.05	11.63
LD40	40.00	8.58	PZ40	490.80	86.74	9.75
LL40	40.00	13.03	PZ32	220.40	105.74	10.69
LM40	40.00	6.66	PZ32	220.40	73.98	9.08
LS30	30.00	23.53	PZ32	220.40	69.95	7.50
LN40	40.00	13.44	PLZ23	203.75	107.92	10.81
LT40	40.00	20.97	PZ27	184.20	148.17	12.61

where, H is the free wall height, D is the depth of penetration, I is the moment of inertia of the pile section, M_{\max} is the maximum moment, and A_p is the anchor force.

Selection of Finite Element Grids and Other Analysis Parameters

In this section the selection of the finite element analysis parameters and other details are discussed. This includes the of selection of; (a) grid size, (b) element subdivision or grid generation procedure, (c) number of substeps to be used, and (d) determination of the anchor stiffness to be used.

Rectangular grids, which are finite element grids made up of rectangular elements, were used in all cases. This type of grids has the advantage of facilitating the automatic generation of data. However, in a rectangular grid very thin and long elements occur

toward the boundaries. Such elements may introduce inaccuracies in a finite element analysis especially if they occur in the zones of interest where stress concentrations occur. In the current problem, however, the region of interest is around the sheet pile wall. Since the long and thin elements are distant enough from the region of interest this should not be very significant.

Selection of Grid Size

The soil layer thickness was set as $3H$ below which is bedrock, where H is the free wall height. The width of a finite element grid in geotechnical problems is usually arbitrary because there is no natural boundary on the two sides. For a rational selection of the grid width to be used a series of runs were made; five different widths were considered and each case was analyzed to see the how the width affects the results. The widths were taken as $1H$, $2H$, $3H$, $4H$ and $5H$ on both sides of the wall (Figure 3.3). Analyses were performed for both excavation and backfilling cases. The maximum deflection, maximum moment, and the anchor force values were noted as a basis for comparisons. The results for DD40 and LM40 cases are given in Table 3.5.

The first observation made is that the maximum deflection of the wall increased as the grid width increased. This was observed in all cases. This effect can be explained as the bulk deformation of the larger soil profile as the grid width is increased.

The calculated maximum bending moment values decreased as the grid size was increased, in the excavation cases. The opposite was true in backfill cases: as the grid size increased, the maximum bending moment decreased.

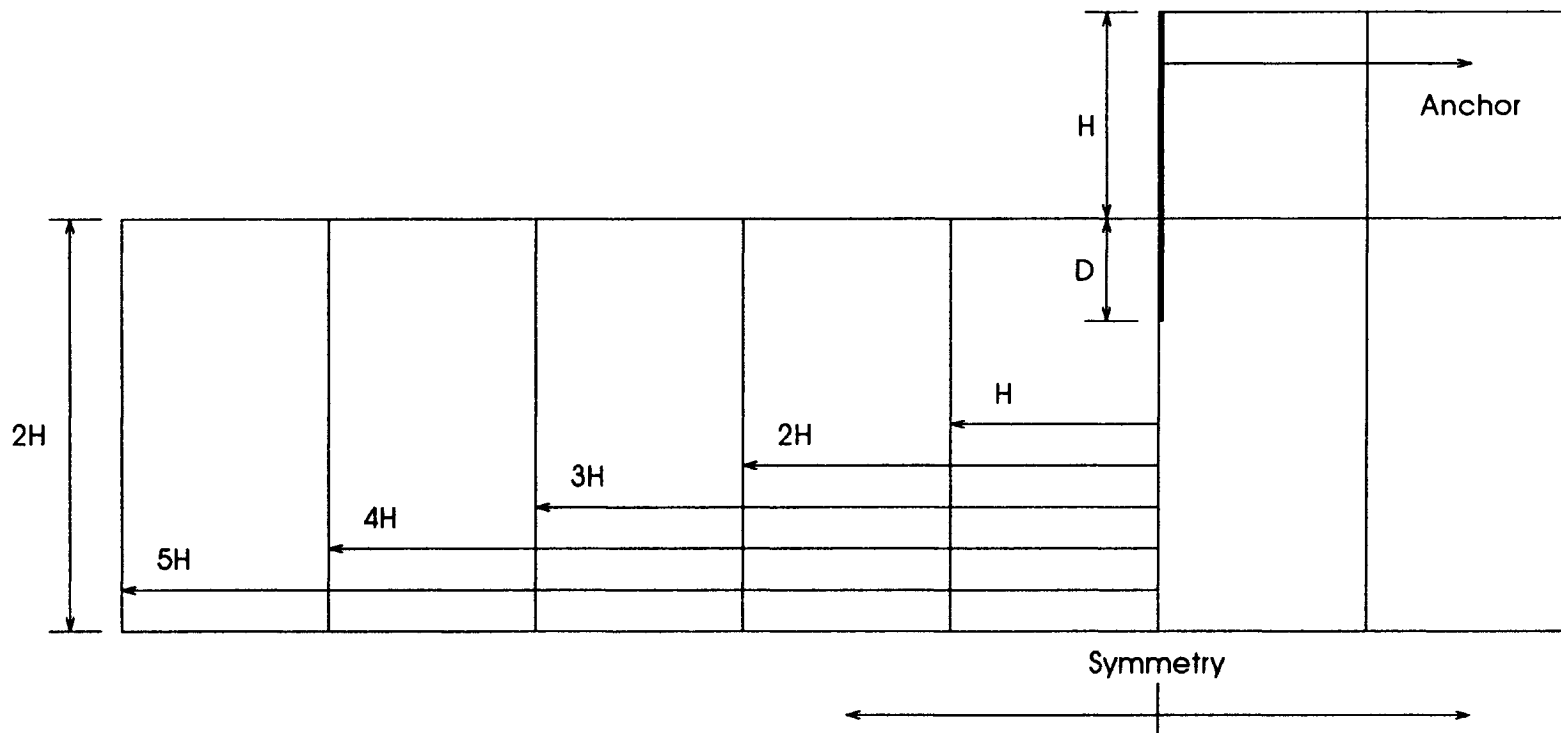


Figure 3.3. Grid Sizes Used to Analyze Grid Size Effect

TABLE 3.5

RESULTS OF ANALYSIS FOR DIFFERENT GRID SIZES

CASE	Depth	Width	Max. Def. (in)	Max. Mom. (k-ft)	Anc. Force (kips)
DD40 (Excavation)	3*H	1*H	-1.33	-42.07	-7.40
	3*H	2*H	-1.45	-40.83	-8.37
	3*H	3*H	-1.54	-39.38	-9.54
	3*H	4*H	-1.60	-39.23	-10.33
	3*H	5*H	-1.61	-39.25	-10.55
DD40 (Fill)	3*H	1*H	-1.79	-50.97	-8.74
	3*H	2*H	-2.11	-54.89	-10.31
	3*H	3*H	-2.31	-57.67	-11.55
	3*H	4*H	-2.40	-58.81	-11.87
	3*H	5*H	-2.42	-58.82	-11.95
LM40 (Excavation)	3*H	1*H	-1.56	-37.44	-9.56
	3*H	2*H	-1.72	-36.08	-11.63
	3*H	3*H	-1.81	-35.41	-12.89
	3*H	4*H	-1.87	-35.26	-13.58
	3*H	5*H	-1.89	-35.18	-13.73
LM40 (Fill)	3*H	1*H	-1.94	-50.19	-9.57
	3*H	2*H	-2.24	-53.40	-11.10
	3*H	3*H	-2.36	-53.60	-11.69
	3*H	4*H	-2.42	-54.25	-11.84
	3*H	5*H	-2.44	-54.15	-11.98

* There is a symmetry on both sides of the wall axis

The calculated anchor forces were higher for larger grid sizes in both excavation and backfill cases. This should be expected since increased deflections that occur in larger grids result in larger elongations in the anchor rods, and consequently, larger anchor forces.

Figure 3.4 shows the change of maximum deflections with increasing grid width. Similarly Figure 3.5 and Figure 3.6 show the change of maximum bending moments and anchor forces, respectively, with increasing grid width. It is observed that there was almost no change in the analysis results for widths of 4H and larger. Therefore, for the main analyses the widths of all grids were set as 4H wide on both sides of the wall.

The boundary conditions imposed are as follows:

1. On the left and right sides: roller or smooth type (fixed in x direction),
2. On the bottom boundary: fixed in both x and y directions.

Selection of the Number of Substeps

The cases in which undrained soft clay were present, excavation and backfill were done in 10 layers, and in the other cases this is done in 11 layers. This is because the free wall height is smaller for the soil profiles containing soft clays. For each layer the load is applied in substeps. It is well known that, for the nonlinear analysis increasing the number of substeps gives better results.

To decide the number of substeps, 1, 2, 4, 8 and 16 substeps were tested by using both methods, excavation and backfilling. The results, maximum deflection, maximum moment and anchor force values, for DD40 and LM40 cases are given on Table 3.6.

The change in the results due to the change in the number of substeps are plotted on the Figures 3.7, 3.8 and 3.9, where Figure 3.7 shows the change in maximum deflections, Figure 3.8 shows the change in maximum moments and Figure 3.9 shows the change in anchor forces.

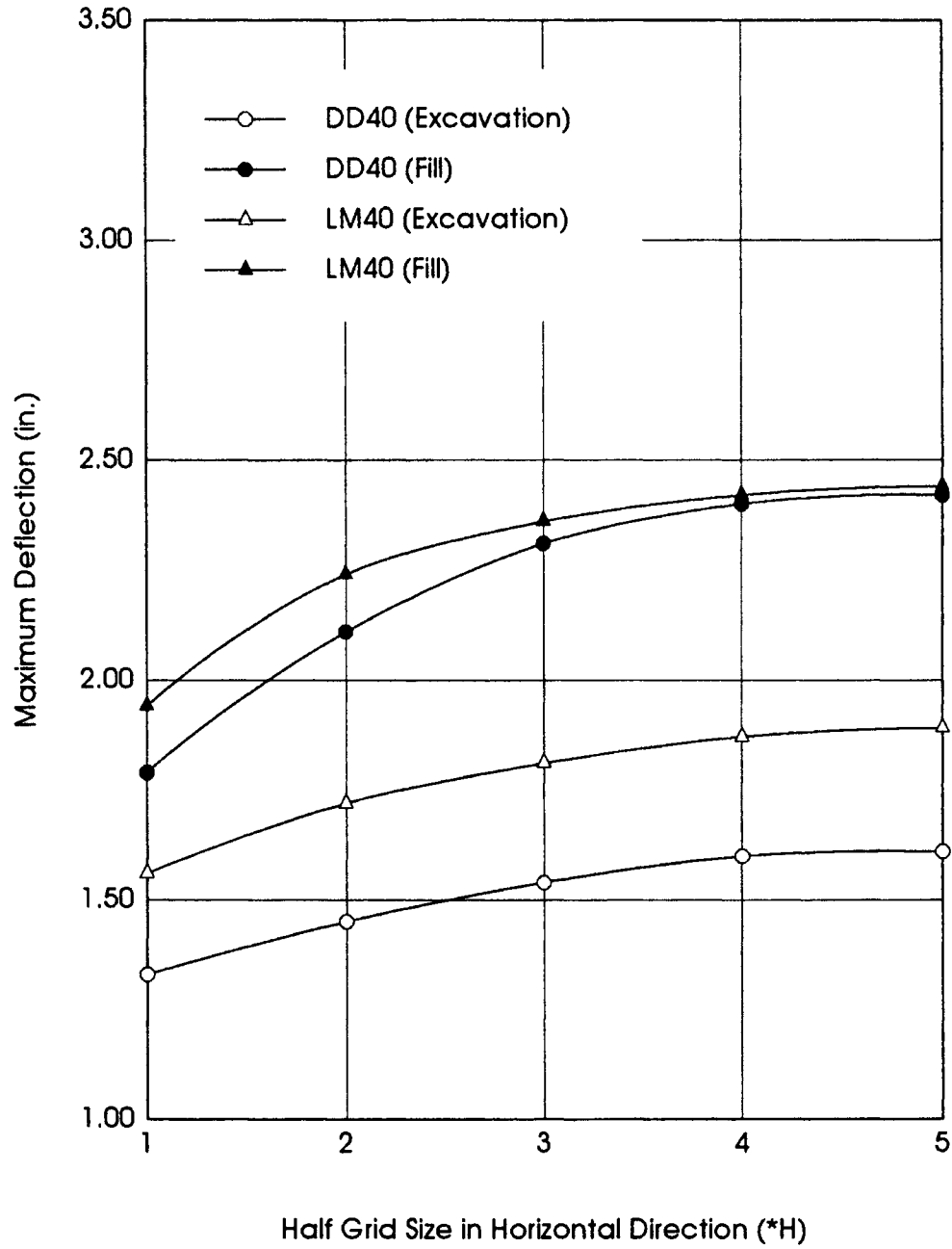


Figure 3.4. Maximum Deflections Obtained Using Different Grid Sizes
(H is the free wall height)

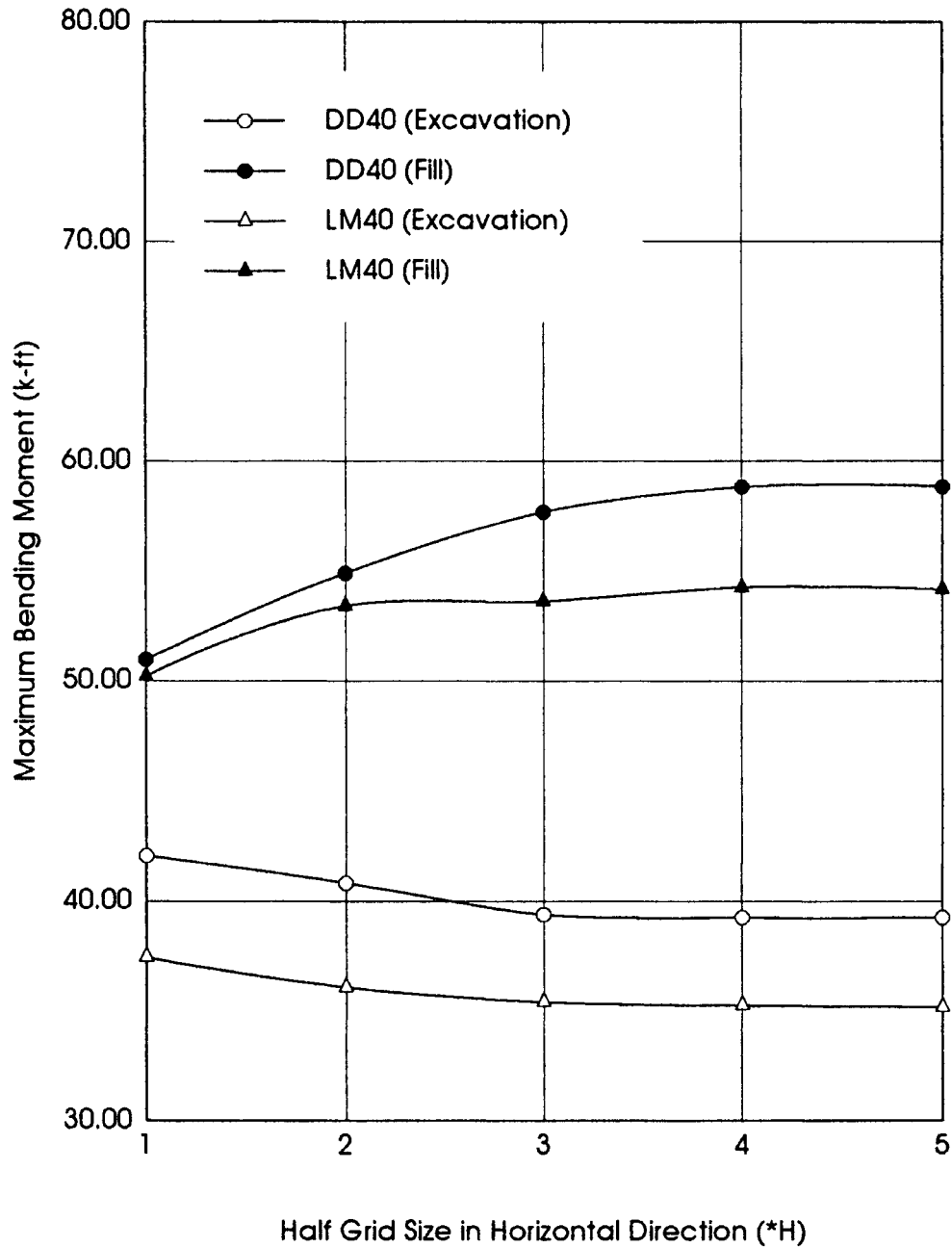


Figure 3.5. Maximum Bending Moments Obtained Using Different Grid Sizes
(H is the free wall height)

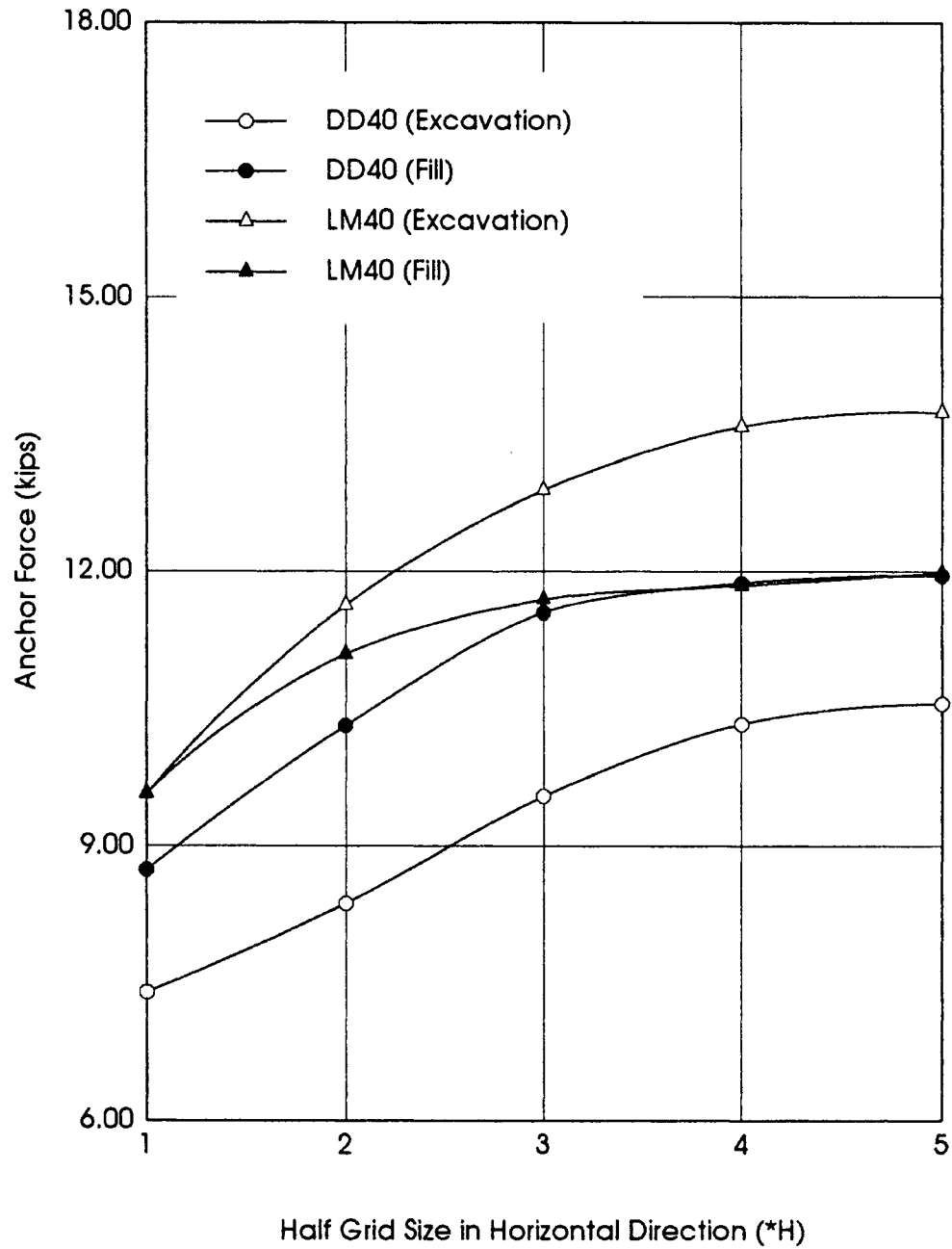


Figure 3.6. Anchor Forces Obtained Using Different Grid Sizes
(H is the free wall height)

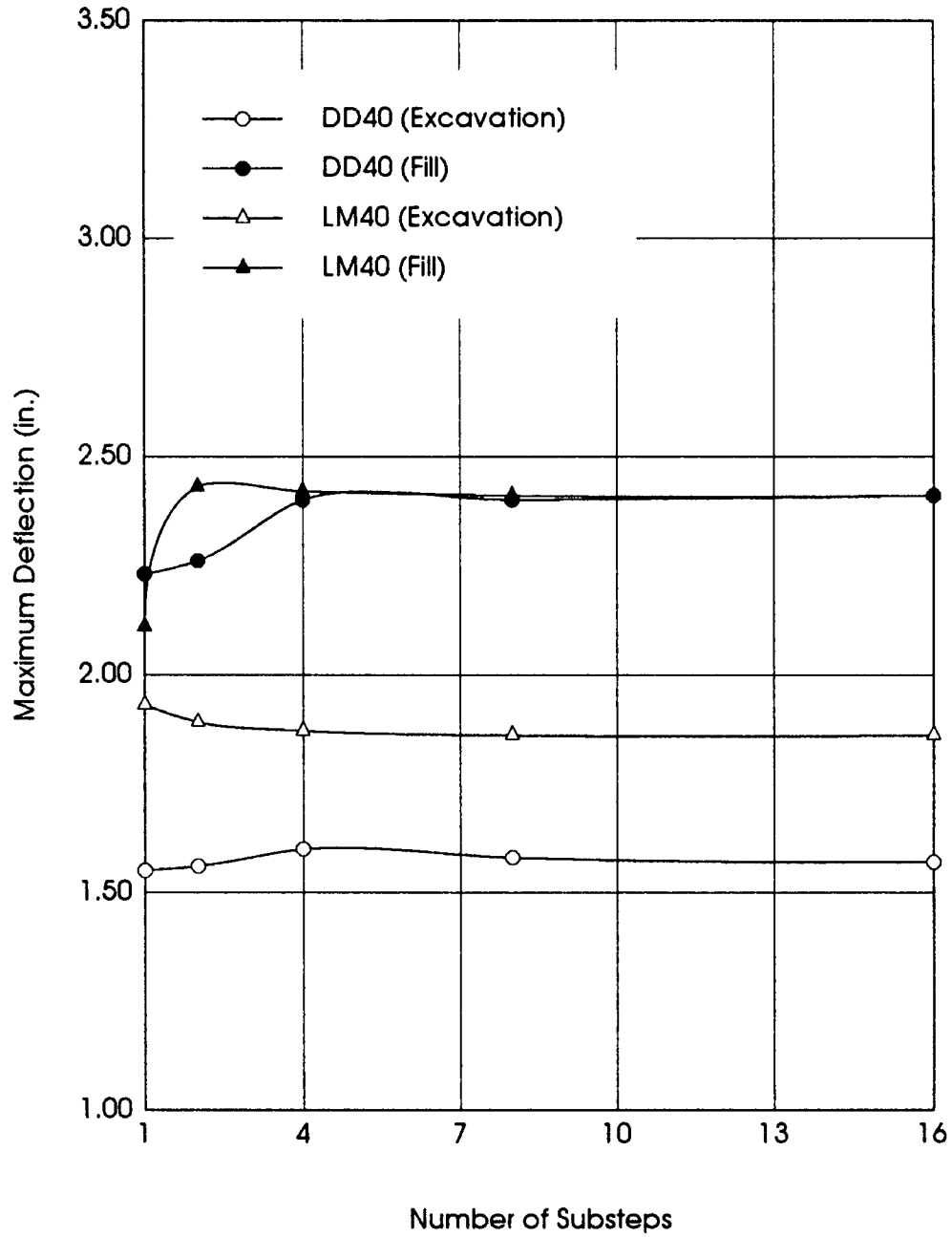


Figure 3.7. Maximum Deflections Obtained Using Different Substeps

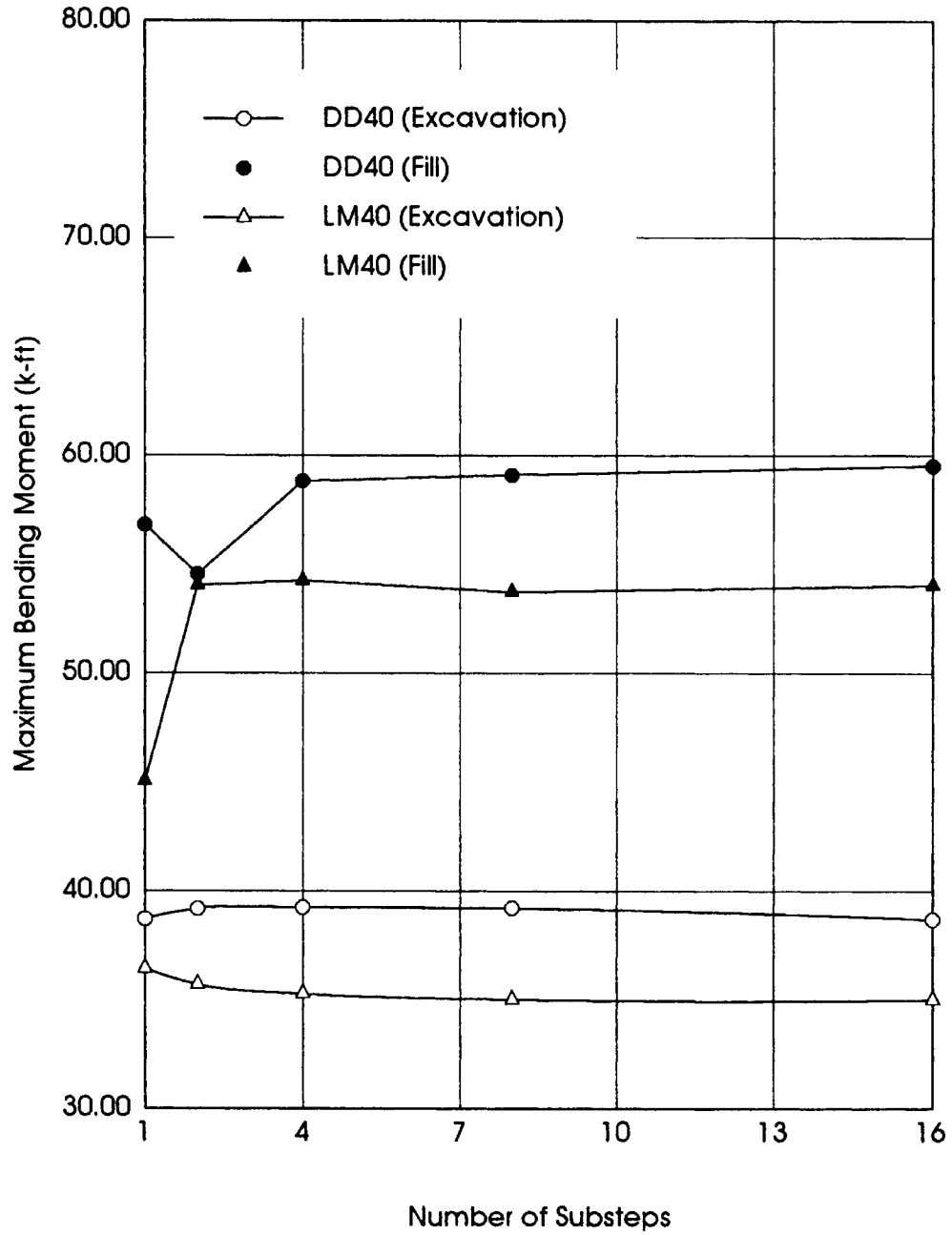


Figure 3.8. Maximum Bending Moments Obtained Using Different Substeps

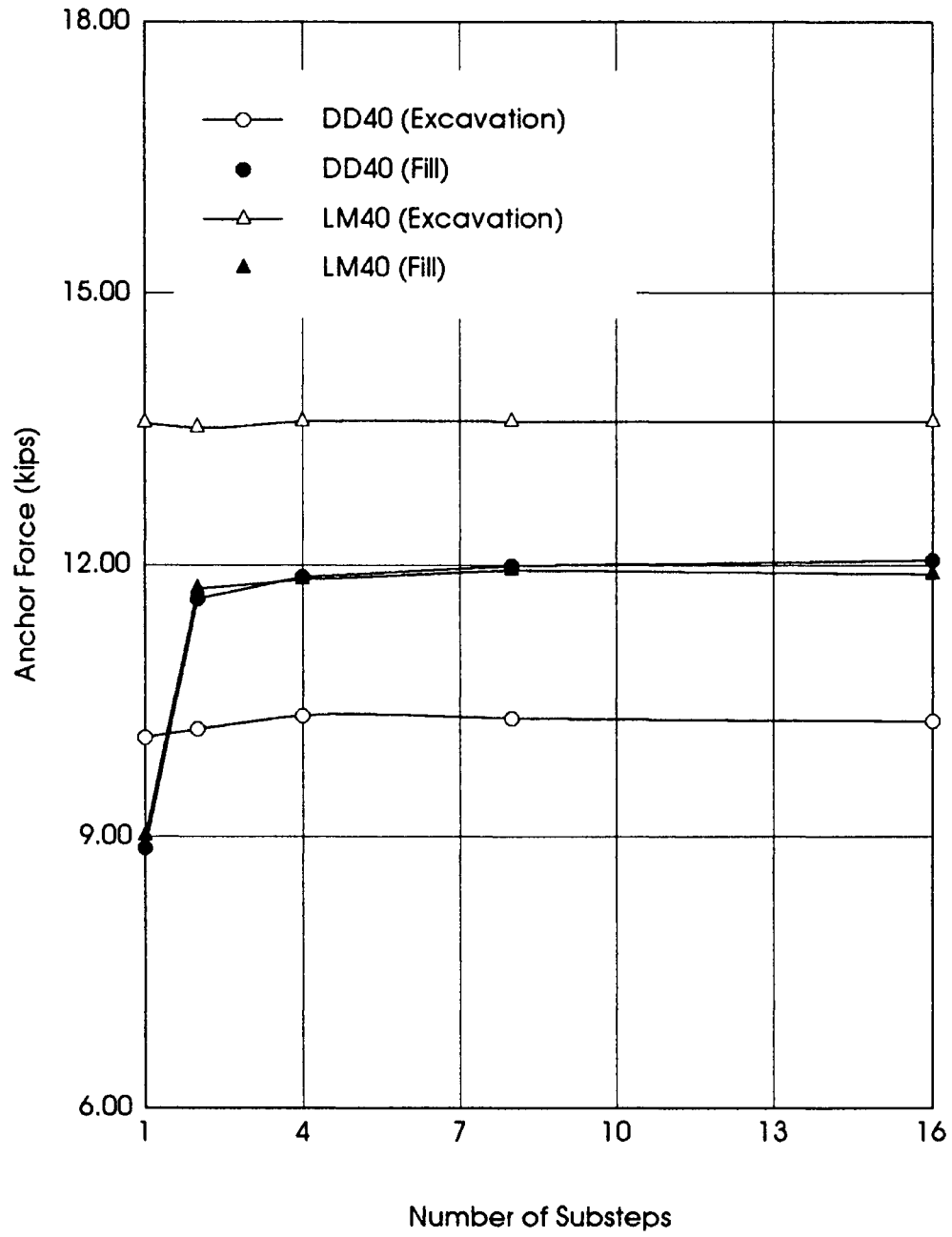


Figure 3.9. Anchor Forces Obtained Using Different Substeps

TABLE 3.6

RESULTS OF ANALYSIS FOR DIFFERENT SUBSTEPS

CASE	SUBSTEPS	Max. Def. (in)	Max. Mom. (k-ft)	Anc. Force (kips)
DD40 (Excavation)	1	-1.55	-38.71	-10.09
	2	-1.56	-39.19	-10.18
	4	-1.60	-39.23	-10.33
	8	-1.58	-39.20	-10.30
	16	-1.57	-38.69	-10.27
DD40 (Fill)	1	-2.23	-56.81	-8.87
	2	-2.26	-54.55	-11.63
	4	-2.40	-58.81	-11.87
	8	-2.40	-59.10	-11.99
	16	-2.41	-59.52	-12.05
LM40 (Excavation)	1	-1.93	-36.43	-13.56
	2	-1.89	-35.68	-13.51
	4	-1.87	-35.26	-13.58
	8	-1.86	-35.00	-13.58
	16	-1.86	-34.99	-13.58
LM40 (Fill)	1	-2.11	-45.04	-9.00
	2	-2.43	-54.02	-11.74
	4	-2.42	-54.25	-11.84
	8	-2.41	-53.71	-11.94
	16	-2.41	-54.03	-11.90

These figures show that the changes in the maximum deflections, maximum moments and the anchor forces are stabilized after 4 substeps and there is almost no change in the results. Therefore, the number of substeps was set as 4 for the analysis of all cases.

The Anchor Stiffnesses

The anchor stiffnesses were chosen based on two criteria:

1. Realistic anchor rod length, L , and cross sectional area, A , were chosen and the anchor stiffnesses (per unit length of the wall) were calculated as:

$$K_{anc} = \frac{AE}{L} \quad (12)$$

where E is the Young's Modulus for steel. The anchor length is determined by the location of the anchor. This location is set by standard procedures which require the anchor block to remain inside the safe zone defined by active and passive regions (Craig, 1989), see Figure 3.10.

The cross sectional area, A , of the anchor rod was determined from the anchor force per unit length of wall, A_p , calculated by free earth support analysis. Thus,

$$A = \frac{A_p}{\sigma_{all}} \quad (13)$$

in which σ_{all} is the allowable tensile stress for the anchor rod.

2. An "expected anchor yield" of $\delta = 0.001H$ (Rowe, 1953, 1955) was considered.

This, combined with A_p from free earth support analysis gives the anchor stiffness as;

$$K_{anch} = \frac{A_p}{\delta} \quad (14)$$

A sample calculation of anchor stiffness for LL40 case using these two criteria is given in Figure 3.11. The anchor force, obtained by conventional method, was used in the calculations. The free wall height, depth of penetration, and internal friction angle were

taken from Tables 3.2 and 3.4. The Young's modulus for the tie rod was taken as 29×10^6 psi. The anchor stiffness found from the two procedures usually agreed closely.

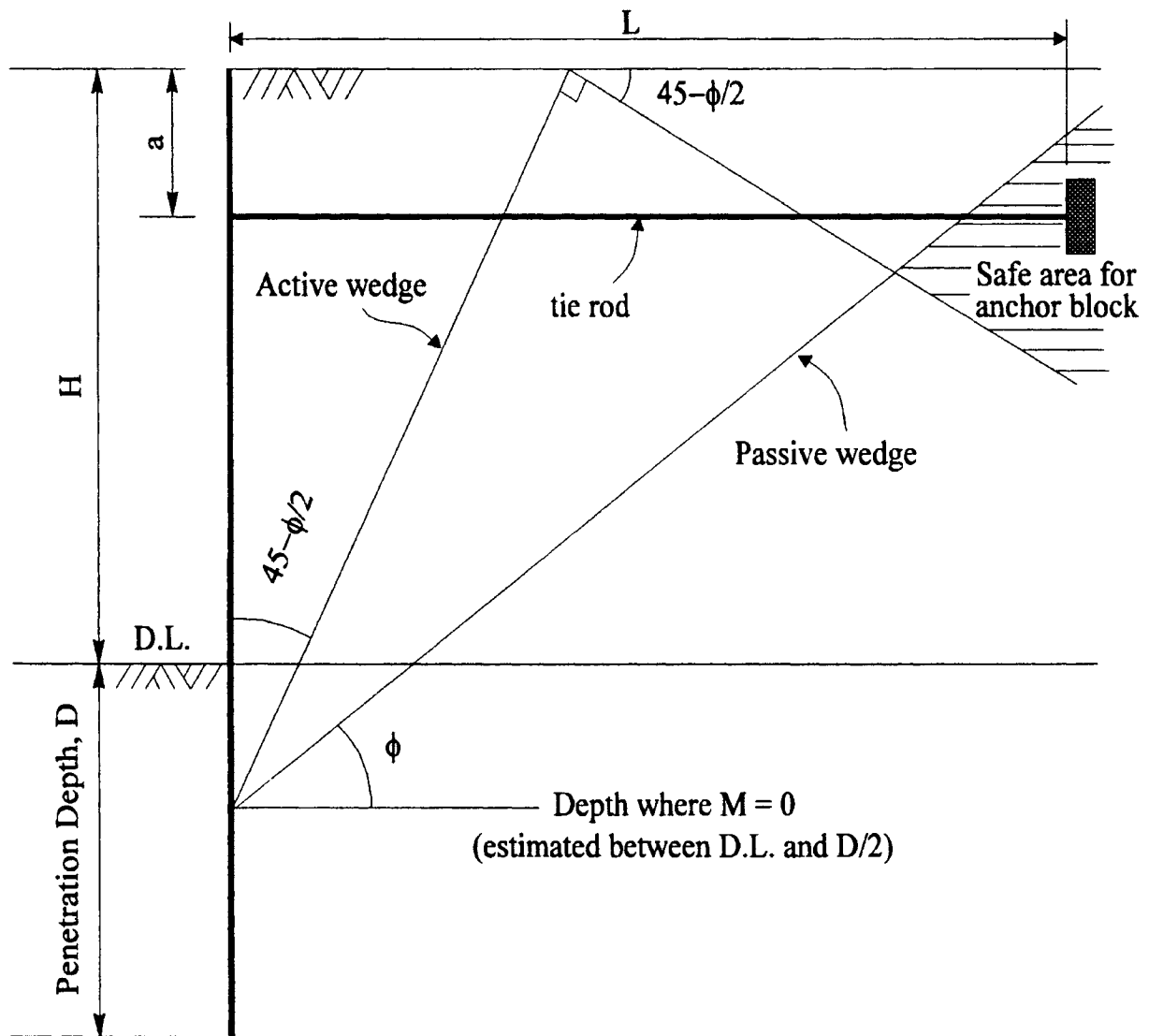
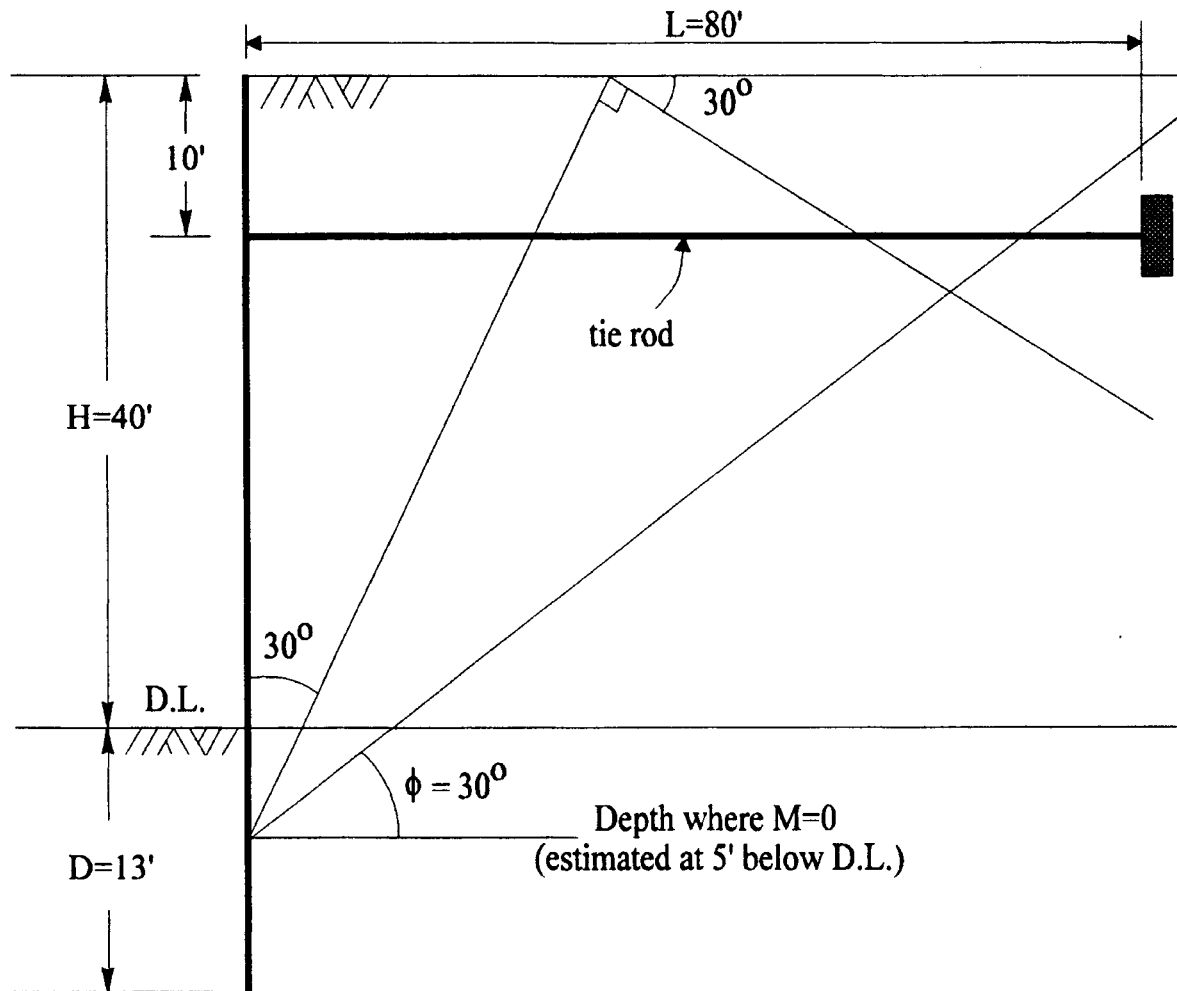


Figure 3.10. Determination of a Safe Location For the Anchor Block



(a) $A_p = 10,693 \text{ lb/ft}$ (FES result)

$$A = \frac{A_p}{\sigma_{all}} = 0.535 \text{ in}^2 / \text{ft} \quad (\sigma_{all} = 20 \text{ ksi})$$

$$K_{anch} = \frac{AE}{L} = \frac{(0.535 \times 29 \times 10^6 \text{ psi})}{80'} = 194 \text{ k / ft}$$

(b) Anchor yield $\delta/H=0.001$; $\delta=0.053'$

$$K_{anch} = \frac{A_p}{\delta} = 202 \text{ k / ft}$$

Figure 3.11. Determination of the Anchor Stiffness For LL Case

CHAPTER IV

RESULTS OF ANALYSES AND COMPARISONS

General

The results obtained from the finite element analyses of the twelve cases, both excavation and backfilling, are given in this chapter. Soil behavior, such as deformation and stresses in the soil (vertical, horizontal and shear stresses) as well as the stress paths, and the degree of mobilization are plotted and the results are compared for the two construction methods. In addition, the deformation and bending moments in the wall and anchor forces are compared for excavation and backfilling methods.

Behavior of the Soil

The cases analyzed are post-processed which produced the plots of the deformed shape of the system, displacement vectors, horizontal, vertical and shear stress and the degree of mobilization contours for both excavation and backfilling methods. As an example, the plots of the DD40 case are shown in this section.

Soil Deformations

Figures 4.1 and 4.2 show the deformed shape of the DD40 case for excavation and

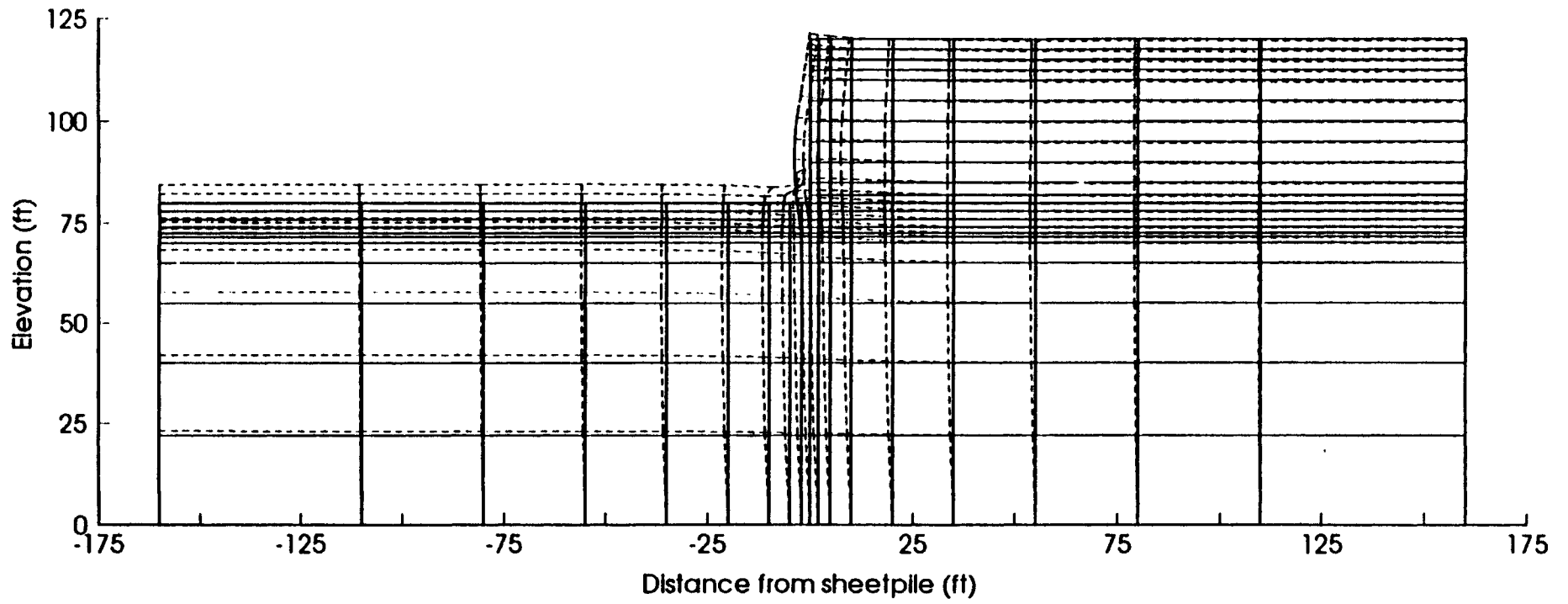


Figure 4.1. DD40 Case - Excavation: Deformed Shape (*30)

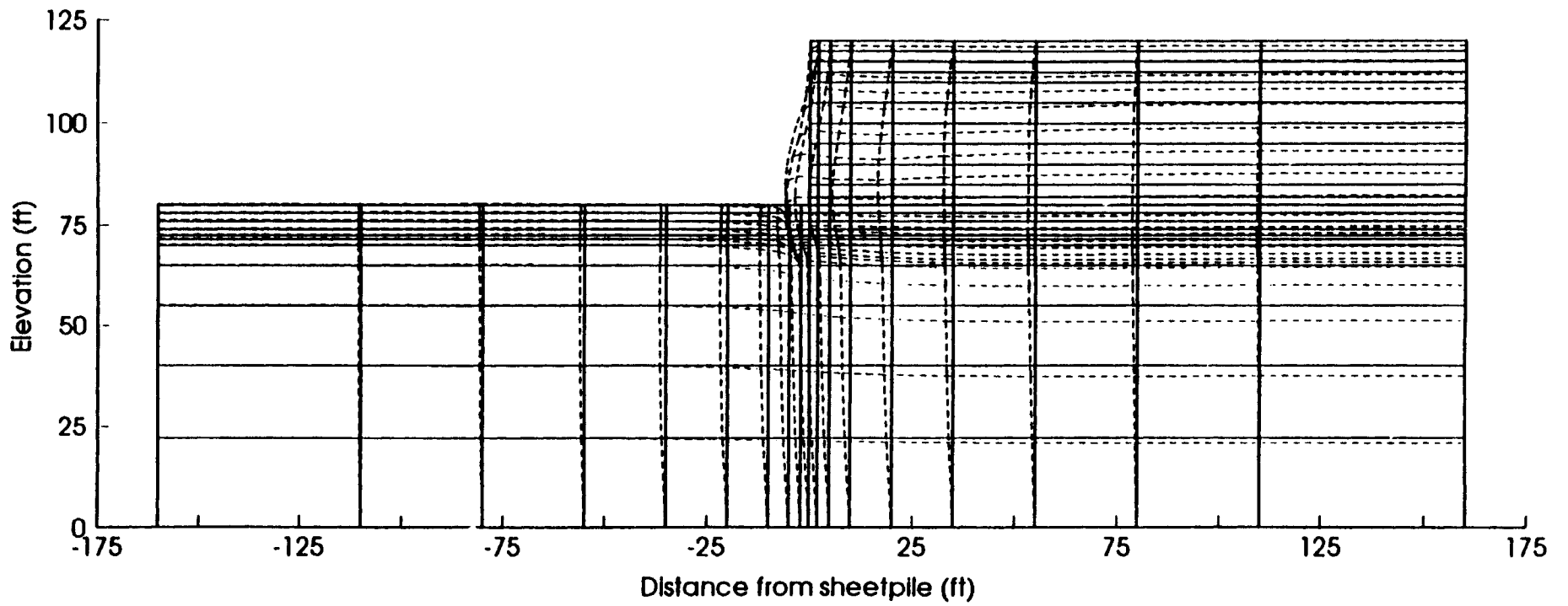


Figure 4.2. DD40 Case - Backfill: Deformed Shape (*30)

backfill respectively. Deformed shapes for LM40 case are given in Appendix B in Figures B.1 and B.2. The deformed shapes were obtained by adding the nodal displacements of finite element mesh to the coordinates of the nodes. In order to see the deformations clearly in the figures, nodal displacements were exaggerated by a factor. For example, the factor is 30 for the DD40 case. Due to this exaggeration factor, the plotted node locations after deformation are not true and this may create the illusion that some parts of the grid intrude on other parts.

The first observation made in these figures is that there is an overall rotational deformation in the soil. In all cases, the soil in front of the wall moved upwards while the soil on the back side of the wall settled, resulting in the overall rotational deformation. In the excavation case, the heave in the front soil was more dominant; this heave was because of the reduced overburden pressure. In the backfill case, the settlement of the soil behind the wall was more dominant part of the soil deformation. This settlement was due to the weight of the fill. The soil behind the wall moved downward in excavation cases and the soil in front of the wall moved upward in backfill cases.

The horizontal deflection of the soil was maximum in the wall axis and it decreased with the distance from the wall. This was expected, and is consistent with the conventional assumptions.

In all cases the sheet pile wall moved upward in excavation cases and downward in backfill cases. This was due to the friction between the wall and the soil; as the soil settled or heaved, the wall friction tried to move the wall with the soil.

Soil deflections in DS30 and LS30 cases were much larger than the other cases.

This was because of the soft foundation clay. For the DM40 and LM40 cases, soil deformations were smaller than average because of the stiffness of the medium-stiff clay foundation.

The soil deformations were excessive in the cases where the foundation soil was soft or medium-stiff clay in drained condition. This was because of the low strength of the soil; large regions in the soil profile failed in these cases producing these large deformations.

Figures 4.3 and 4.4 show the displacement vectors for the DD40 case, excavation and backfill, respectively. The displacement vector plots for LM40 case are given in Appendix B (Figures B.3 and B.4). The arrows show the direction and magnitude of the nodal displacements. The magnitude of the deflections is magnified by a factor to make the plots clearer. In both excavation and fill cases there were an overall, rotational movements in the soil around the wall. The displacement vector plots indicate a more uniform soil deformation in the backfill cases.

Soil Stresses

In order to compare the soil stresses in excavated and backfilled walls, the vertical, horizontal and shear stress contours are plotted for all excavation and backfill cases.

Figures 4.5 and 4.6 show the horizontal stresses at the end of construction in the soil of DD40 case, for excavated and backfilled walls, respectively. The horizontal stress contours for LM40 case are given in Appendix B (Figures B.5 and B.6).

The horizontal stresses increased behind the wall at about the anchor level for both

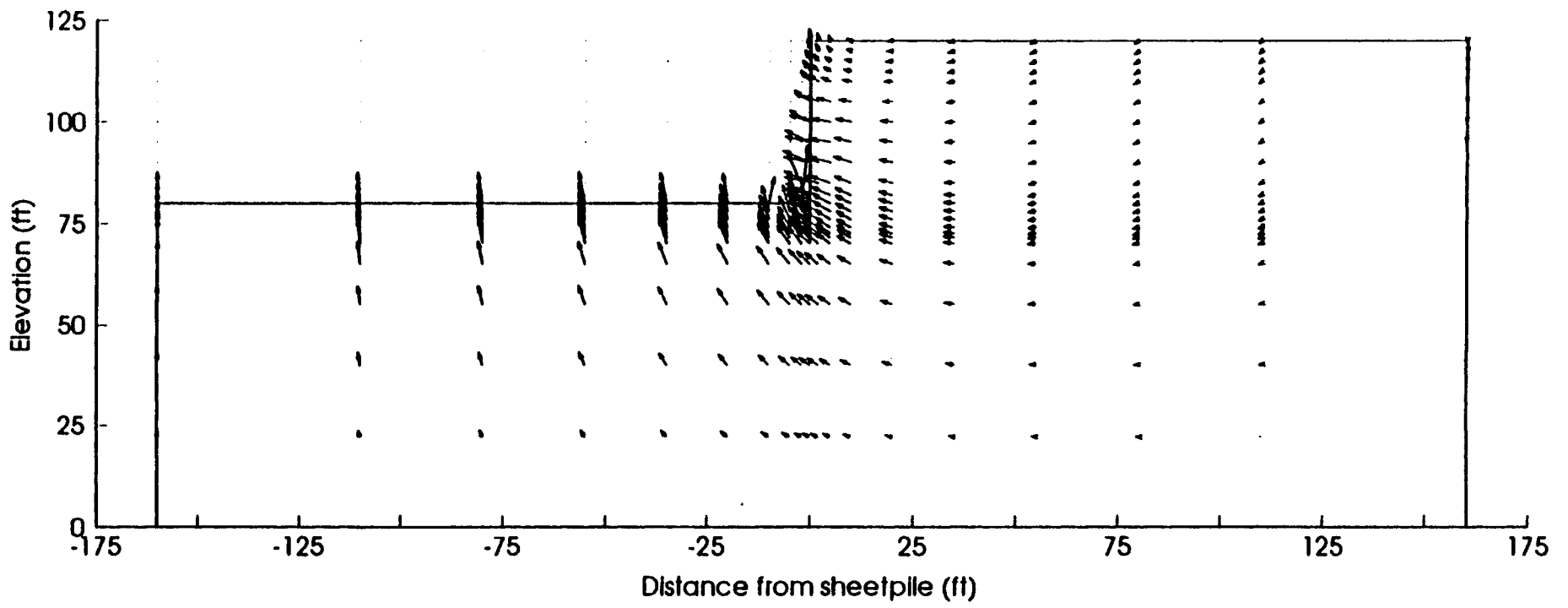


Figure 4.3. DD40 Case - Excavation: Displacement Vectors (*50)

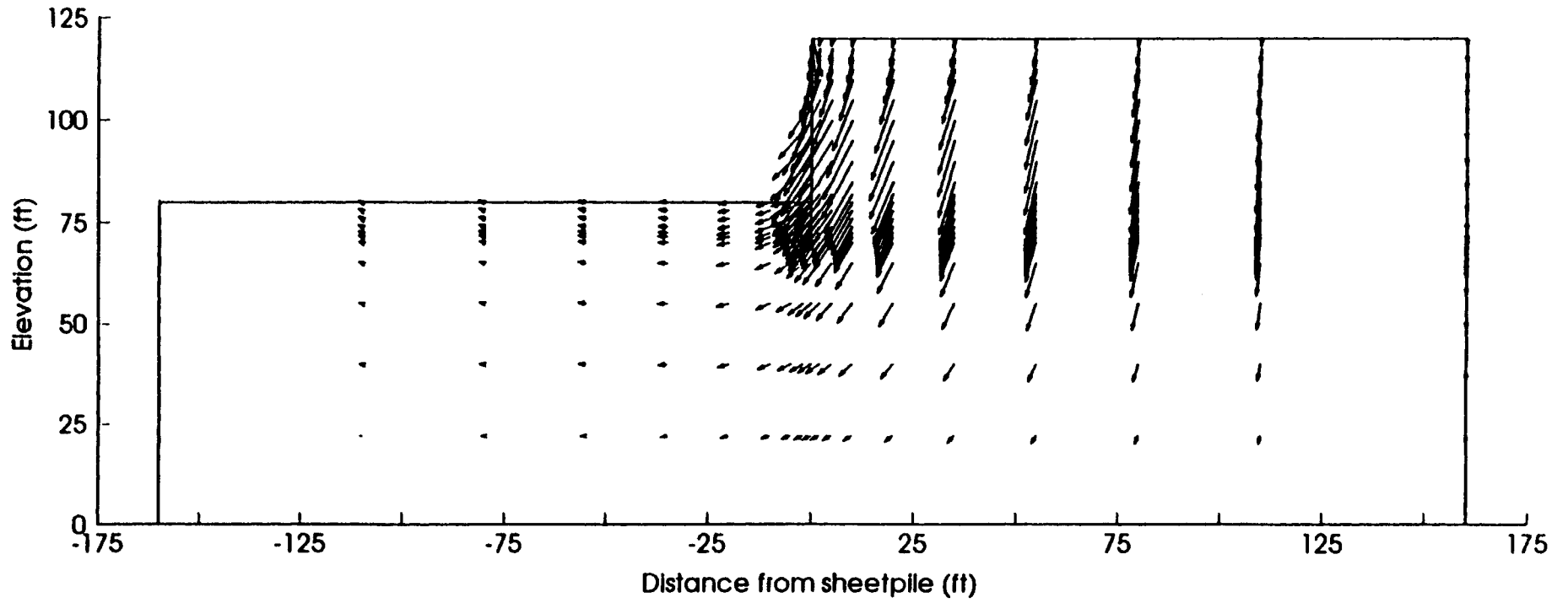


Figure 4.4. DD40 Case - Backfill: Displacement Vectors (*50)

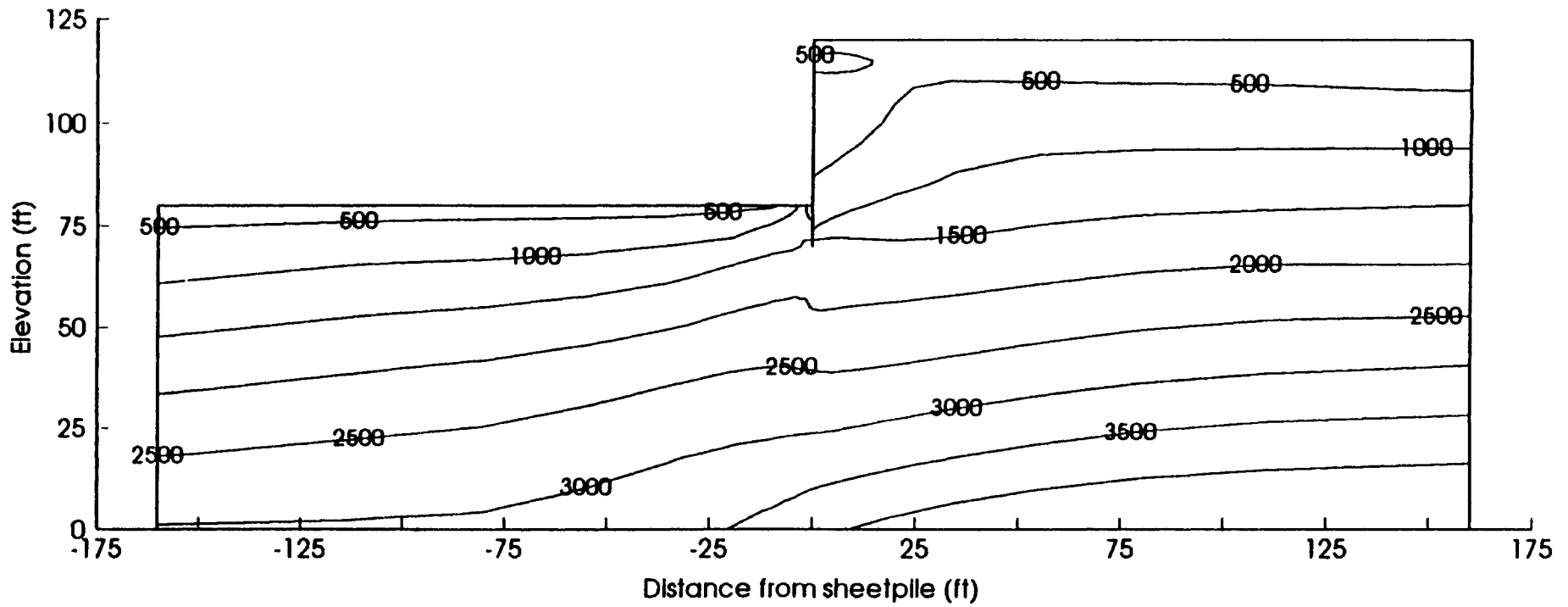


Figure 4.5. DD40 Case - Excavation: Horizontal Stress - σ , (psf)

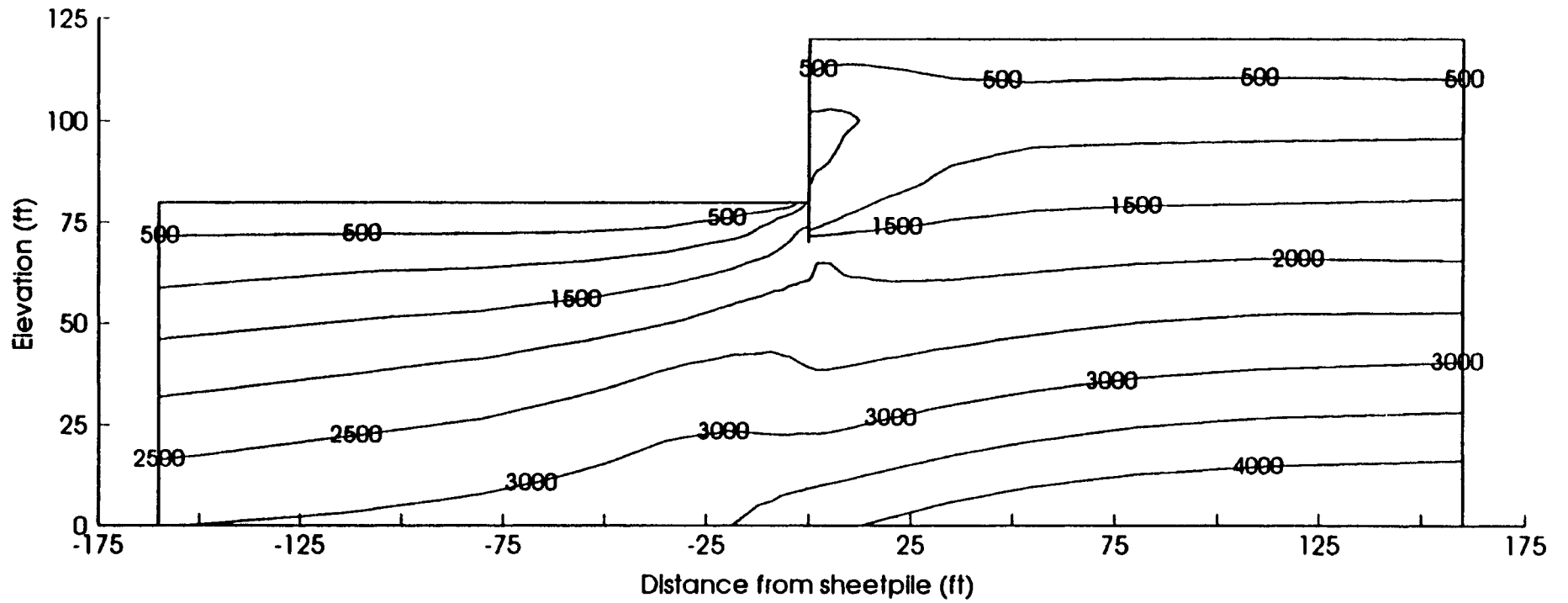


Figure 4.6. DD40 Case - Backfill: Horizontal Stress - σ , (psf)

construction types. Apparently the anchor prevented the displacement of the wall at that level which resulted in an increase in horizontal stress. The horizontal stresses decreased around the middle of the wall height due to the increased deflection of the wall at that level. The soil reached active stress levels in this area, as expected. This was true for both construction methods.

In both construction types, higher lateral stresses occurred in the front soil near the wall, due to the lateral wall movement in this area. This was consistent with the conventional passive pressure assumption.

The horizontal stresses away from the wall were approximately the same for both excavation and backfill cases.

The calculated soil-wall contact stresses in front of the wall for DD40 and LM40 case, for both construction methods, are plotted in Figures 4.7(a) and 4.7(b) respectively. The stresses were smaller than the passive pressures at larger depths, and slightly higher than the passive pressures near the ground surface, for both cases. This was caused by soil-wall friction and/or adhesion that tends to increase the vertical stresses in the soil in this region. It is well known from conventional passive pressure studies that the wall friction increases the passive pressures considerably. It is found that this effect occurs at shallower elevations.

Figures 4.8 and 4.9 show the vertical stresses in the soil for DD40 case at the end of construction, for excavated and backfilled walls, respectively. The vertical stress contours for LM40 case are given in Appendix B (Figures B.7 and B.8).

The vertical stresses in the soil at large distances from the wall were not affected

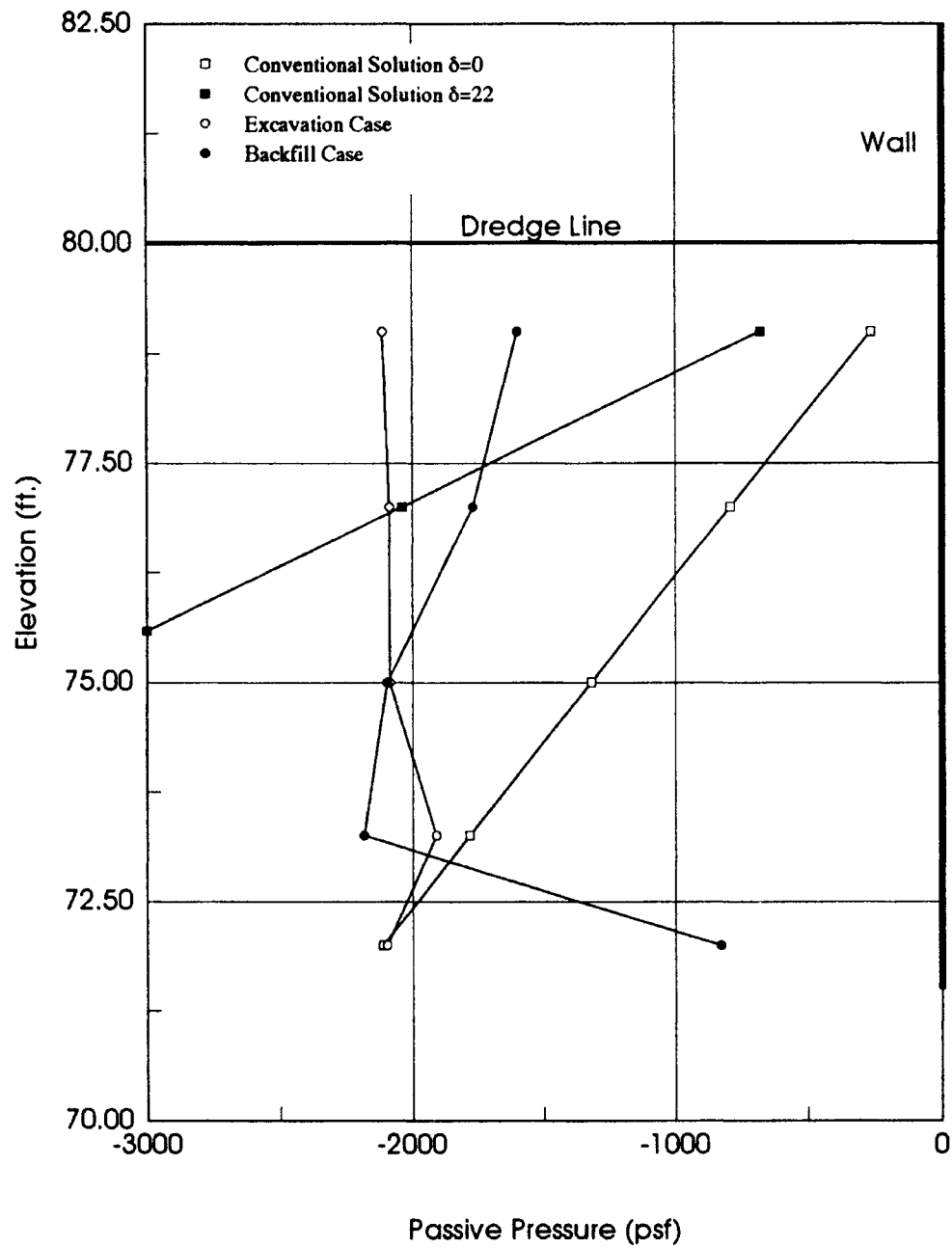


Figure 4.7(a). Passive Pressure in Front of the Wall
(DD40 Case)

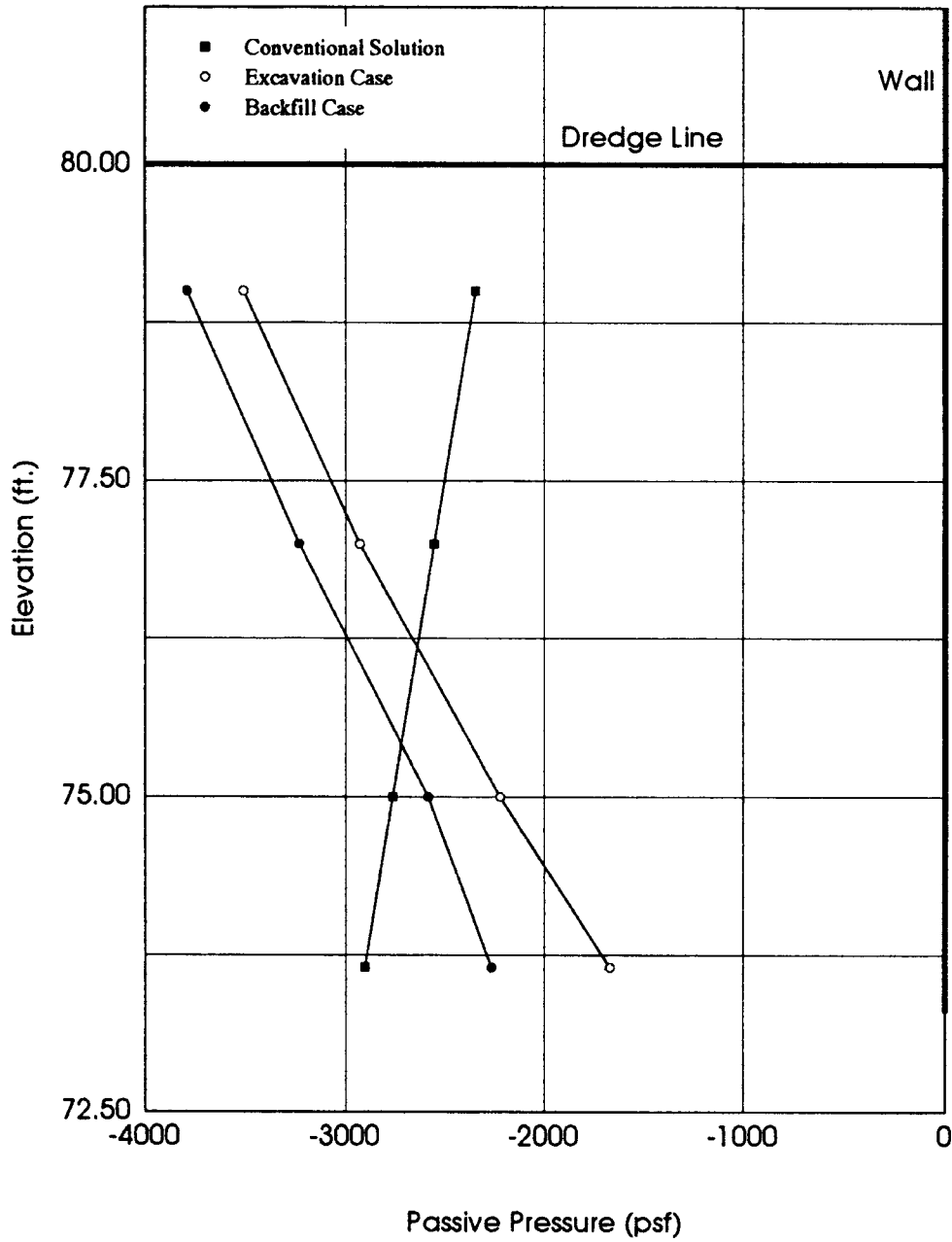


Figure 4.7(b). Passive Pressure in Front of the Wall
(LM40 Case)

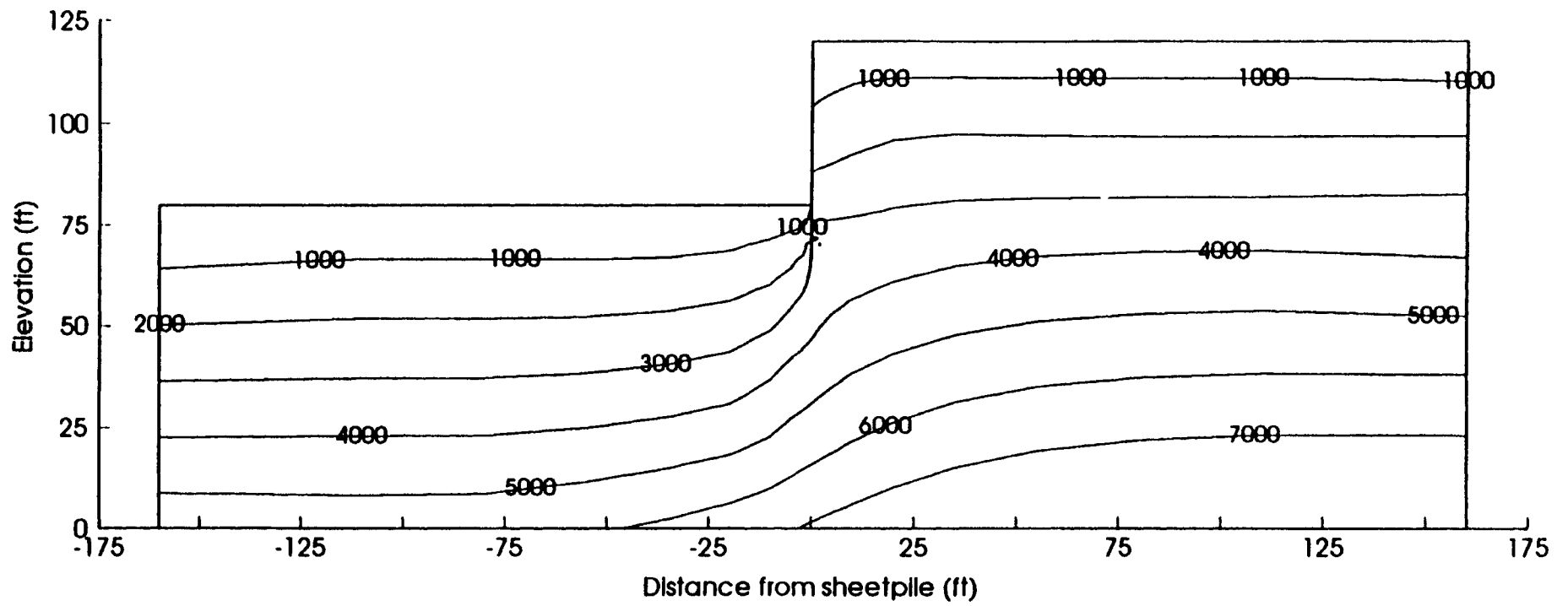


Figure 4.8. DD40 Case - Excavation: Vertical Stress - σ , (psf)

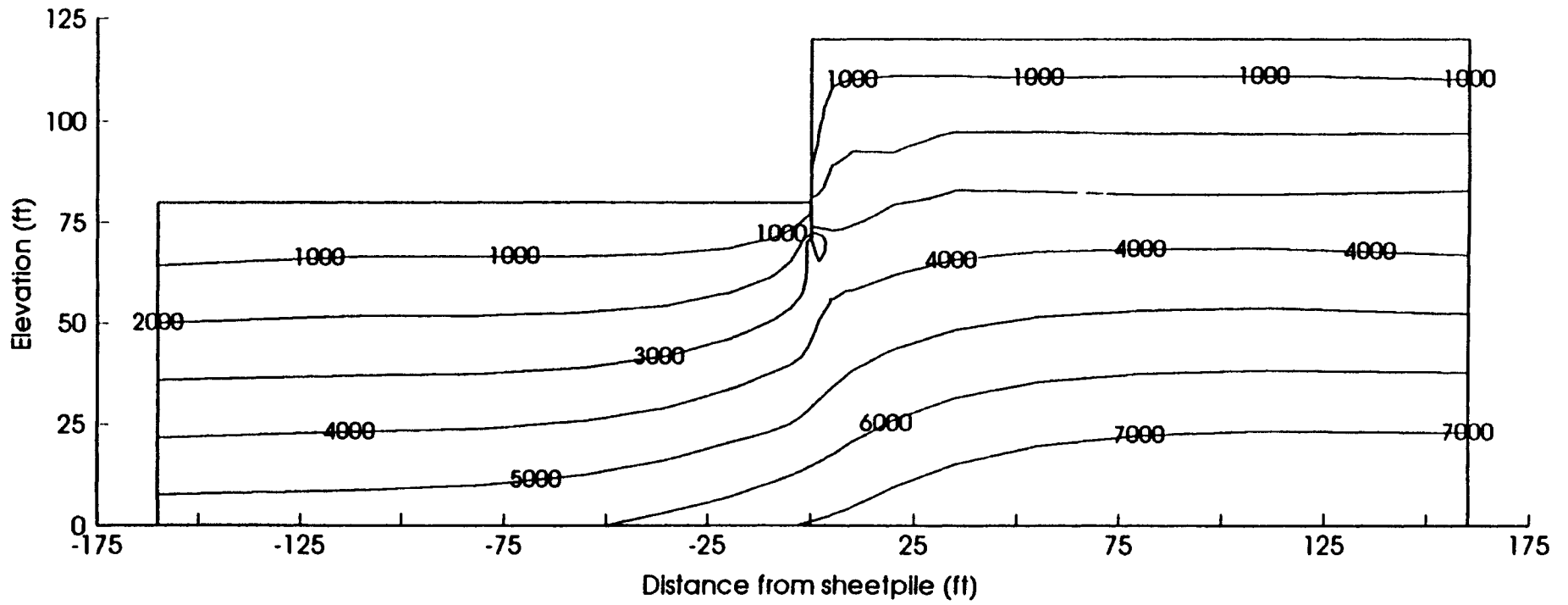


Figure 4.9. DD40 Case - Backfill: Vertical Stress - σ , (psf)

significantly by the construction method. The differences were localized around the wall, approximately within 10 feet in most cases.

The vertical stresses behind the wall above the dredge line in backfill cases were less than those in excavation cases. In a backfill case, the wall deflected laterally more than the corresponding excavation case. This decreased the friction between the wall and the soil and, therefore the vertical stress decreased more in backfill cases in the back side of the wall.

The vertical stresses in both construction types were higher near the wall in the front of the wall. This occurred due to the deflection of the wall. As the wall deflected, it pushed the soil downward which in turn caused the increase in the vertical stress in that region.

Figures 4.10 and 4.11 show the shear stresses at the end of construction in the soil of DD40 case for both excavated and backfilled walls respectively. The shear stress contours for LM40 case are given in Appendix B (Figures B.9 and B.10).

The shear stresses in both cases changed near the wall. In both cases, excavation and backfill they were nearly the same in the zones more than 10 feet from the wall.

The shear stresses increased around the tip of the wall and below the dredge line. This was because of the vertical deflection wall. The friction between the wall and soil caused the increase in the shear forces around the tip of the wall.

Degree of Mobilization

Figures 4.12 and 4.13 show the degree of mobilization contours of the DD40 case

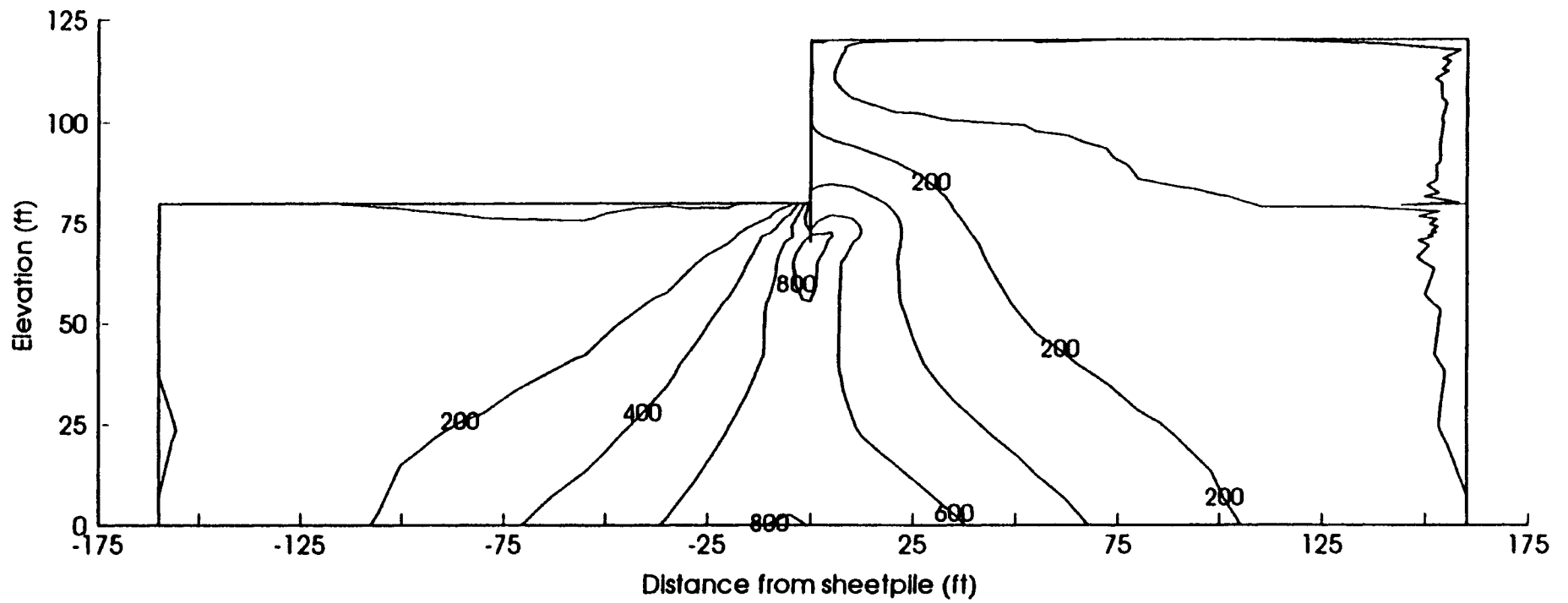


Figure 4.10. DD40 Case - Excavation: Shear Stress - τ_v (psf)

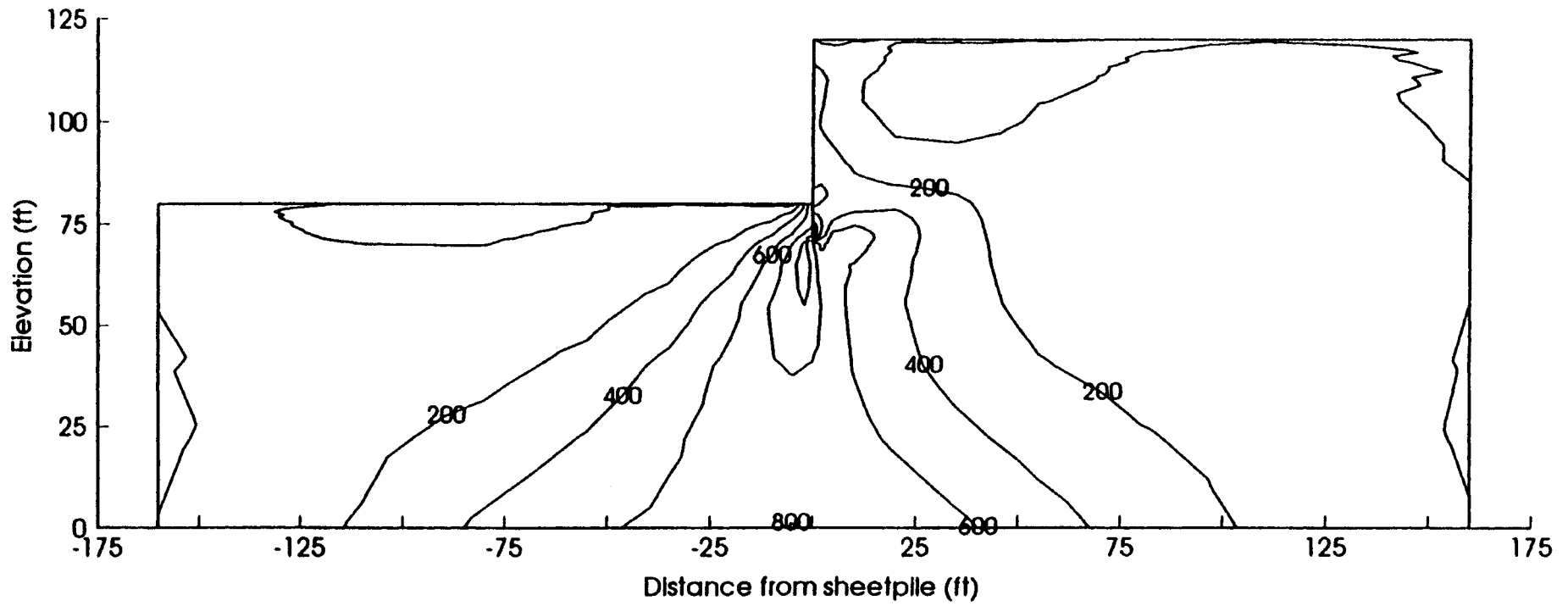


Figure 4.11. DD40 Case - Backfill: Shear Stress - τ_v (psf)

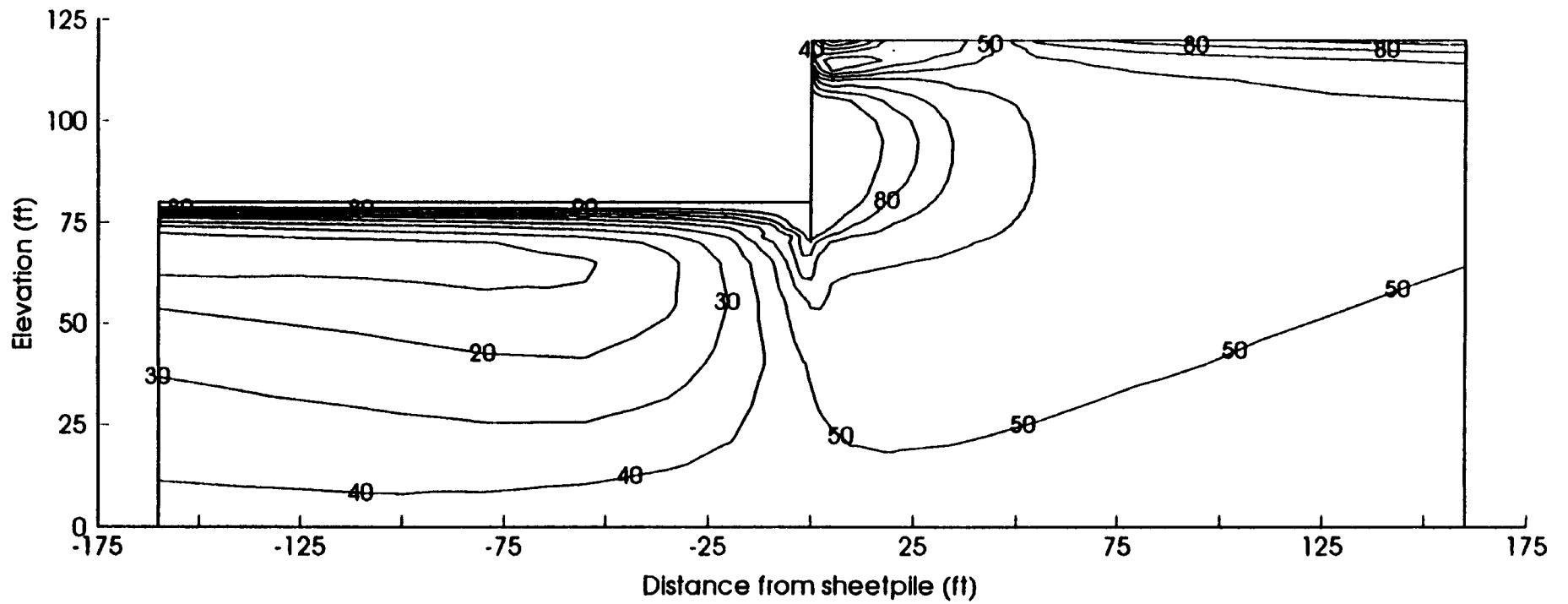


Figure 4.12. DD40 Case - Excavation: Degree of Mobilization - f (%)

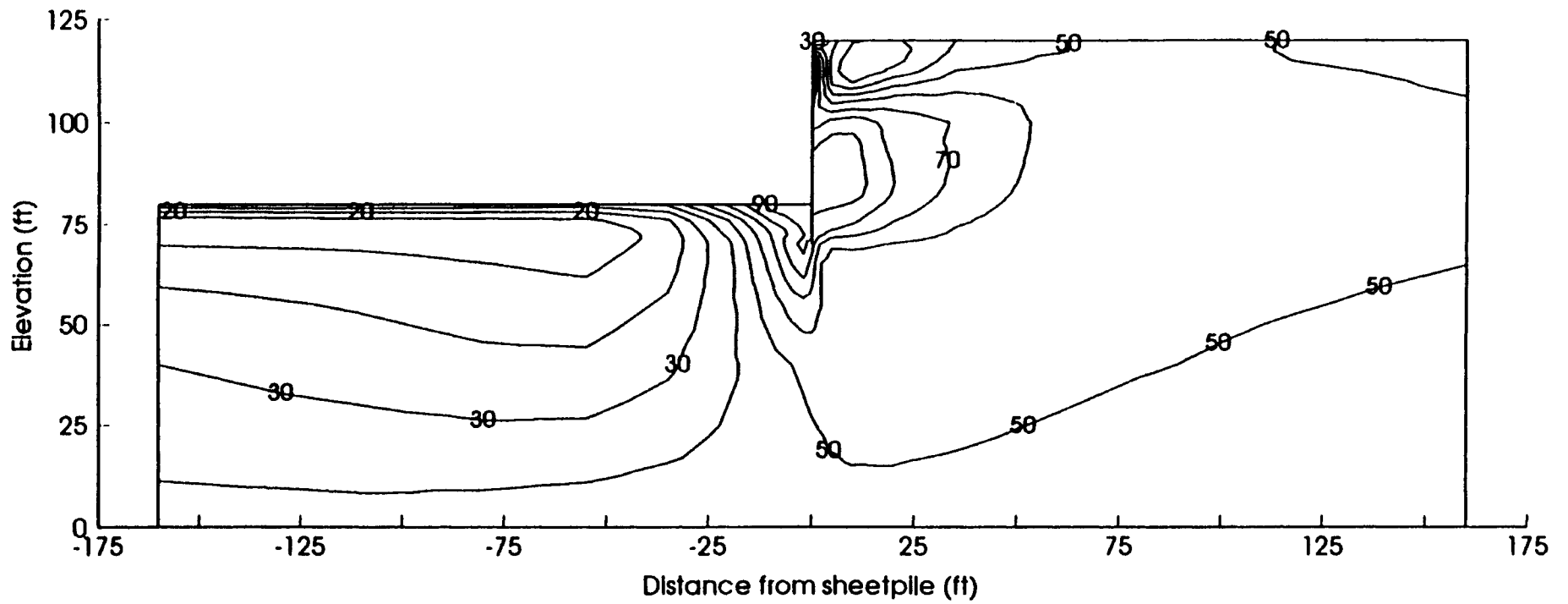


Figure 4.13. DD40 Case - Backfill: Degree of Mobilization - f (%)

for excavation and backfill respectively. Degree of mobilization, f , contours for LM40 case are given in Appendix B in Figures B.11 and B.12.

The degree of mobilization contours show that there was a local failure that occurred around the sheet pile wall in each case. In the areas away from the wall, the same contours were obtained.

In excavation cases, the upper soil layers failed in front of the wall if the foundation soil was sand or drained clay. This was because of an imperfection in the simulation of unloading in the finite element.

Comparison of the degree of mobilization contours shows that smaller regions failed in backfill cases as opposed to the larger failed areas in excavation cases, i.e. the soil remains at a safer stress level in the backfill cases.

In the profiles containing drained clay as the foundation soil, the soil mass above the dredge line failed over wide areas, within the last few analysis steps. This occurred in both excavation and backfill cases (Figures B.13 through B.18). It is known that the FEM is not accurate after large areas of soil fail. So the FEM results for these cases may not be as accurate in the last few analysis steps. Therefore, the last two steps were discarded - which was equivalent to assuming that the free wall heights were approximately 8% smaller in these cases. When this was done more reasonable f contours were obtained; both the distribution and the values of f agree with the other cases. This means that in walls designed by conventional methods, the engineer has to be more concerned if the foundation soil is clay because one should expect large areas of failure in long term, drained condition.

Failure zones in front of the wall were passive type failures (i.e. the horizontal stress was larger than the vertical stress) whereas the failure zones behind the wall were consistent with active earth pressure theory. These results were expected from conventional analyses of the sheet pile wall problems.

Stress Paths

To examine the behavior of the soil in the critical regions around the sheet pile wall, stress paths were used. A stress path describes the changes in the state of stress by plotting the top points of the conventional Mohr's circles. A plot of p versus q was used to draw the stress paths, where

$$p = \frac{\sigma_1 + \sigma_3}{2} \quad (15)$$

and

$$q = \frac{\sigma_1 - \sigma_3}{2} \quad (16)$$

where σ_1 and σ_3 are principal stresses.

In discussing the stress paths in this section two cases, DD40 and LM40, were used as typical cases. Stress paths for soil elements at different locations around the wall were plotted for both excavation and backfill cases for comparison. In each of these figures there are two stress paths: one is for the excavated wall case, and the other is for the backfilled wall case.

The stress path in Figure 4.14 is for a location identified as 'point 1' in the following. The soil element at point 1 was at a passive failure condition, i.e., the horizontal stress was larger than the vertical stress and the Mohr circle representing the stresses at

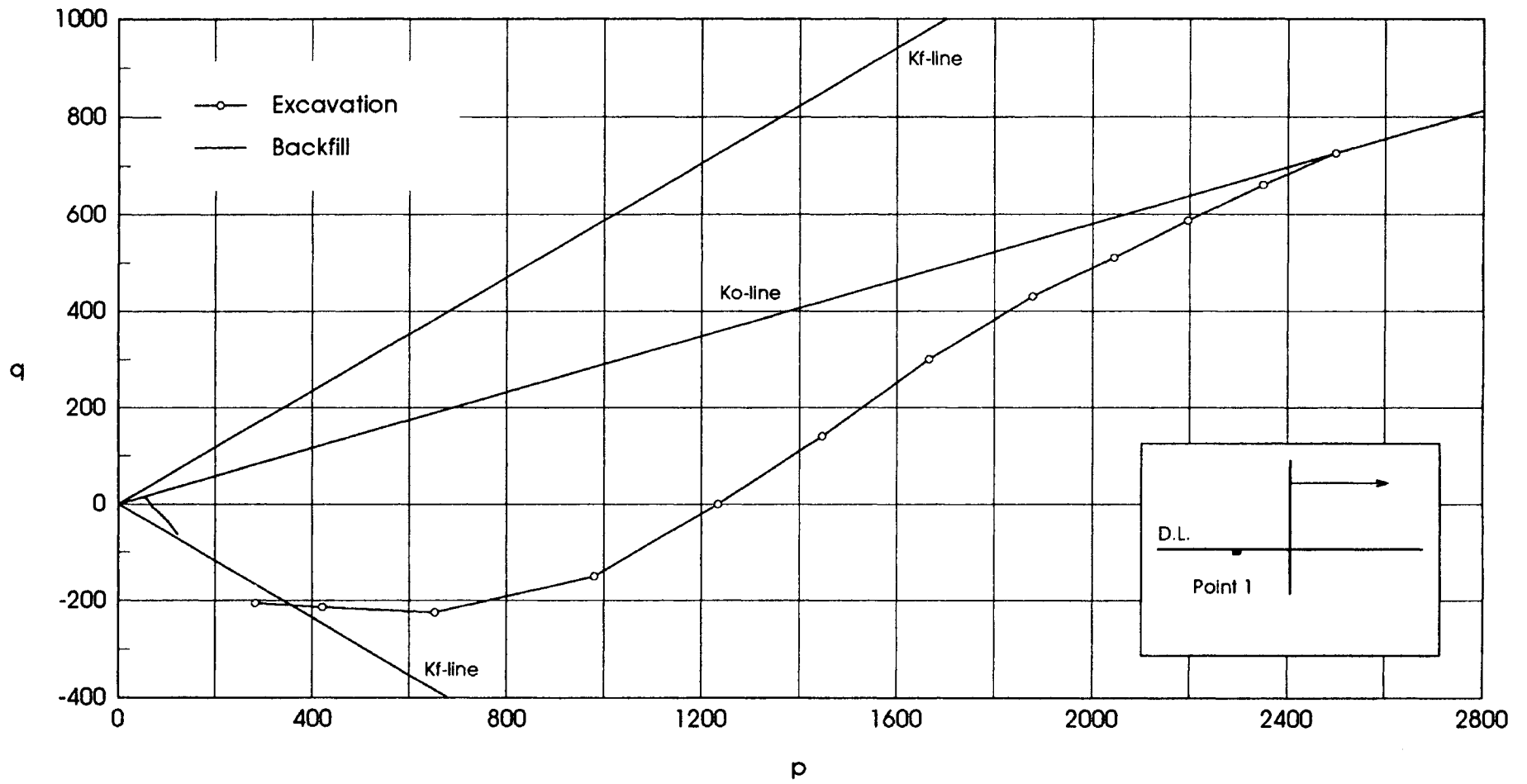


Figure 4.14. Stress Paths For Point 1 - DD40 Case

this point was tangent to the failure envelope. This result was consistent with conventional theories. Stress path for the excavation case shows that both horizontal and vertical stresses decreased, but the rate of decrease in the vertical stresses was greater. Therefore a passive failure occurred at point 1 at the end of excavation. In the backfill case, the horizontal stresses increased while the vertical stresses decreased. The failure was still of passive type.

Figure 4.15 shows the stress paths for point '2.' There was an active zone at this point in both cases, as expected. Failure was reached in the excavation case while the backfill case was still safe, though very close to failure. In the excavated wall, both vertical and horizontal stresses decreased. The rate of decrease in the horizontal stress was more than that in the vertical stress. In the backfilled case, both horizontal and vertical stresses increased. Vertical stresses increased adjacent to the wall due to the friction between the wall and the soil.

Point '3' in Figure 4.16 was also in an active zone in both cases. There was an active failure in the excavation case while the backfill case was still safe. In the excavated wall, the vertical stresses increased while the horizontal stresses decreased. The rate of change in horizontal stresses was greater than the vertical stresses. In the backfill case, both horizontal and vertical stresses increased. The change in horizontal stress was much higher.

For LM40 case the stress paths for the points A, B, C, and D are plotted in Figures 4.17 through 4.20. These points were near the dredge line and progressively farther away from the wall. The locations of these points were selected in order to see the

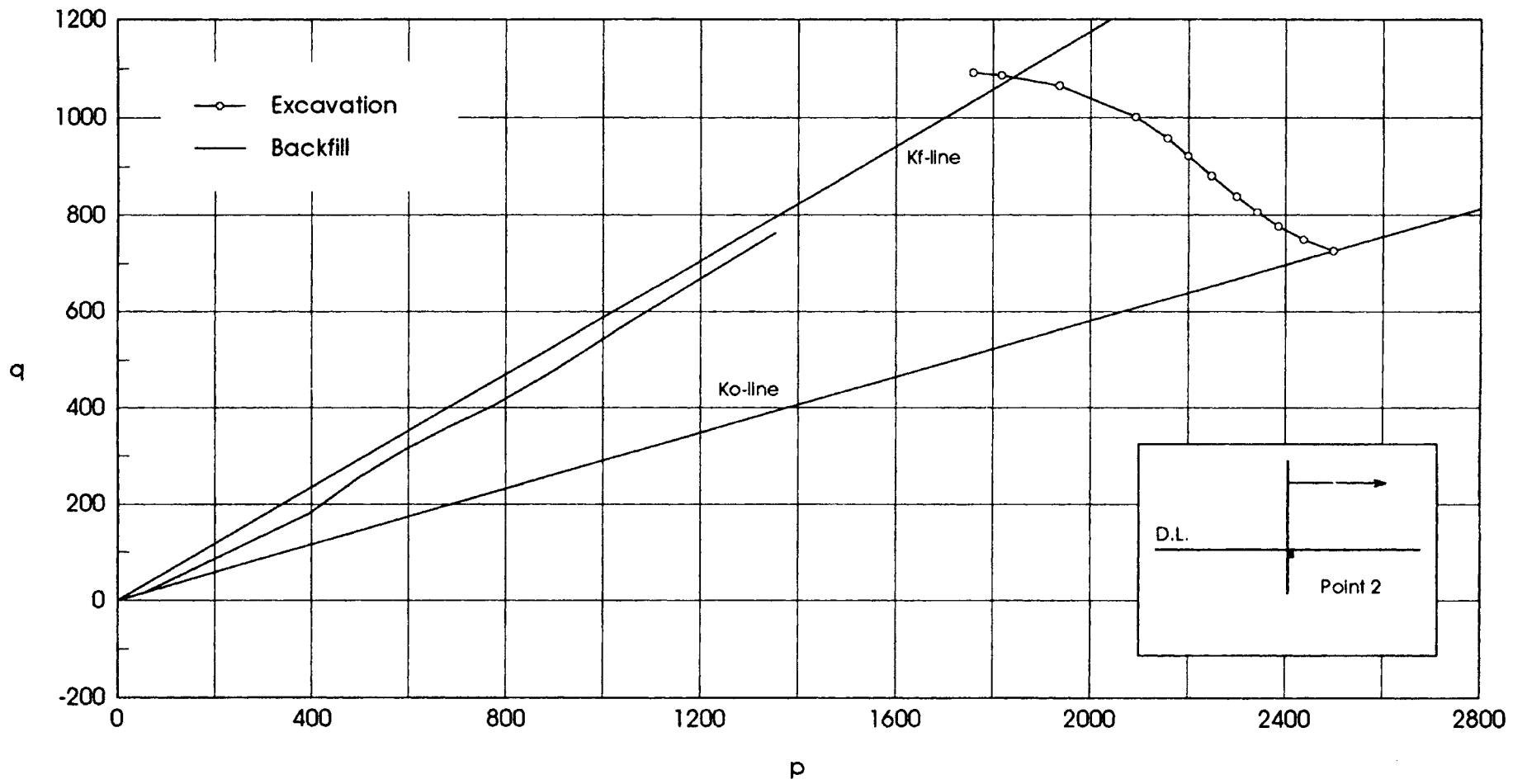


Figure 4.15. Stress Paths For Point 2 - DD40 Case

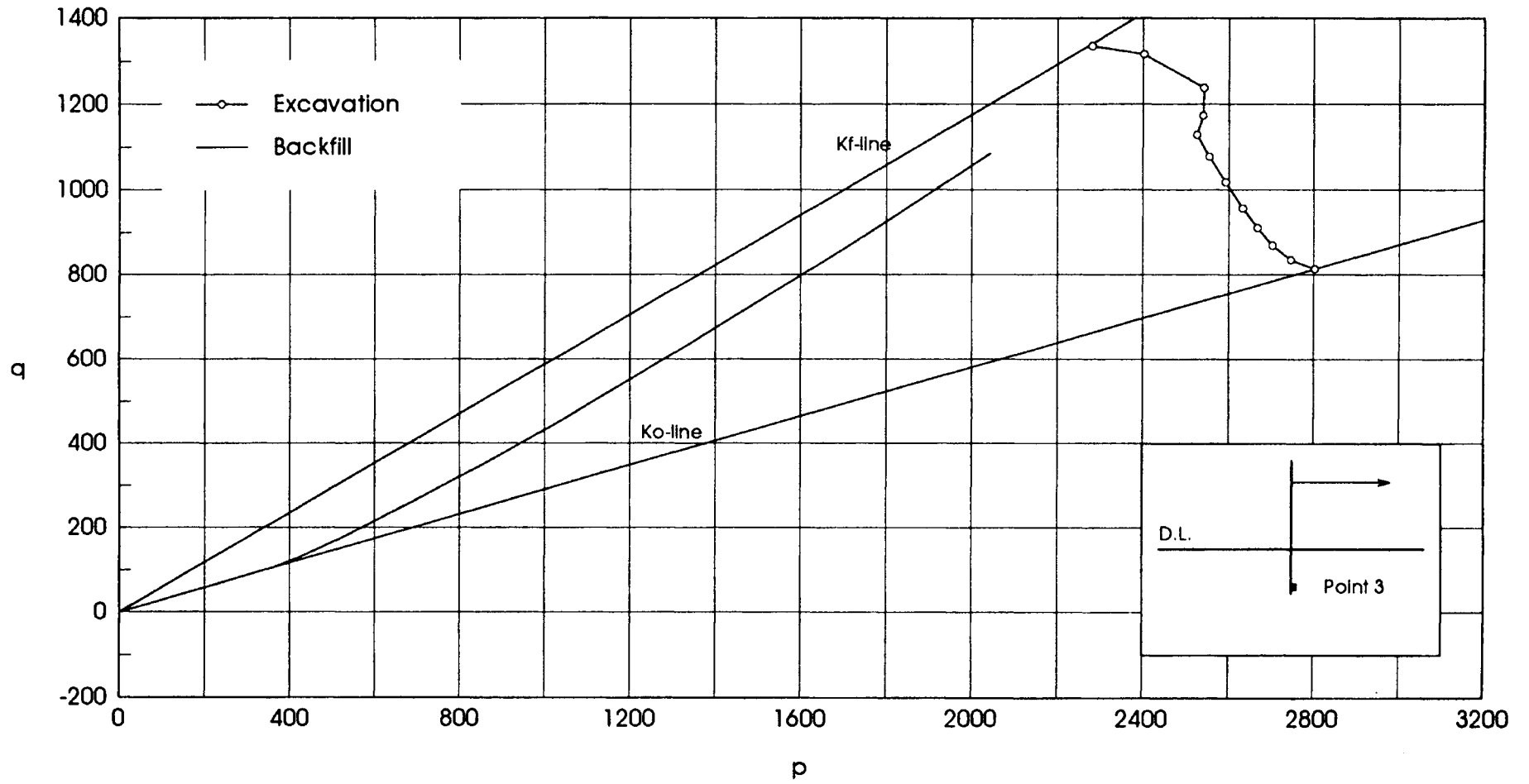


Figure 4.16. Stress Paths For Point 3 - DD40 Case

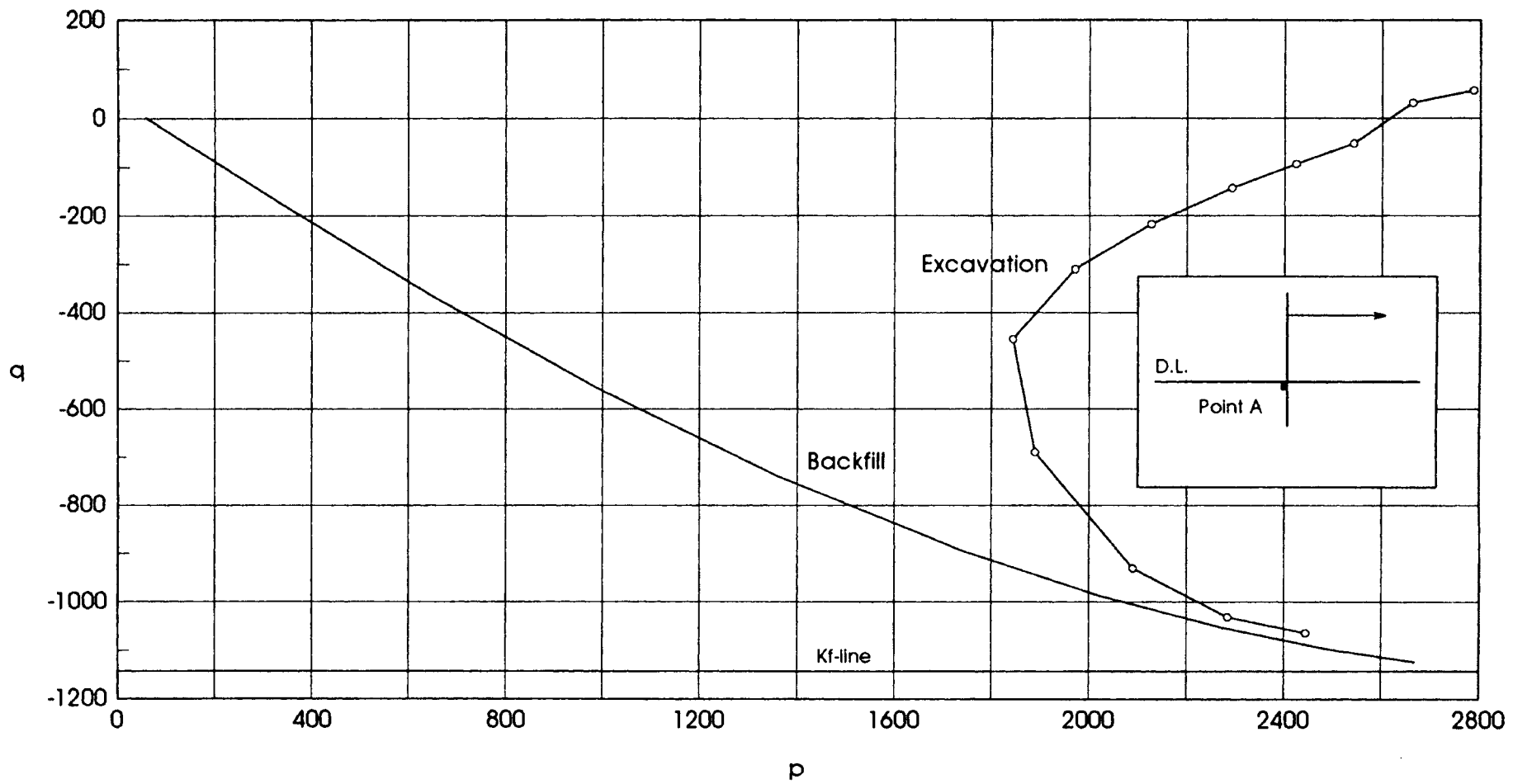


Figure 4.17. Stress Paths For Point A - LM40 Case

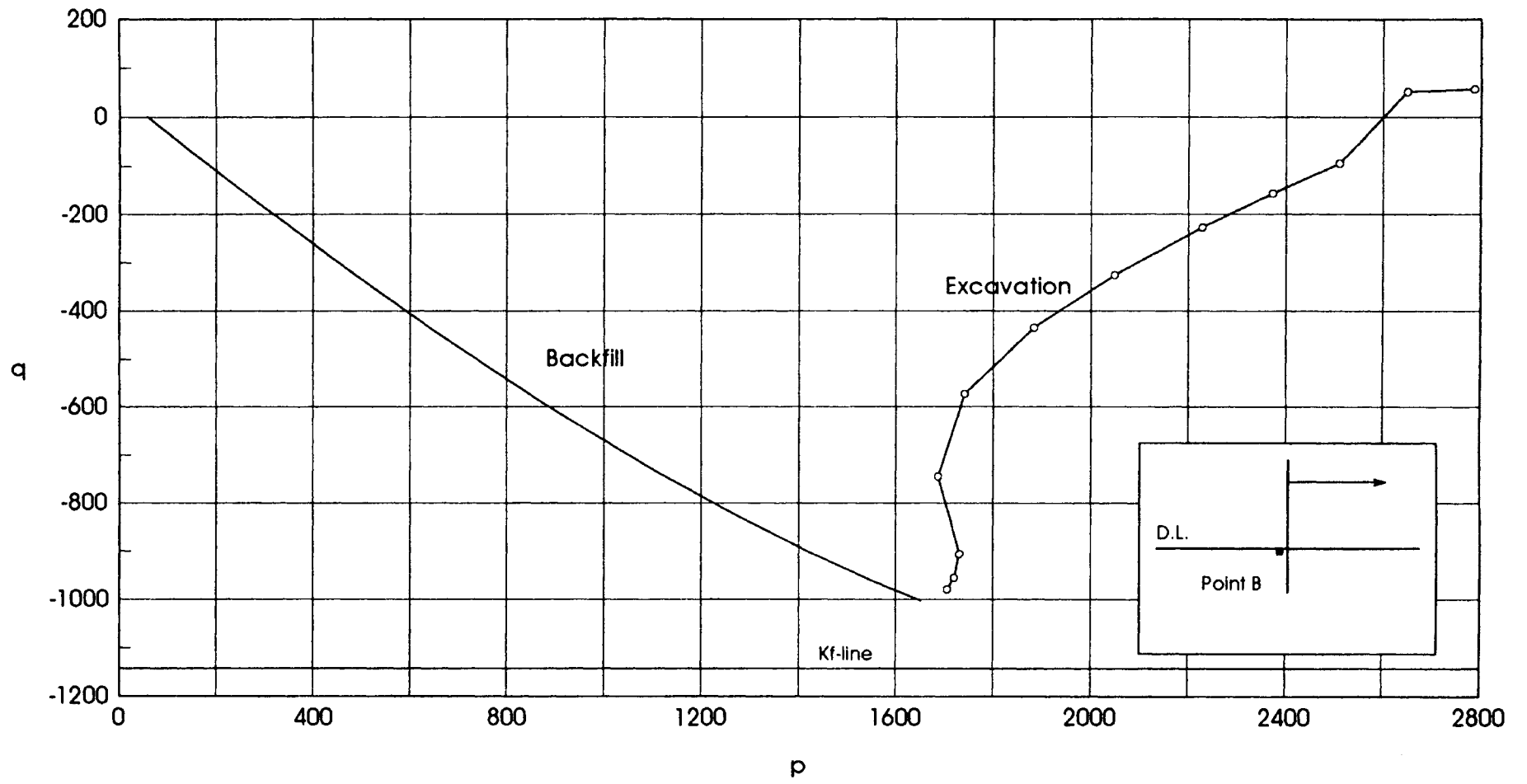


Figure 4.18. Stress Paths For Point B - LM40 Case

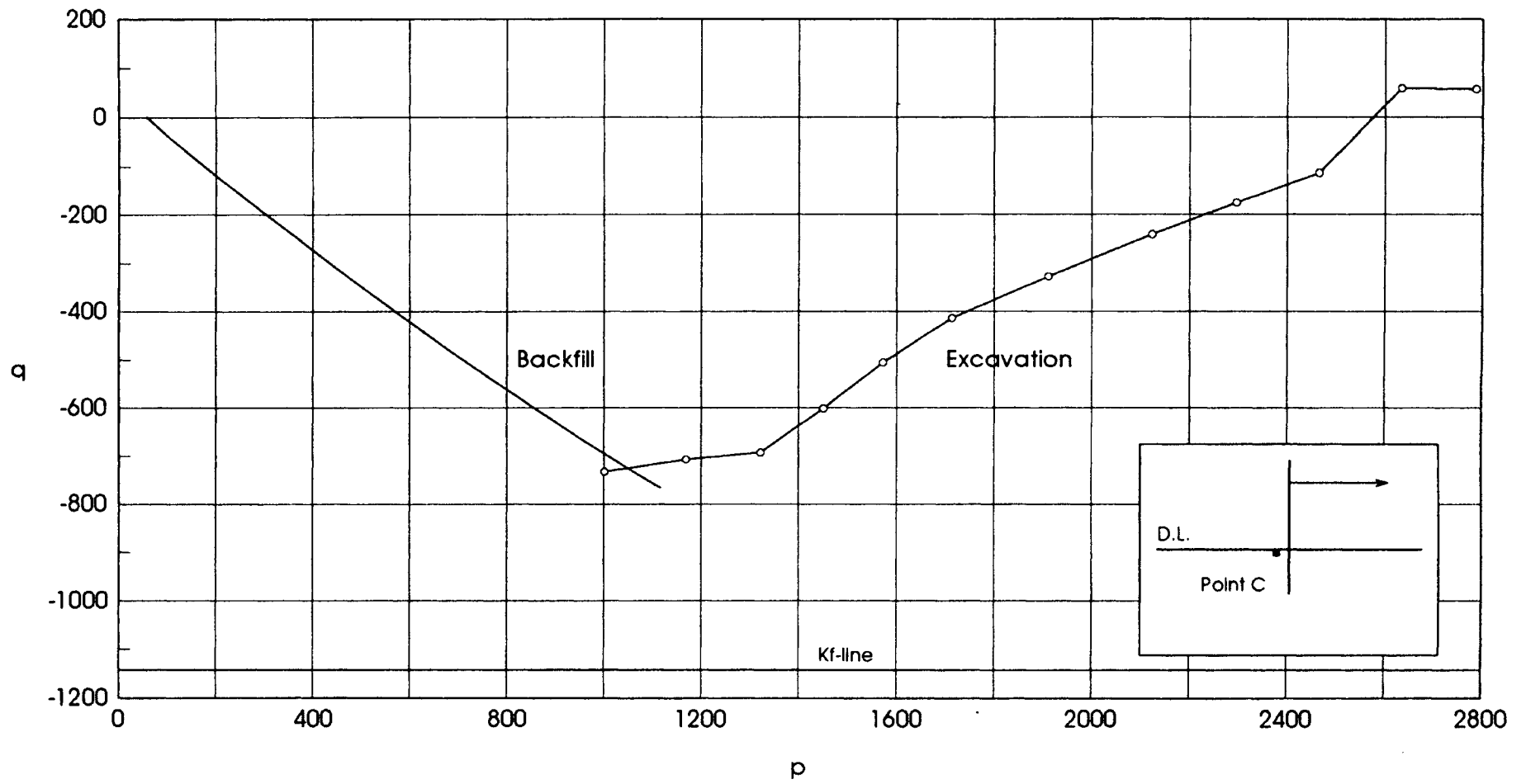


Figure 4.19. Stress Paths For Point C - LM40 Case

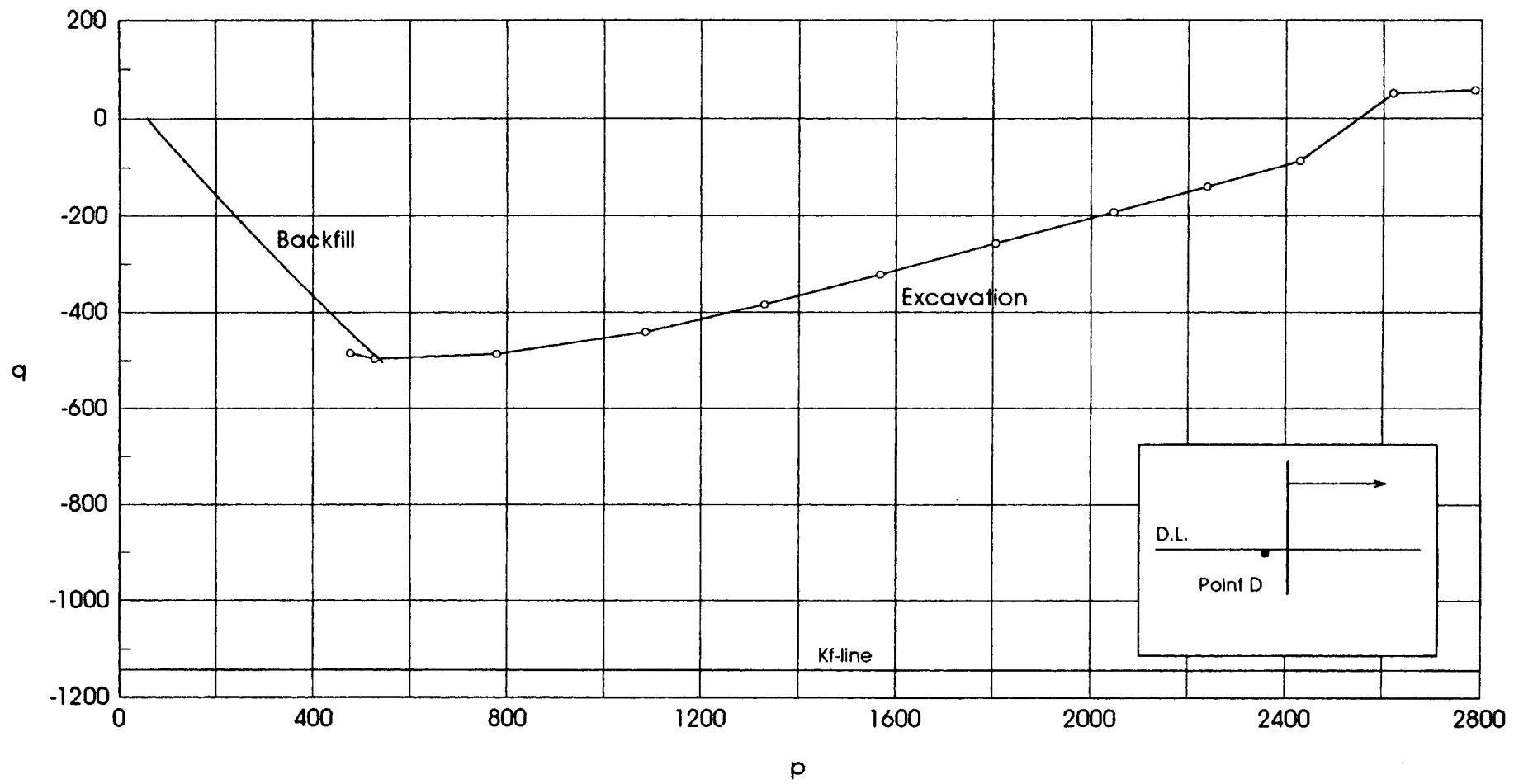


Figure 4.20. Stress Paths For Point D - LM40 Case

effect of the proximity of the wall on the soil stresses. In point A the soil failed because horizontal stresses increased due to wall deflection. At the beginning of excavation both horizontal and vertical stresses decreased. But at later stages, the deflected wall caused an increase in both stresses. While the distance of the element to the wall increased, the effect of the wall on the soil decreased and the soil did not fail. This shows that the passive-like stresses around the wall were indeed highly localized.

Behavior of the Structure

The behavior of the wall was discussed in this section in terms of the deflections and the bending moments in the wall, and the anchor forces. These were extracted from the analysis results of all cases for comparison of the excavation and backfill cases.

Wall Deflections

The deflections of the sheet pile wall throughout the construction steps are shown in Figures 4.21 through 4.26 for cases DD40, LM40 and DT40. Figures 4.21, 4.23 and 4.25 show the excavation results and Figures 4.22, 4.24 and 4.26 show the backfill results. The same scale was used in the plots of these results to facilitate comparison. The observations made in these figures are presented below.

DD40 Case

It may be observed that at the initial stages of the excavation the wall underwent a horizontal rigid body translation, while it underwent a rigid body rotation around the anchor point at the initial stages of the backfill case (Figures 4.21 and 4.22). At later

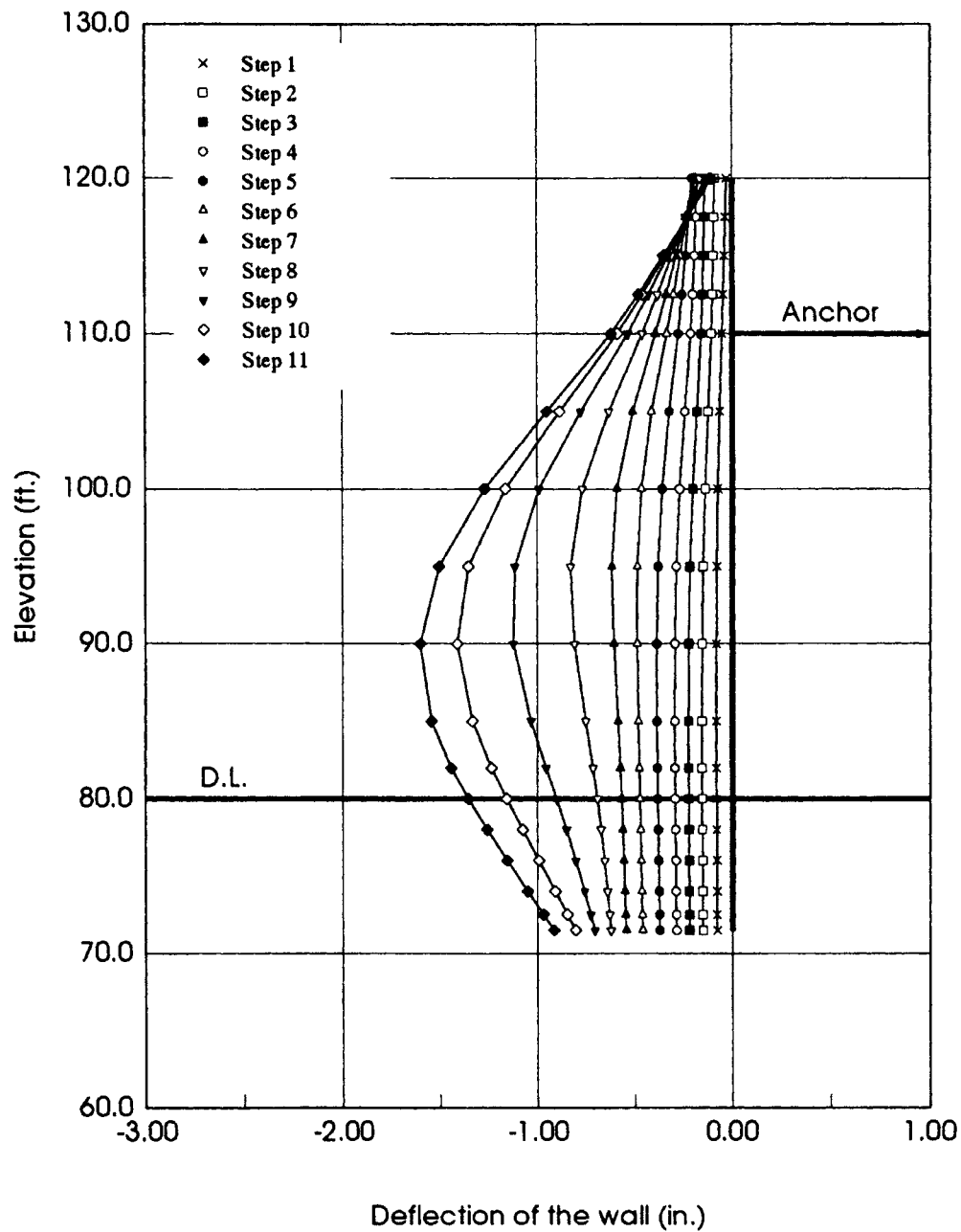


Figure 4.21. Deformed Shape of the Wall at the End of Each Step
(DD40 Excavation Case)

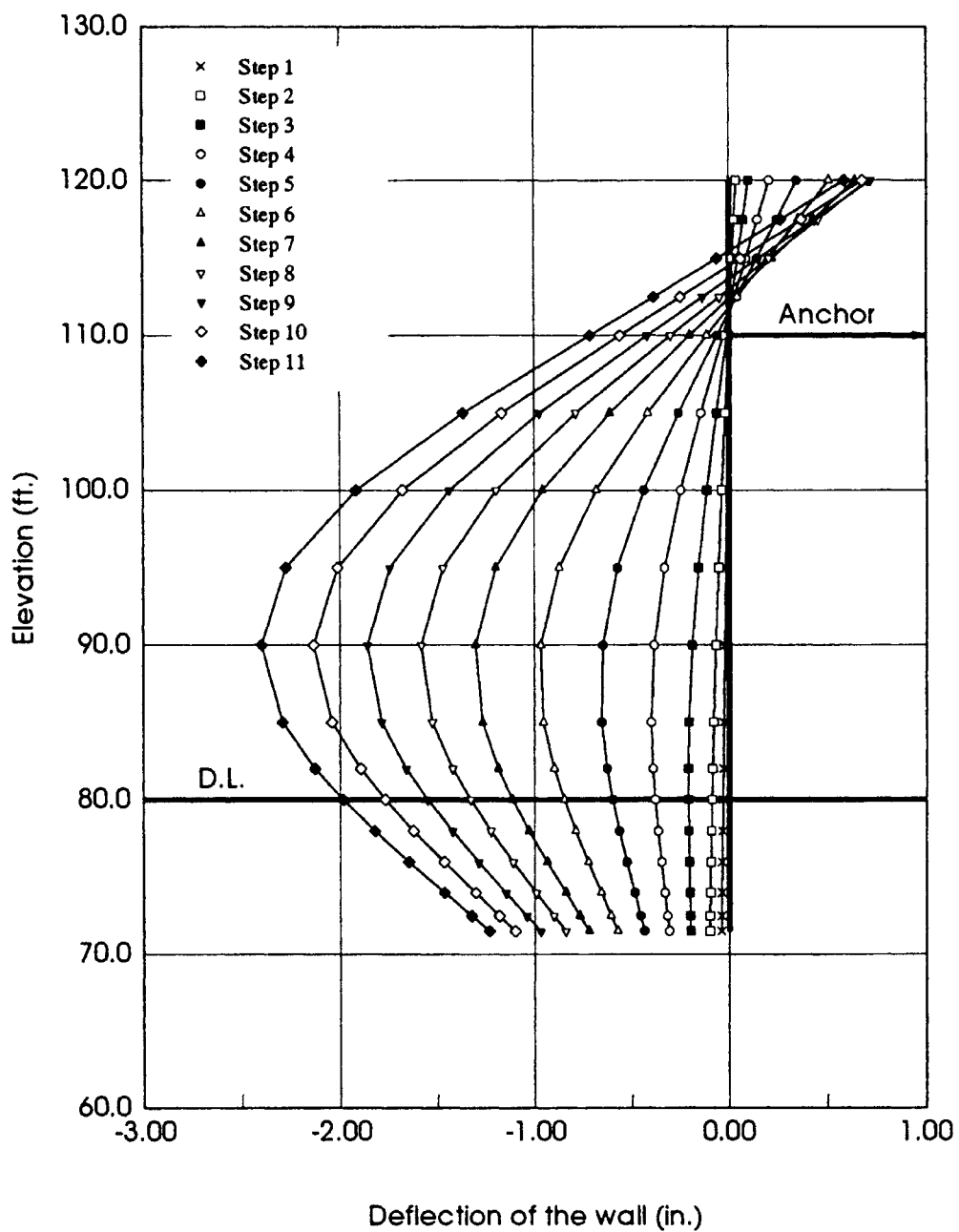


Figure 4.22. Deformed Shape of the Wall at the End of Each Step
(DD40 Backfill Case)

stages of the excavation or backfill, the wall started to bend near mid-height. This was because, when the first a few layers were excavated, the stresses in front of the wall decreased while the stresses in back side of the wall remained high. So the foundation soil started moving towards the front of the wall. The wall can not rotate easily because almost all of it is still buried. Therefore rigid body translation occurred. In the backfill case, as the first a few layers were filled the foundation soil started to behave as in the excavation case. But since the wall was not initially buried in this case, it simply rotated around the anchor point because of the lateral movement of the foundation soil.

The second difference between the excavation and backfill cases was the *amount* of the deflections: the deflections were larger in the backfilled wall by about 60%. This was related to the rigidity of the system. In the excavation case, since there was soil all around the wall initially the system was more rigid. In the backfill case, the wall penetrated the soil only a small depth and the rest of the wall was not supported by the soil. This made the system more flexible compared to the excavation case.

In the backfilled wall, the top of the wall deflected backwards while it deflected forwards in the excavated case. This was simply because in backfilling there was no soil in the back of the wall at higher levels until the final stages of construction. This made the system stiffer in the excavated case and therefore the deflections in the excavated type wall were smaller.

Finally, there was a difference in the rate of development of wall deflections. In the excavated wall, the deflection development rate was slower at the beginning and much higher towards the end of the construction. In the backfilled case, the rate of deflection

development was almost constant.

LM40 Case

In this case, during the initial stages of the excavation the wall underwent a rigid body translation. This was in contrast to the rigid body rotation around the anchor point in the backfill case (Figures 4.23 and 4.24). As the excavation or backfill progressed the wall started to bend near the middle. These were similar to the observations in DD40 case.

The deflections were larger in the backfilled wall by about 75% in this case. This was related to the rigidity of the system. In the excavation case, the system was more rigid initially since there was soil all around the wall. In the backfill case, the wall penetrated the soil only by a small depth and the rest of the wall was not supported by the soil. This made the system more flexible.

In the backfilled case, the top of the wall deflected backwards while it deflected forwards in the excavated case. This was because in backfilling there was no soil in the back of the wall until the later stages of construction. This made the system stiffer in the excavated wall and therefore the deflections in the excavated wall were smaller.

The tip deflections of the walls were approximately the same. This was remarkable since there was a difference in the maximum and top deflections of nearly 75% between the excavated and backfilled cases.

Finally, there was a difference in the rate of development of wall deflections as in the previous case.

DT40 Case

The first difference observed in this case is that, unlike the DD40 and LM40 cases

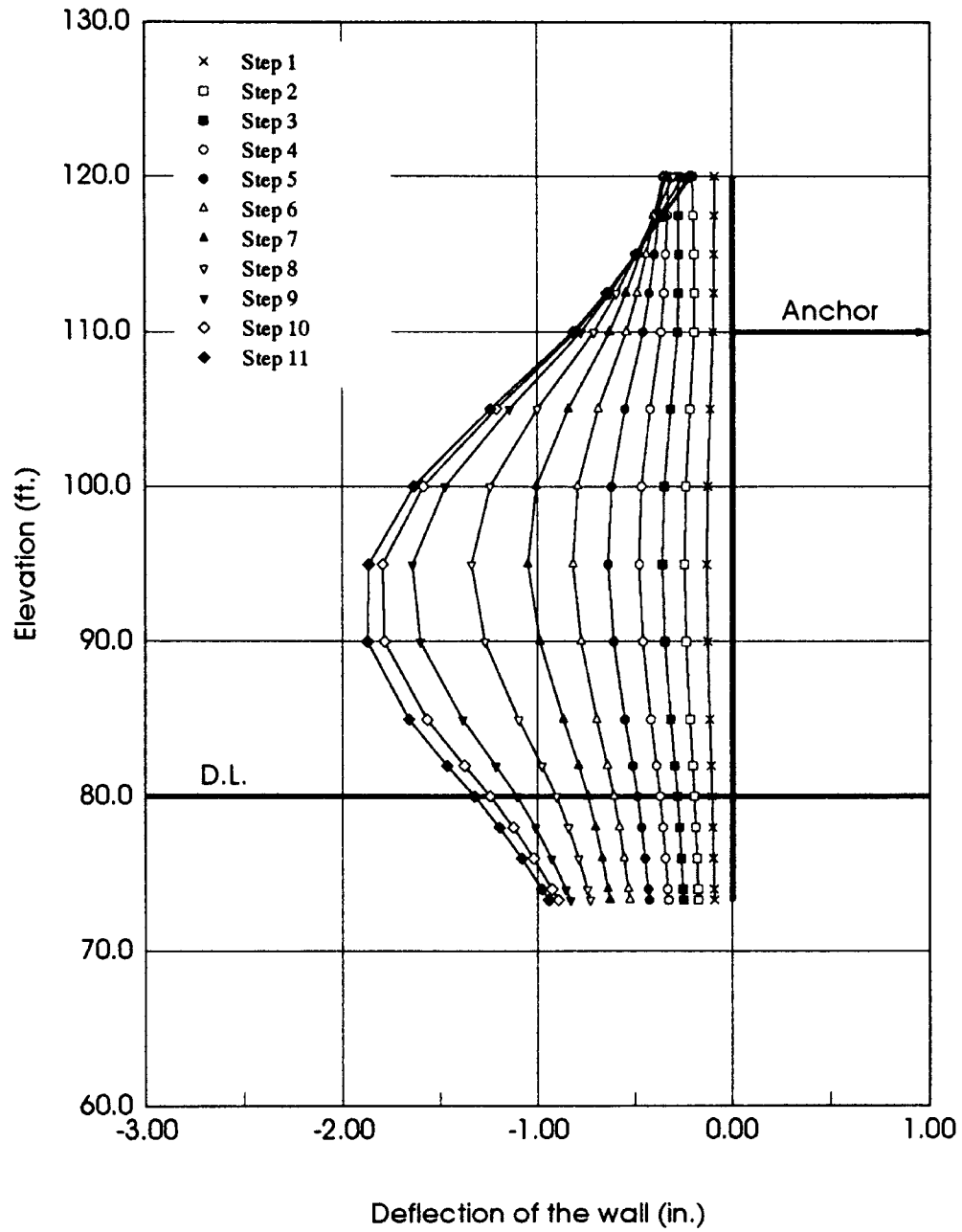


Figure 4.23. Deformed Shape of the Wall at the End of Each Step (LM40 Excavation Case)

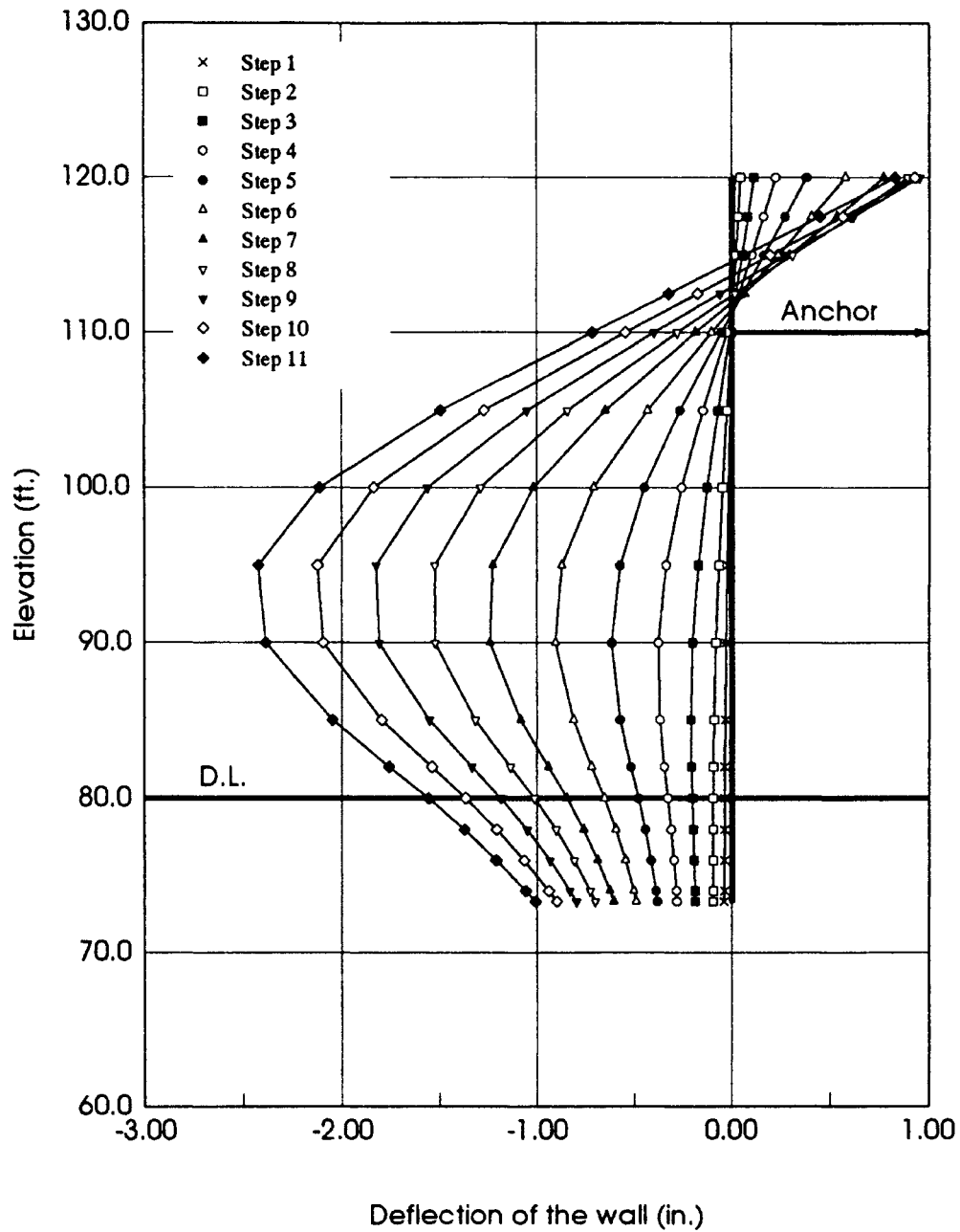


Figure 4.24. Deformed Shape of the Wall at the End of Each Step
(LM40 Backfill Case)

at the beginning stages of both excavation and backfill types, the wall underwent a rigid body rotation around the anchor point (Figures 4.25 and 4.26). After the excavation or backfill increased, the wall started to bend around mid-height. This was because the foundation soil was drained soft clay which was the softest soil used in this study. Because of the drained soft foundation clay, the deformation of the foundation layer, i.e. rotational or lateral movement of foundation soil was very large. This made the wall rotate around the anchor point.

The deflections were larger in the backfilled wall by about 60%. This was again related to the rigidity of the system. But the deflections were very large in this case when compared to the cases given above, because of the soft foundation soil.

For this case, the top of the wall deflected backwards in both the excavated and backfilled walls.

Finally, there was a difference in the rate of development of wall deflections as in the other cases.

The results of wall top displacements and wall maximum displacements for all twelve cases analyzed are given on Table 4.1 and Table 4.2 respectively. In the tables, “*X*” represents the excavation cases and “*F*” represents the backfill cases. The ratios $R_{d,top}$ and $R_{d,max}$ used in the tables are defined as follows:

$$R_{d,top} = \frac{\text{Wall top deflection obtained from excavation analysis}}{\text{Wall top deflection obtained from backfill analysis}} \quad (17)$$

and

$$R_{d,max} = \frac{\text{Maximum Wall deflection obtained from excavation analysis}}{\text{Maximum Wall deflection obtained from backfill analysis}} \quad (18)$$

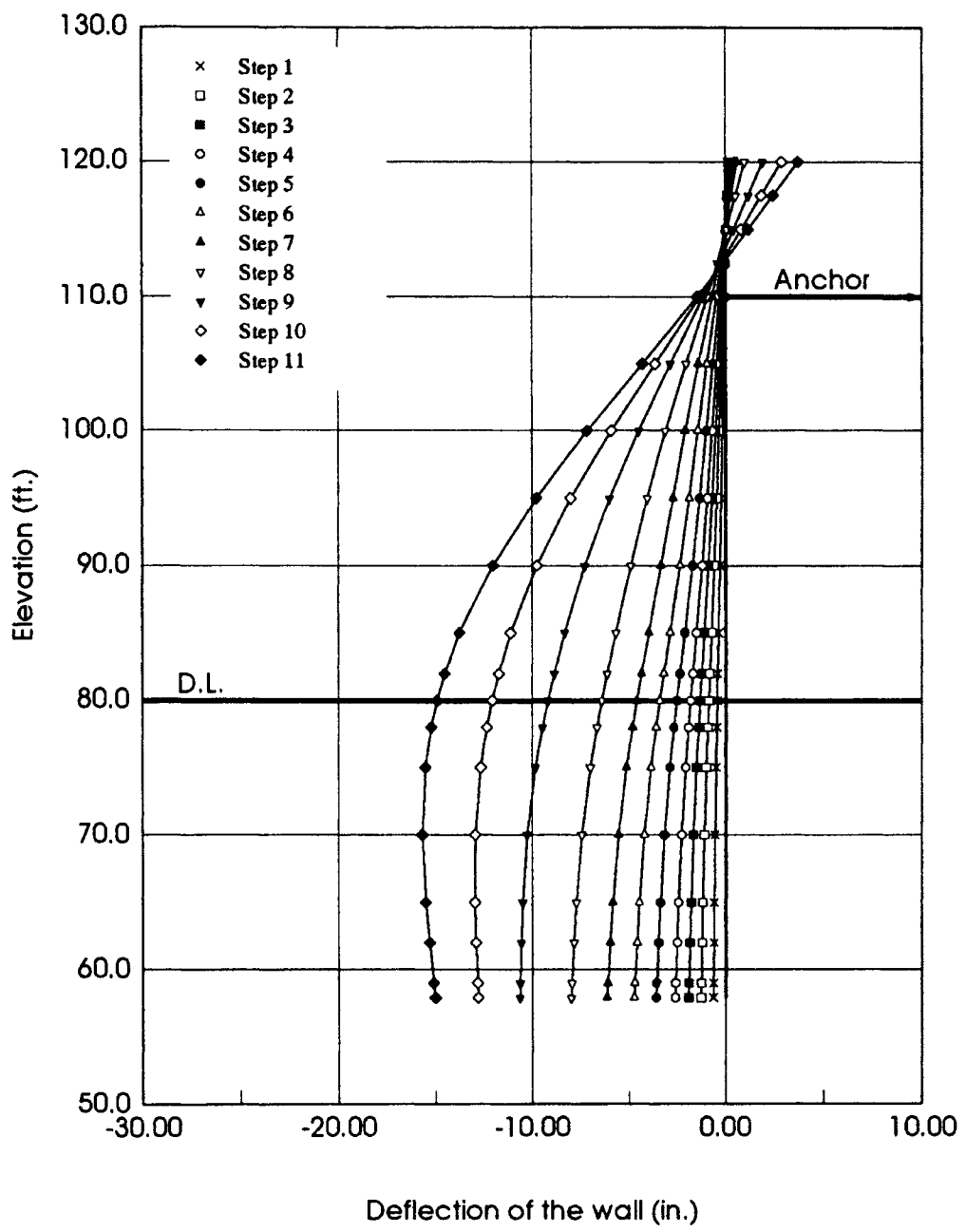


Figure 4.25. Deformed Shape of the Wall at the End of Each Step (DT40 Excavation Case)

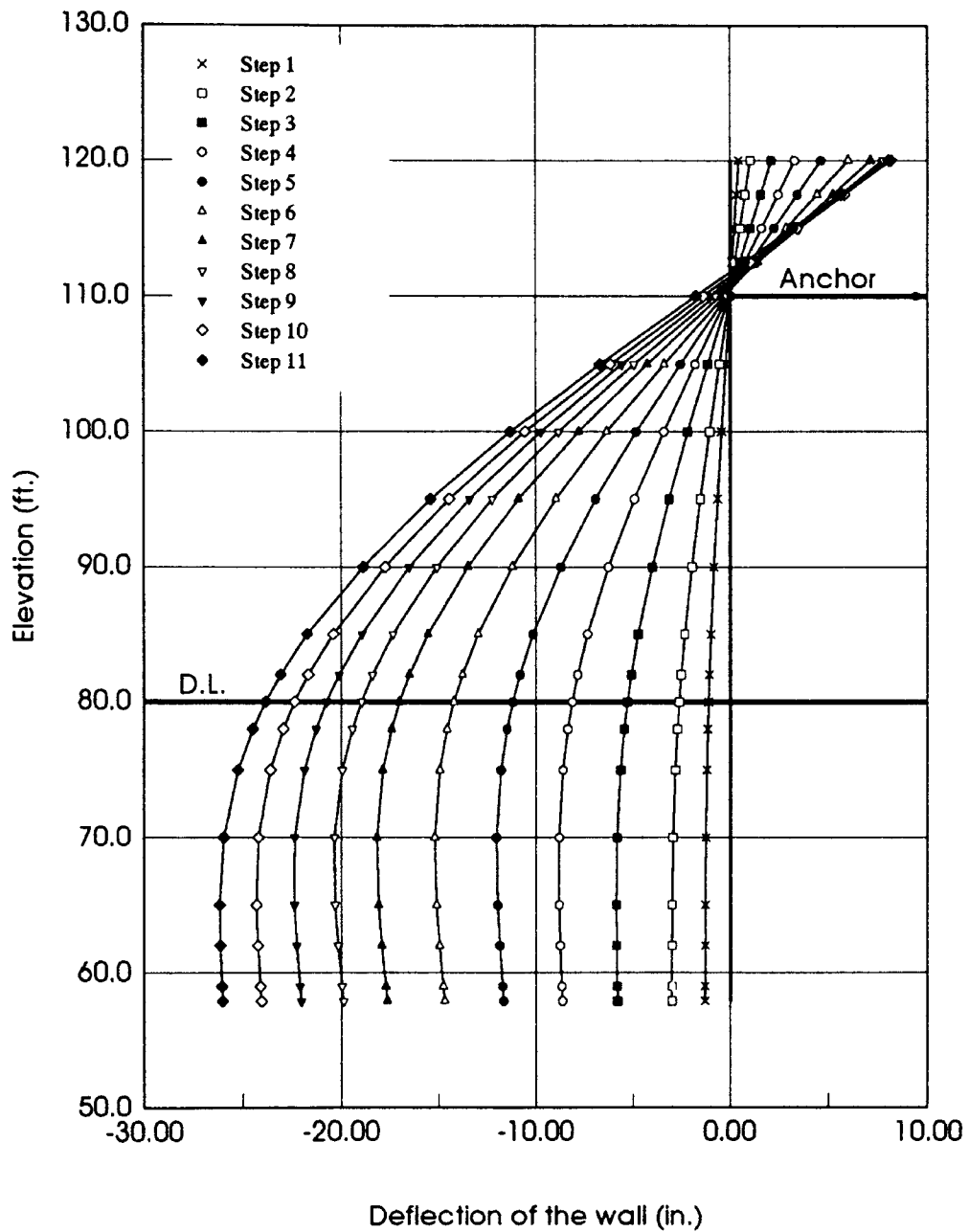


Figure 4.26. Deformed Shape of the Wall at the End of Each Step (DT40 Backfill Case)

In the backfilled walls, it was observed that the top of the wall moved backwards in all cases. In the excavation cases, the top of the wall deflected forward in some cases and backward in other cases. This was related to the foundation soil. The tip of the wall deflected more when the foundation soil was softer; and due to the restraint of the anchor, the top of the wall deflected backward. However, if the foundation soil was stiffer the tip deflection was smaller and the soil on the back of the wall did not allow the wall to deflect backward.

TABLE 4.1

COMPARISON OF WALL TOP DEFLECTIONS FOR
EXCAVATION AND BACKFILL CASES

	Top Deflection (in.)		
	X	F	$R_{d,top}$
DD40	-0.10	0.58	-0.17
DL40	0.06	1.42	0.04
DM40	-0.40	0.53	-0.75
DS30	-0.11	0.71	-0.15
DN40	1.57	3.28	0.48
DT40	3.72	8.05	0.46
LD40	-0.06	0.54	-0.11
LL40	0.29	2.07	0.14
LM40	-0.21	0.83	-0.25
LS30	0.08	0.81	0.10
LN40	1.74	4.32	0.40
LT40	3.90	9.08	0.43

In backfill cases, however, since there was no soil at the beginning stages of the construction, the wall rotated around the anchor point due to the deflection of the

foundation soil. The top deflections were in the range of 0.53" to 9.08" in backfill cases.

The maximum wall deflections obtained from the analysis of all cases are given on Table 4.2. The maximum deflections obtained from the analysis of backfilled wall cases were always larger than obtained from the excavated wall. Because the soil was more stiff in the excavation cases due to the soil all around the wall at the beginning of the construction. However, in the backfilled case there was no soil around the wall above the dredge line at the beginning of the construction. This made these cases, i.e. backfilled cases, more flexible. Therefore the maximum deflections were larger in backfilled cases. The ratios $R_{d,max}$ changed between 0.60 and 0.86 (with an average of 0.70).

TABLE 4.2
COMPARISON OF MAXIMUM WALL DEFLECTIONS FOR
EXCAVATION AND BACKFILL CASES

	Max. Deflection (in.)		
	X	F	$R_{d,max}$
DD40	-1.60	-2.40	0.67
DL40	-2.74	-4.33	0.63
DM40	-1.52	-1.92	0.79
DS30	-2.70	-3.13	0.86
DN40	-7.55	-10.30	0.73
DT40	-15.66	-26.18	0.60
LD40	-1.79	-2.65	0.68
LL40	-3.18	-5.18	0.61
LM40	-1.87	-2.42	0.77
LS30	-2.57	-3.04	0.85
LN40	-7.25	-11.21	0.65
LT40	-15.56	-25.80	0.60
		Average :	0.70

In Figure 4.27, the results of maximum deflections are plotted for excavation versus backfill cases. The deflections for the cases which have drained clayey foundation soils were very large. This was because at the end the construction most of the soil elements failed in these cases (Figures B.13 through B.18).

Bending Moments in The Wall

The bending moments in the sheet pile wall throughout the construction steps are shown in Figures 4.28, 4.29, 4.30 and 4.31 for the cases DD40 and LM40. Figures 4.28 and 4.30 show the excavation results and Figures 4.29 and 4.31 show the backfill results. While plotting the results of an any case, the same scale was used in the figures for both construction type, excavation and backfilling, to be able to see the differences and to facilitate comparison. The differences noticed in the wall deflection for the cases DD40 and LM40 are given below:

DD40 Case

The most important difference noticed in this case was that the bending moments were larger in the backfilled wall by about 67% (Figures 4.28 and 4.29). There was positive moments around the tip of the wall in the excavation case. The bending moments at the anchor level were greater in the excavated wall. Finally, there was a difference in the rate of development of wall deflections. In the excavated wall, the deflection development rate was slower at the beginning and much higher towards the end of the construction. In the backfilled case, the rate of deflection development was almost constant.

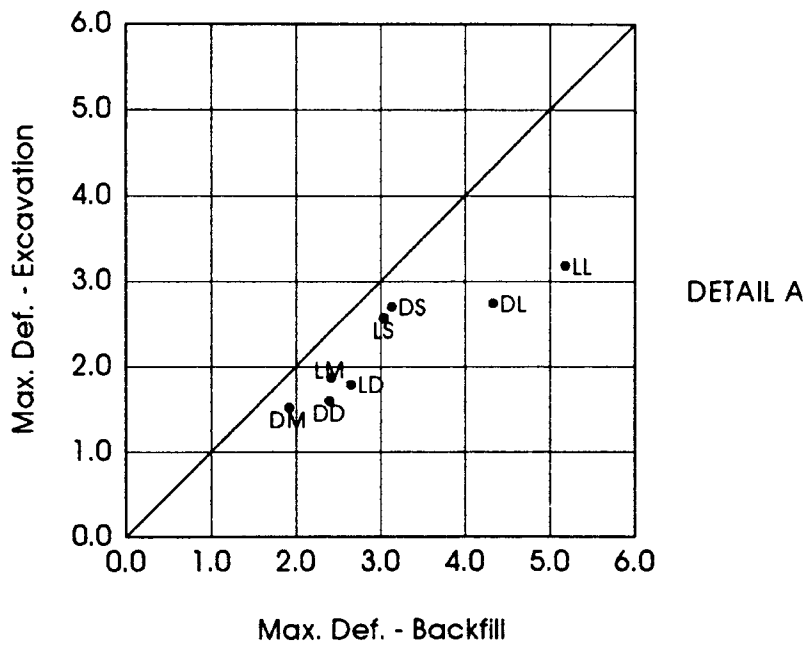
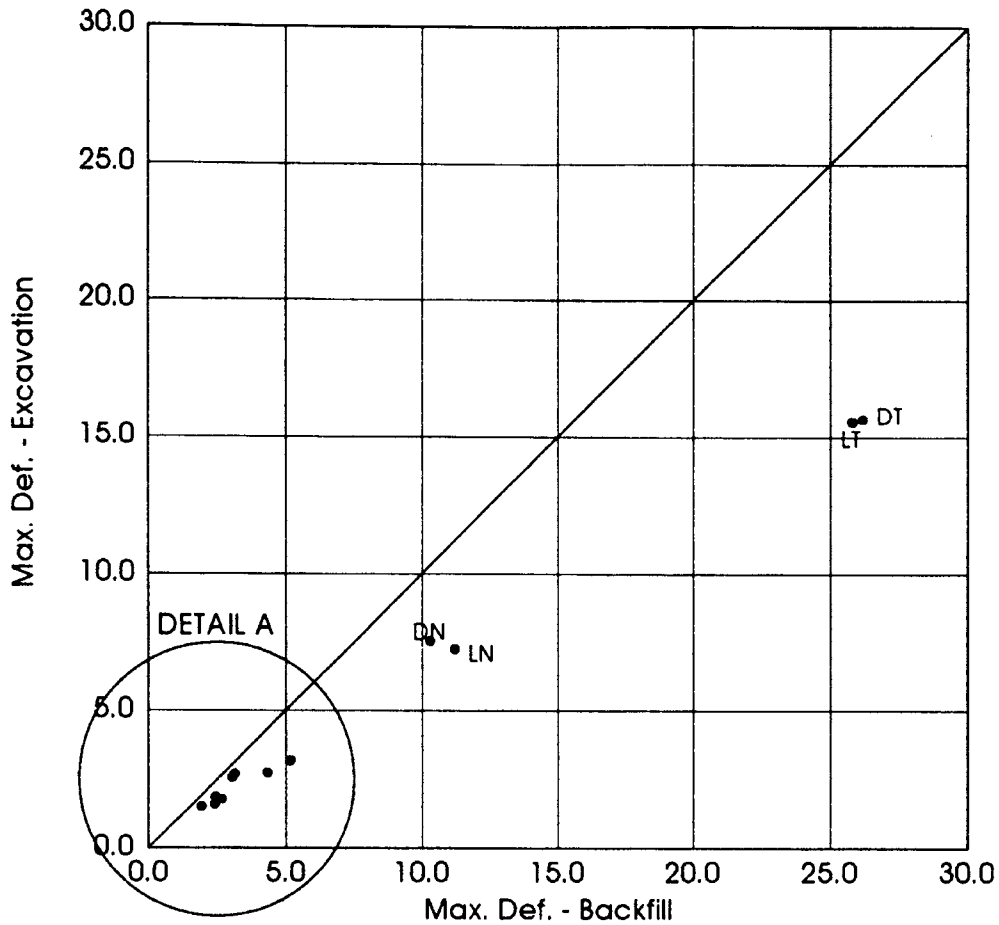


Figure 4.27. Comparison of Maximum Wall Deflections (in in.)
For Excavation and Backfill

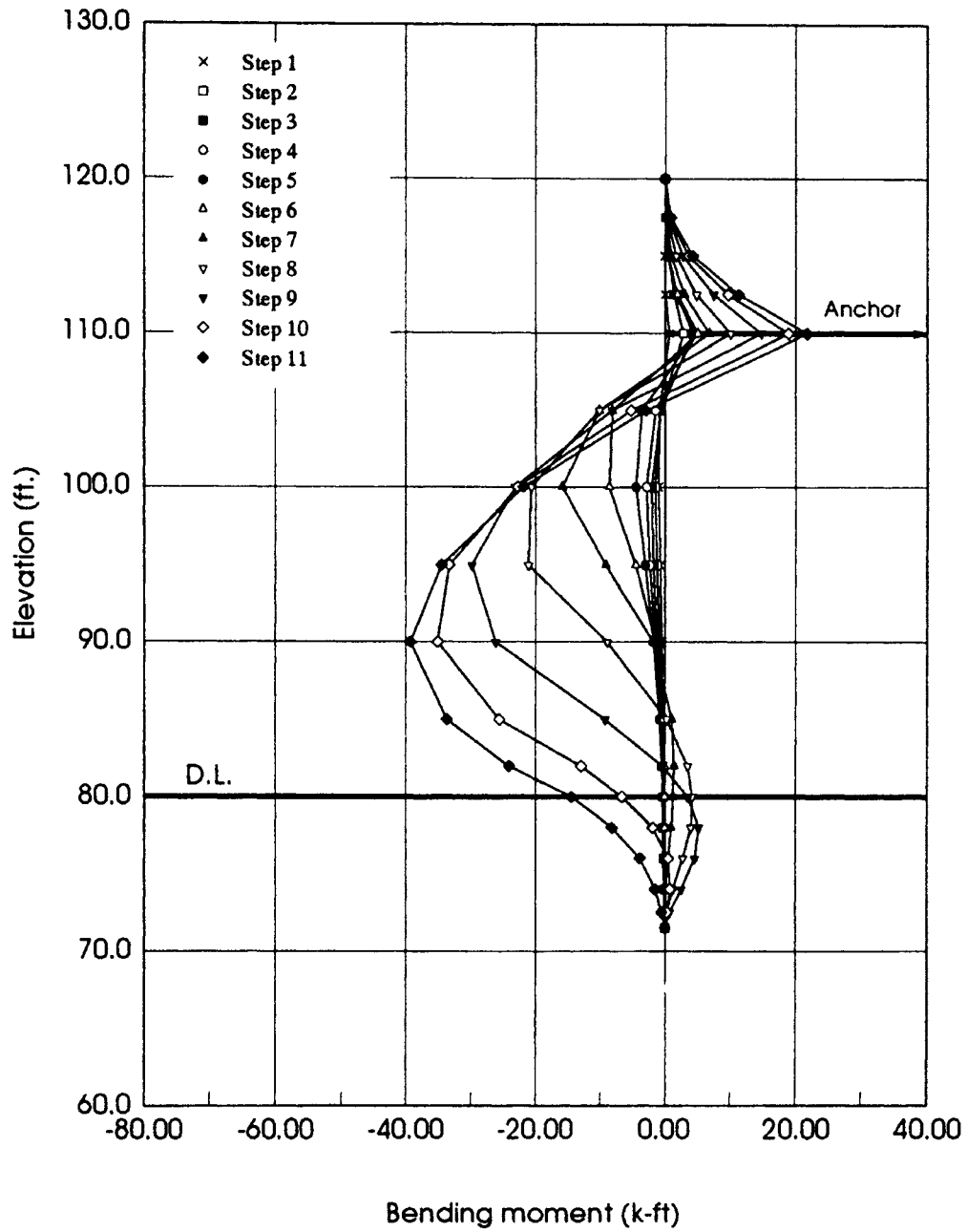


Figure 4.28. Bending Moment Diagram of the Wall at the End of Each Step
(DD40 Excavation Case)

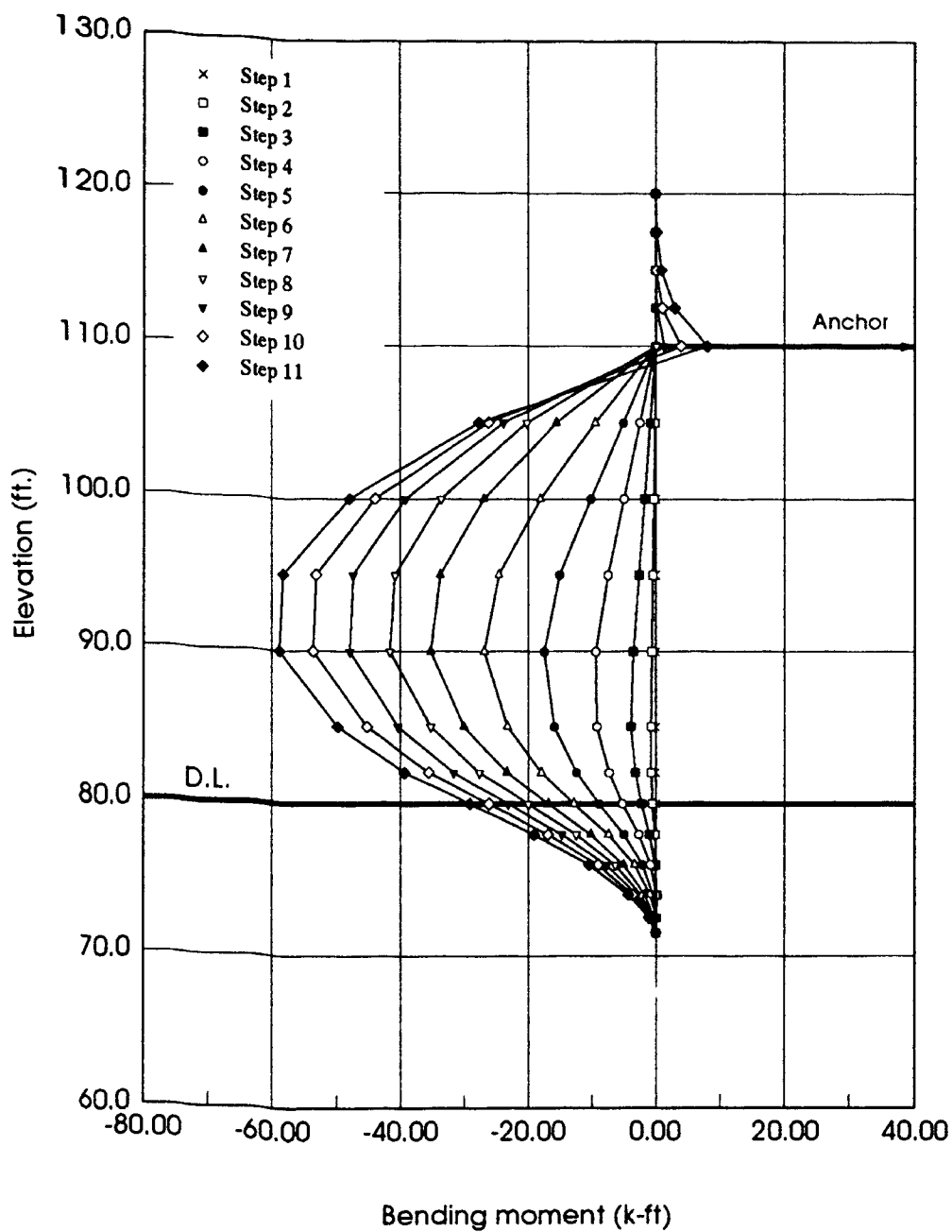


Figure 4.29. Bending Moment Diagram of the Wall at the End of Each Step
(DD40 Backfill Case)

LM40 Case

The most important difference noticed in this case was that the bending moments were larger in the backfilled wall by about 65% (Figures 4.30 and 4.31). Unlike the DD40 case, there were positive moments around the tip of the wall in both excavation and backfill cases. The bending moments at the anchor level were greater in the excavated wall. Finally, there was a difference in the rate of development of wall deflections like in DD40 case. In the excavated wall, the deflection development rate was slower at the beginning and much higher towards the end of the construction. In the backfilled case, the rate of deflection development was almost constant.

The results of wall bending moments for all twelve cases analyzed are given in Table 4.3. The ratio, R_m used in the table is defined as;

$$R_m = \frac{\text{Maximum bending moment obtained from excavation analysis}}{\text{Maximum bending moment obtained from backfill analysis}} \quad (19)$$

R_m changed between 0.64 and 0.95 (average of 0.71) as shown in the Table 4.3. It can be seen that the maximum moment ratios for DN40, DT40, LN40 and LT40 cases were quite high. This was because of the failure of the soil elements in the profile. For this reason, since DN40 case gives the maximum R_m value, it can be eliminated. Then R_m value changes from 0.64 to 0.70 with an average of 0.67.

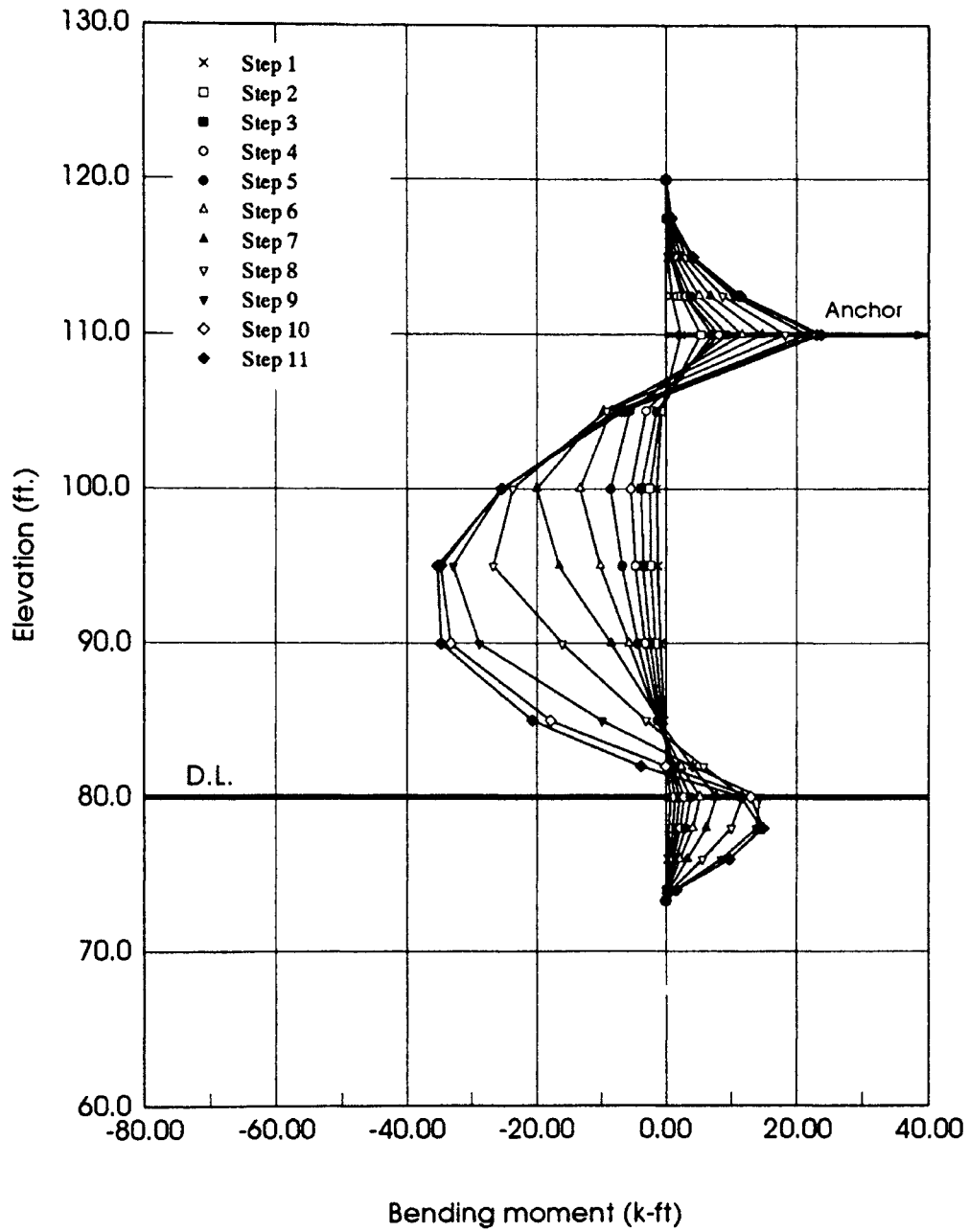


Figure 4.30. Bending Moment Diagram of the Wall at the End of Each Step (LM40 Excavation Case)

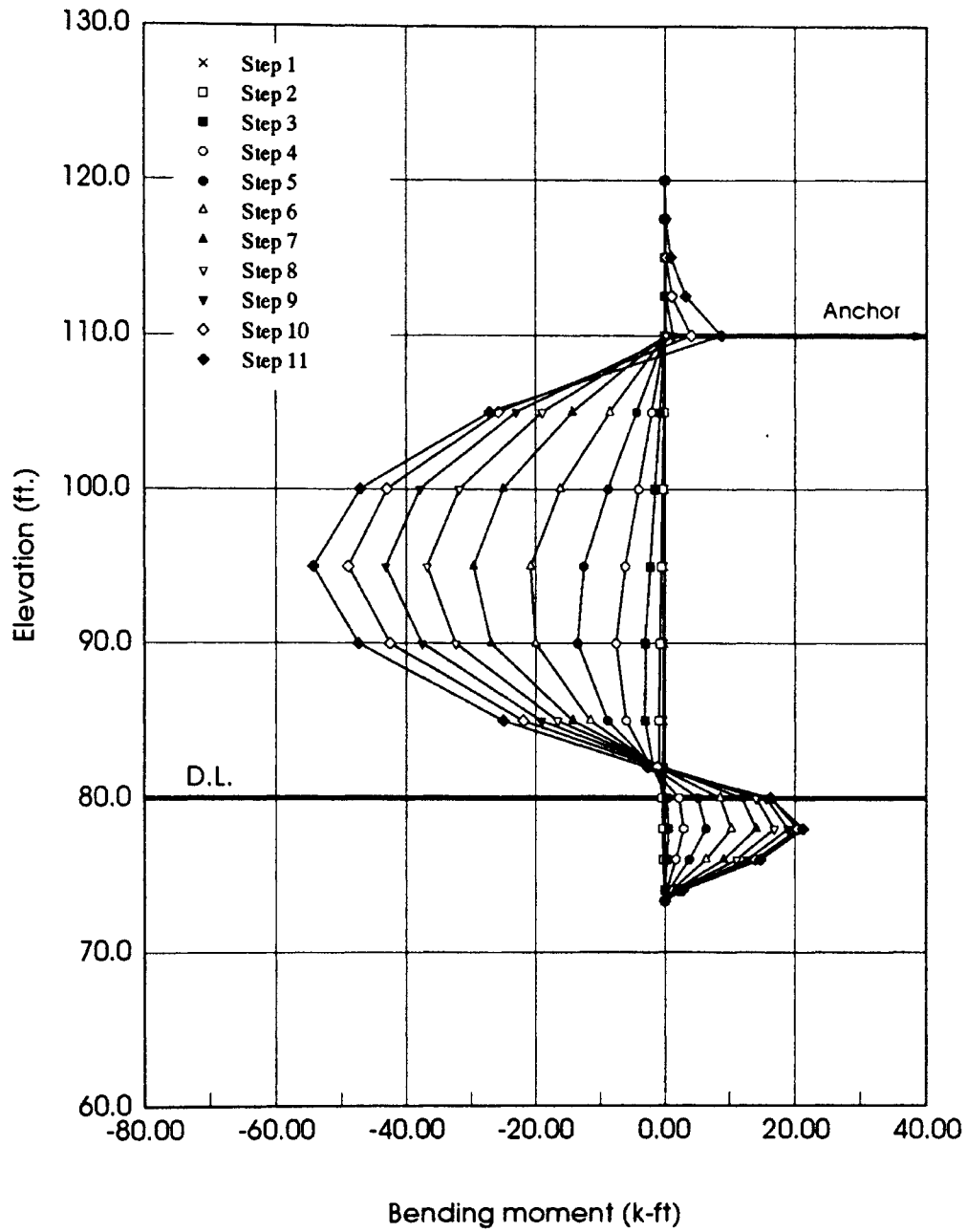


Figure 4.31. Bending Moment Diagram of the Wall at the End of Each Step (LM40 Backfilling Case)

TABLE 4.3
COMPARISON OF BENDING MOMENTS IN THE WALL FOR
EXCAVATION AND BACKFILL CASES

	Maximum Moment (k-ft)			
	Walsht	X	F	R_m
DD40	76.06	39.23	58.81	0.67
DL40	95.95	33.25	47.45	0.70
DM40	62.05	25.83	39.21	0.66
DS30	68.99	26.18	37.93	0.69
DN40	98.09	51.37	54.00	0.95
DT40	145.05	78.98	102.50	0.77
LD40	86.74	58.72	90.10	0.65
LL40	105.74	45.41	71.31	0.64
LM40	73.98	35.26	54.25	0.65
LS30	69.95	31.08	46.38	0.67
LN40	107.92	55.50	82.83	0.67
LT40	148.17	82.43	109.60	0.75
Average :				0.71

In Figure 4.32, the results of maximum bending moments are plotted for excavation versus backfill cases. The moments for the cases, which have the drained clayey foundation soils, were larger because of soil failure.

Anchor Forces

Anchor force is one of the critical factors in designing an anchored sheet pile wall. The results obtained from the analyses are given in Figure 4.33 and Table 4.4.

The results showed that, on the average the anchor force obtained from both analyses (excavation and backfilling) does not change significantly.

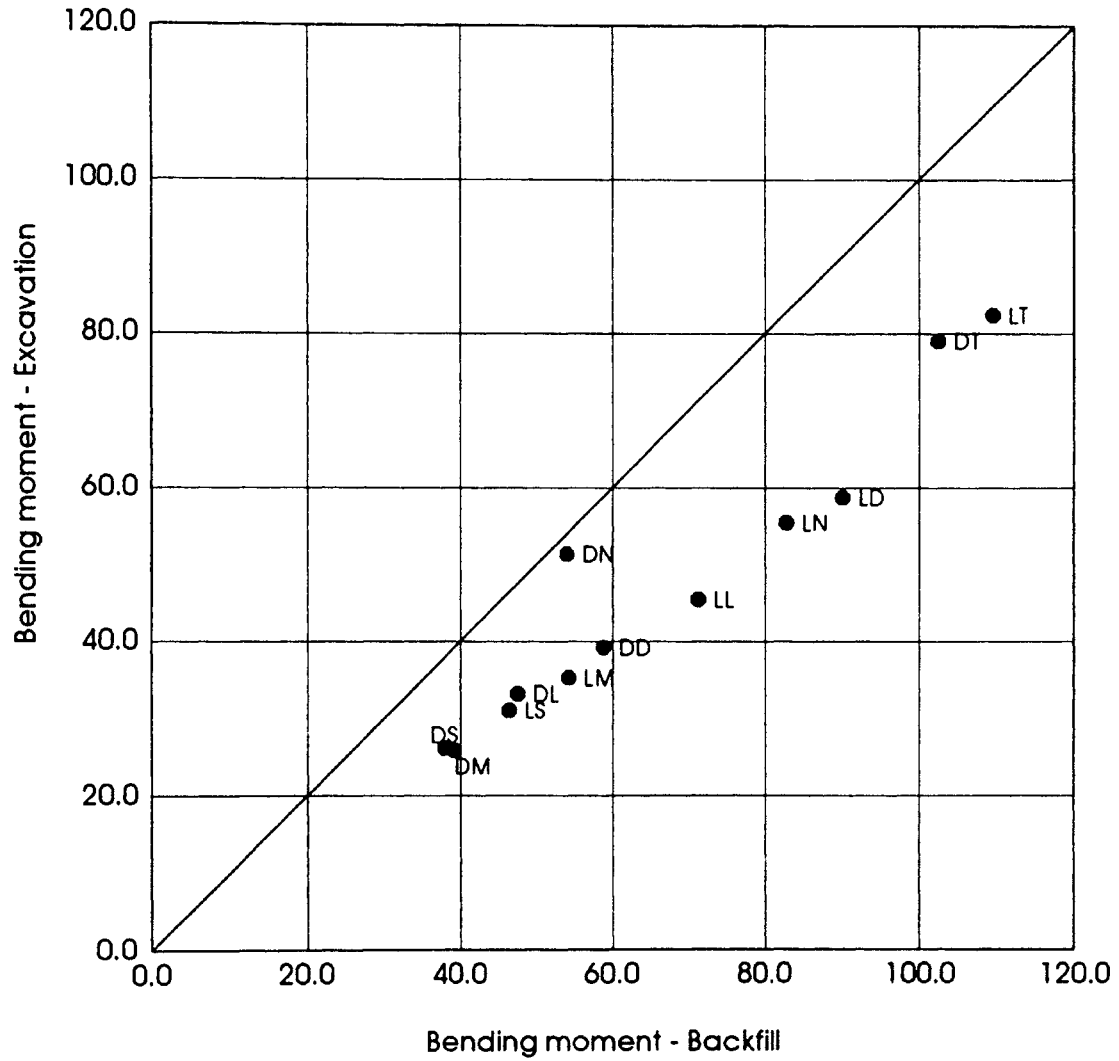


Figure 4.32. Comparison of Maximum Bending Moments (in k-ft)
For Excavation and Backfill Cases

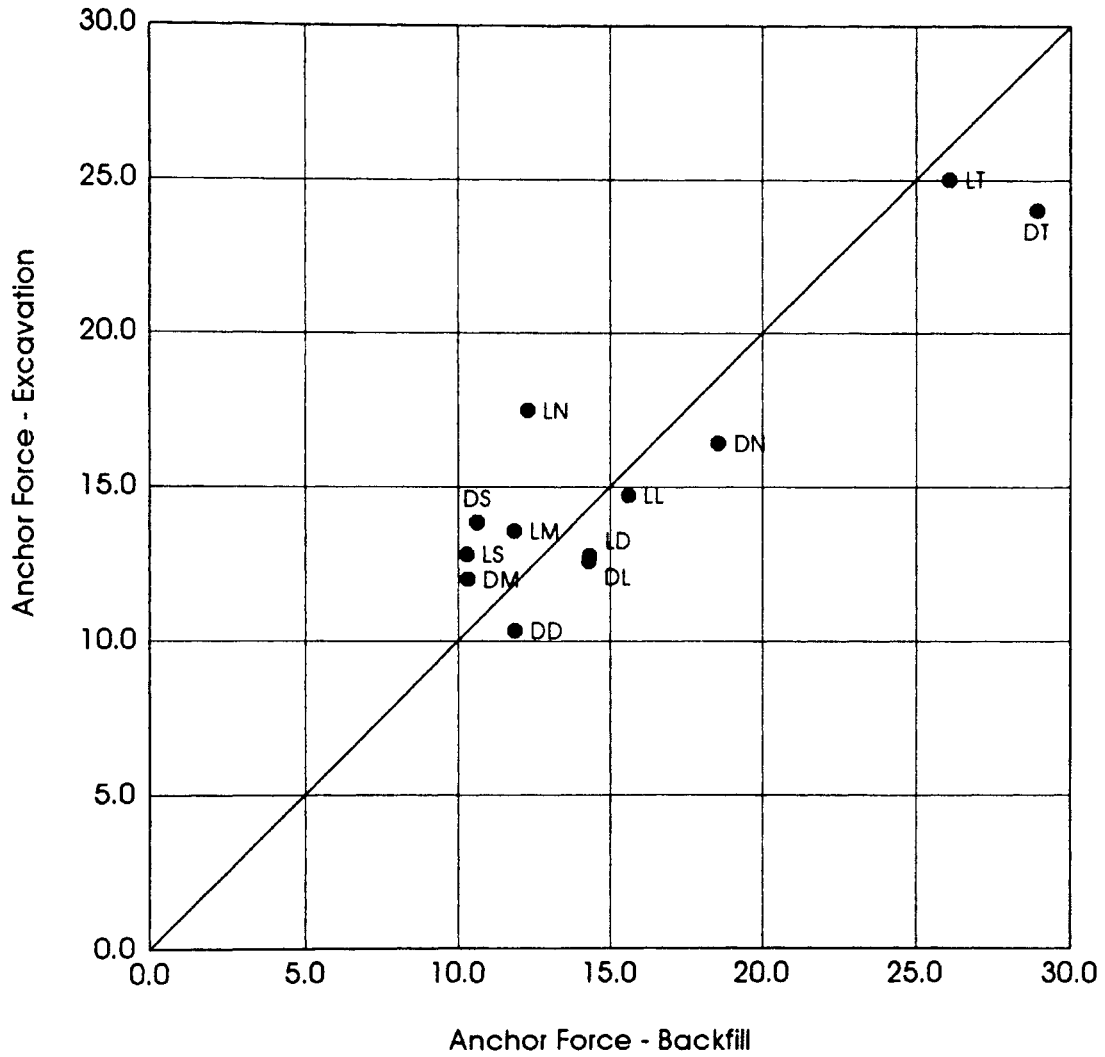


Figure 4.33. Comparison of Anchor Forces (in kips) For Excavation and Backfill

The ratio, R_{af} ;

$$R_{af} = \frac{\text{Anchor force obtained from excavation analysis}}{\text{Anchor force obtained from backfill analysis}} \quad (20)$$

varied between 0.83 and to 1.42, but the DT40 (0.83) and the LN40 (1.42) cases both failed in a large areas. When these two cases were not considered, R_{af} changed between 0.87 (DD40 case) and 1.3 (DS30 case) with an average of 1.05.

If the foundation soil was undrained clay then the excavation cases gave larger anchor forces than the backfill cases. Otherwise, the anchor forces was larger in backfilled cases than those in excavation cases.

TABLE 4.4

COMPARISON OF ANCHOR FORCES FOR
EXCAVATION AND BACKFILL CASES

	Anchor Force (kips)			
	Walsht	X	F	R_{af}
DD40	8.52	10.33	11.87	0.87
DL40	9.50	12.60	14.31	0.88
DM40	7.77	12.01	10.32	1.16
DS30	6.95	13.85	10.63	1.30
DN40	9.60	16.43	18.57	0.88
DT40	11.63	24.02	28.94	0.83
LD40	9.75	12.77	14.33	0.89
LL40	10.69	14.73	15.61	0.94
LM40	9.08	13.58	11.84	1.15
LS30	7.50	12.82	10.30	1.24
LN40	10.81	17.49	12.29	1.42
LT40	12.60	25.02	26.10	0.96
Average:				1.04

Table 4.4 indicates that the conventional method gives smaller anchor forces than finite element analysis results. In backfilled walls, the differences in the results were greater if the foundation soil was sand. Sowers and Sowers (1967) concluded that most anchored sheet pile wall failures occurred due to the failure of anchorage. The FEM results also show that the anchor force based on the free earth support method is not safe.

The Effects of the Anchor Installation Time

Theoretically, it is possible to install the anchor any time during the backfilling process, a factor that is not considered in conventional calculations. Here, the possible effects of placing the anchor at different times was investigated.

The two extremes for anchor placement are: (1) the beginning of the filling process, and (2) when the fill level reached the anchor level. The anchor can be placed at any fill level between these two extremes. In previous runs, the analysis was done by placing the anchor at the beginning of backfilling. Here the analyses were repeated by placing the anchor when different fill heights were reached. Fill heights of 2, 5, 10, 15, 20, 25 and 30 feet were considered. The maximum deflection of the wall, maximum bending moment in the wall and the anchor force values obtained from the analysis for the fill heights given above. The results for the cases DD40 and LM40 are tabulated on Table 4.5.

TABLE 4.5

**THE EFFECTS OF INSTALLING THE ANCHOR
WHILE THE FILL IS AT DIFFERENT LEVELS**

CASE	Height (ft)	Max. Def. (in)	Max. Mom. (k-ft)	Anc. Force (kips)
DD40 (Fill)	0	2.40	58.81	11.87
	2	2.38	58.04	11.74
	5	2.40	55.02	11.80
	10	2.61	51.84	11.90
	15	2.92	43.81	10.98
	20	3.98	38.88	10.46
	25	6.37	31.68	9.89
	30	9.52	21.94	8.95
LM40 (Fill)	0	2.42	54.25	11.84
	2	2.44	54.13	11.83
	5	2.48	53.84	11.83
	10	2.64	52.68	11.75
	15	2.84	44.63	11.58
	20	3.37	36.30	11.05
	25	5.05	28.91	10.32
	30	8.58	20.26	9.34

* Fill height when the anchor is placed

Anchor Placement Time Effect on Deflection of The Wall

The maximum deflection of the sheet pile wall increased when installation of the anchor was delayed. For example, if the anchor was placed when the fill height reaches 1/3 of the anchor height, the increase in the maximum deflection was around 9% (8.75% for DD40 case, 9.09% for LM40 case). The increase in the deflection was around 20% (21.67% for DD40 case, 17.35% for LM40 case) when the anchor was placed as the fill

height reached $1/2$ of an anchor height. This was because the anchor normally prevented the deflection of the wall; therefore if it was placed at the beginning of the construction the wall deflected less. As shown in Figure 4.34 the rate of increase in maximum deflection was slow at lower fill heights and increased rapidly as the anchor placement was postponed. The wall deflections can be unreasonably high if the anchor was placed very late. For example the maximum deflection grew from approximately 2 to about 9 inches in the cases analyzed, see Figure 4.34.

The deformed shapes of the walls at the end of construction are given in Figures 4.35 and 4.36 for DD40 and LM40 cases, respectively. The wall deflection characteristics in the two cases were almost the same except that there was a curvature around the wall tip in LM40 case which accompanied the positive moments in that area.

Anchor Placement Time Effect on Bending Moments

The maximum bending moment in the wall decreased by placing the anchor at later stages in construction instead of at the beginning. This was because the wall deformed freely at the earlier stages of backfilling. Therefore, the bending moments were lower. The rate of decrease in bending moments was roughly the same for DD40 and LM40 cases (Figure 4.37).

In the DD40 case, the decrease in the bending moment was around 63% if the anchor was placed when the fill height reached the anchor height. In the LM40 case, the maximum bending moment value decreased by 37% if the anchor was placed when the fill height reached the anchor height.

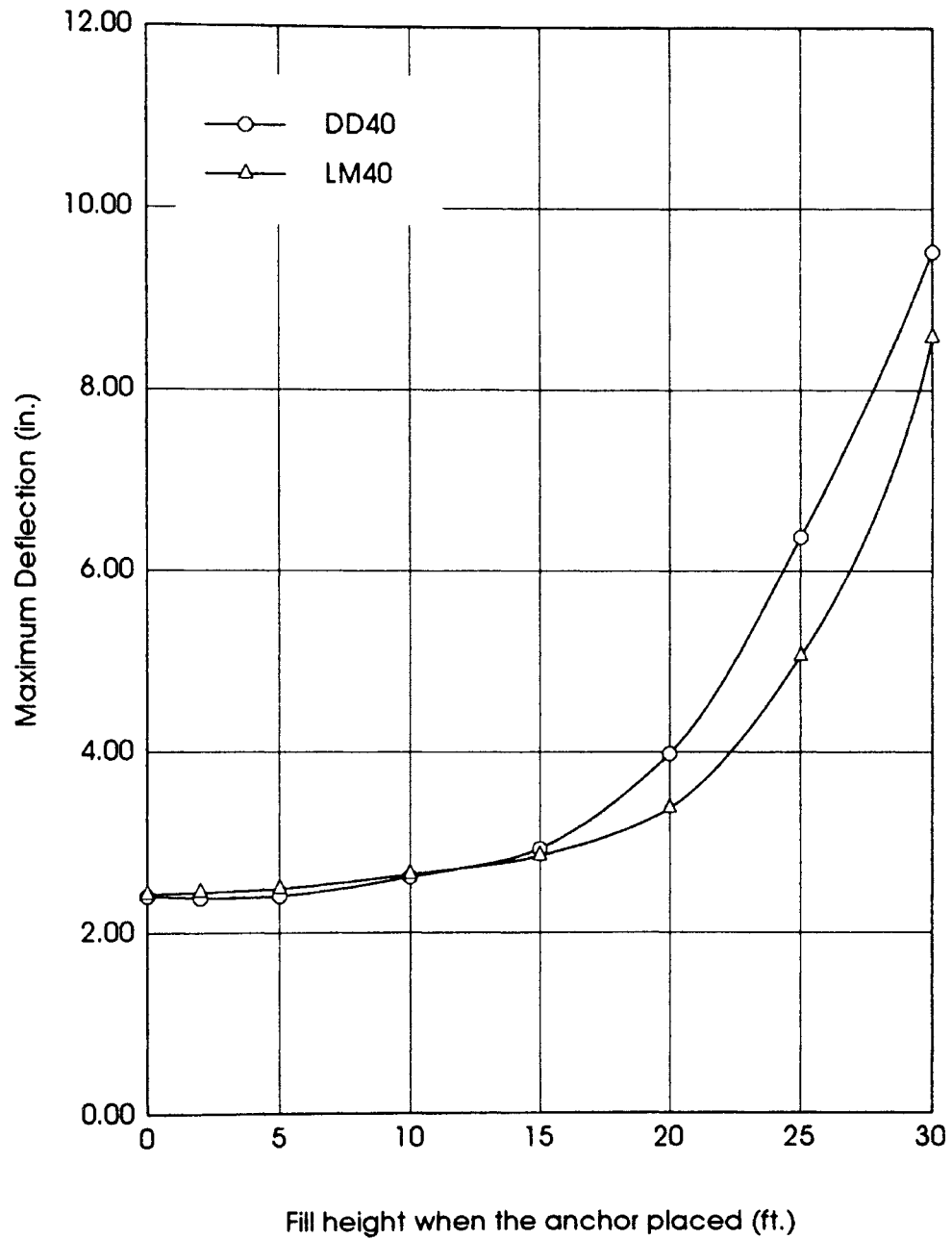


Figure 4.34. Maximum Wall Deflections Obtained When the Anchor is Placed at Different Fill Levels

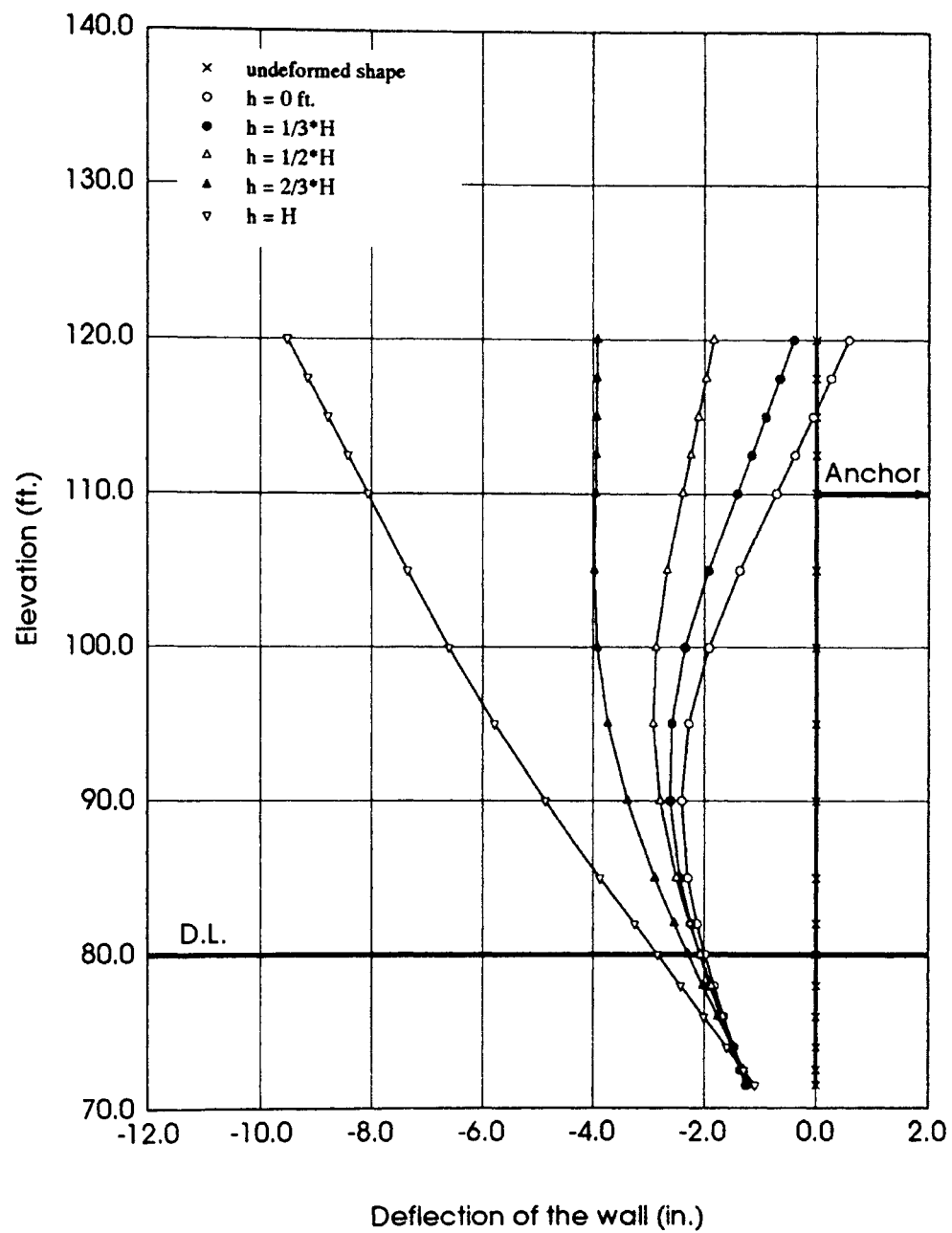


Figure 4.35. Wall Deformed Shape for DD40 Case When the Anchor is Placed at Different Fill Levels

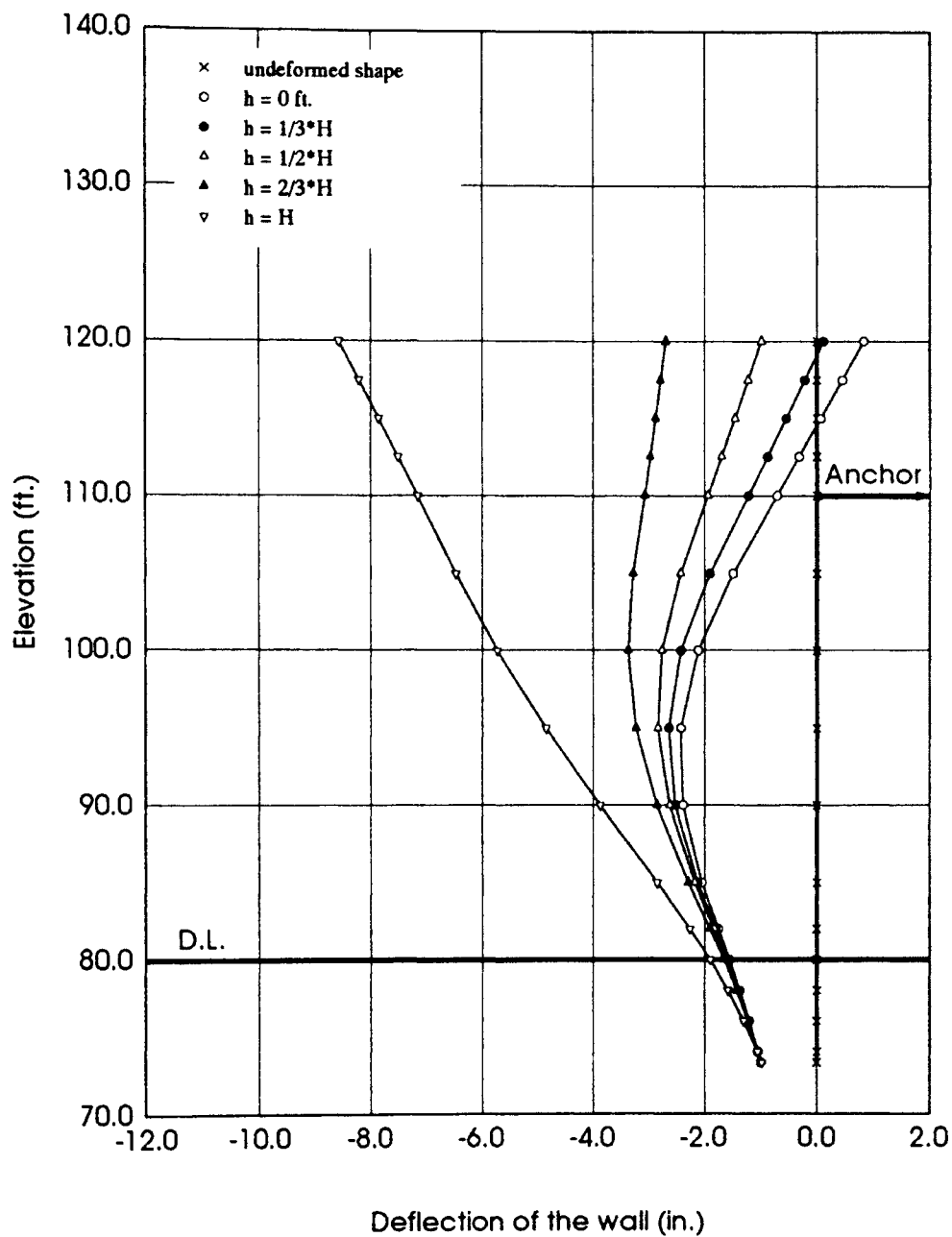


Figure 4.36. Wall Deformed Shape for LM40 Case When the Anchor is Placed at Different Fill Levels

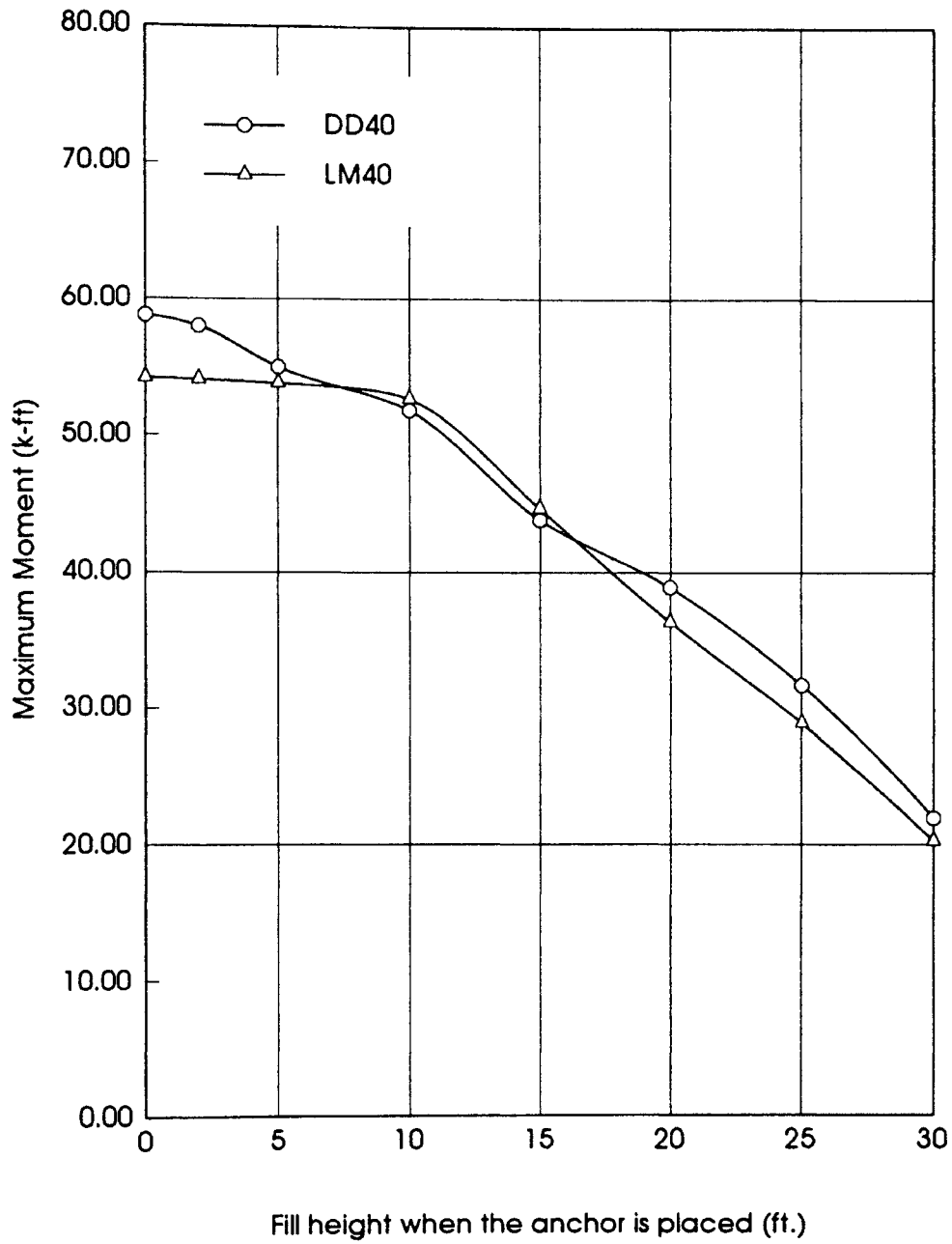


Figure 4.37. Maximum Bending Moments Obtained When the Anchor is Placed at Different Fill Levels

The bending moments obtained from these analysis along the wall section were given in Figures 4.38 and 4.39. The difference observed in these figures was that in the LM40 case the positive moment values were larger than those in DD40 case around the tip of the wall. The positive moment can be seen in Figure 4.36. The curvature in the figure near the tip of the wall caused these positive moments. This shows that some degree of fixity developed in these walls although the wall was designed by free earth support method.

Anchor Placement Time Effect on Anchor Forces

The calculated anchor force was affected by the time of installation of the anchor. Figure 4.40 shows this effect for the DD40 and LM40 cases. In this figure, the anchor force decreased with the delay in installing the anchor. The anchor force was essentially the same when the anchor was placed at the beginning (fill height = 0), and when the fill was about 10 ft high. But there was a large decrease when the anchor was placed after the fill height reached that level. The highest decrease occurs for the case where the anchor is placed when the fill was at 30 feet. At this point, the anchor force decreased by approximately 25%. The decrease in the anchor force with placement delay can be explained as follows. When the anchor was placed at the beginning of filling, the anchor restrained the wall and, took up large amounts of tension. When the anchor installation was delayed, the wall deformed freely at the initial stages until the anchor was tied, the anchor only took up tension after that point. Therefore the larger the delay, the smaller the anchor force.

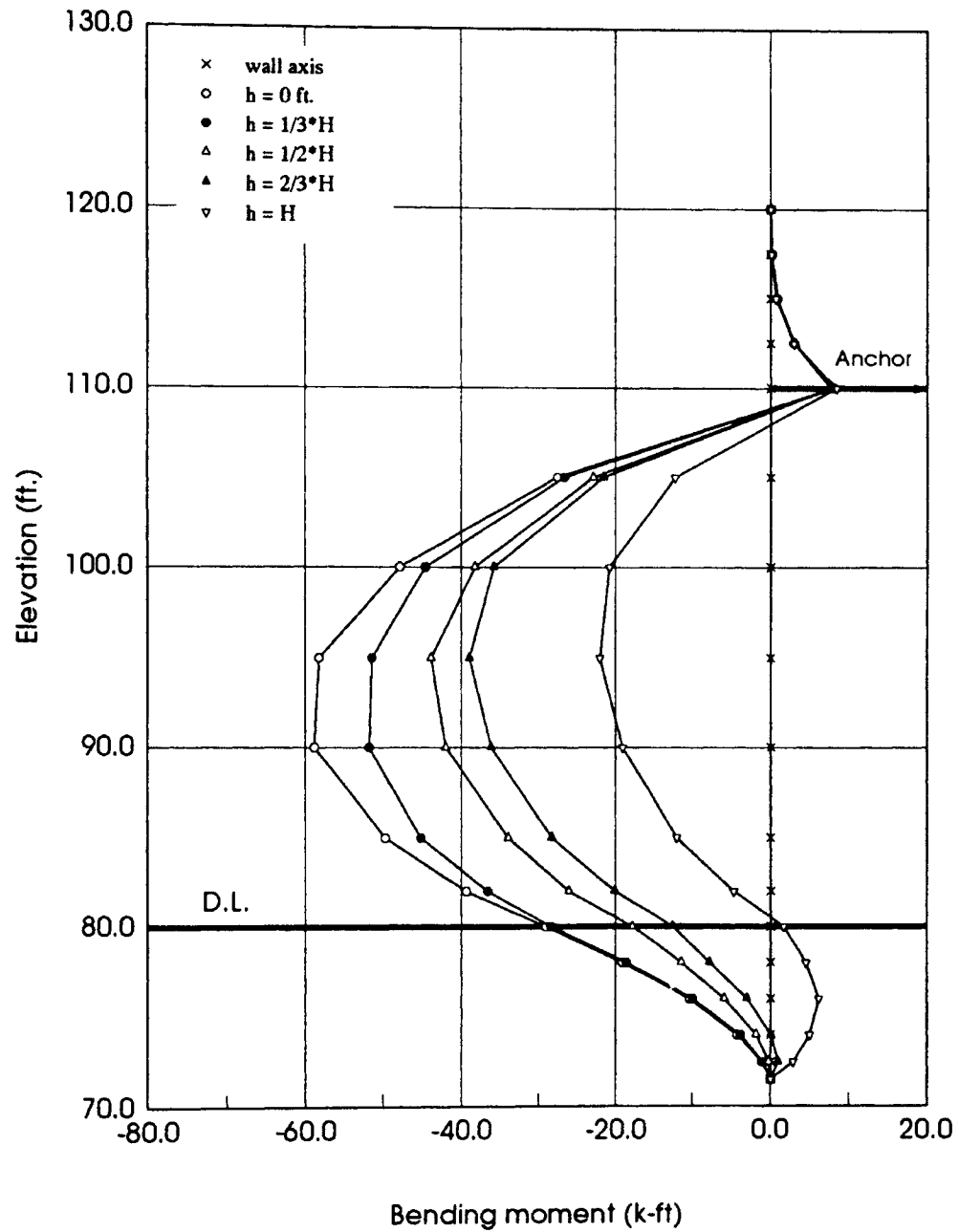


Figure 4.38. Bending Moments for DD40 Case When the Anchor is Placed at Different Fill Levels

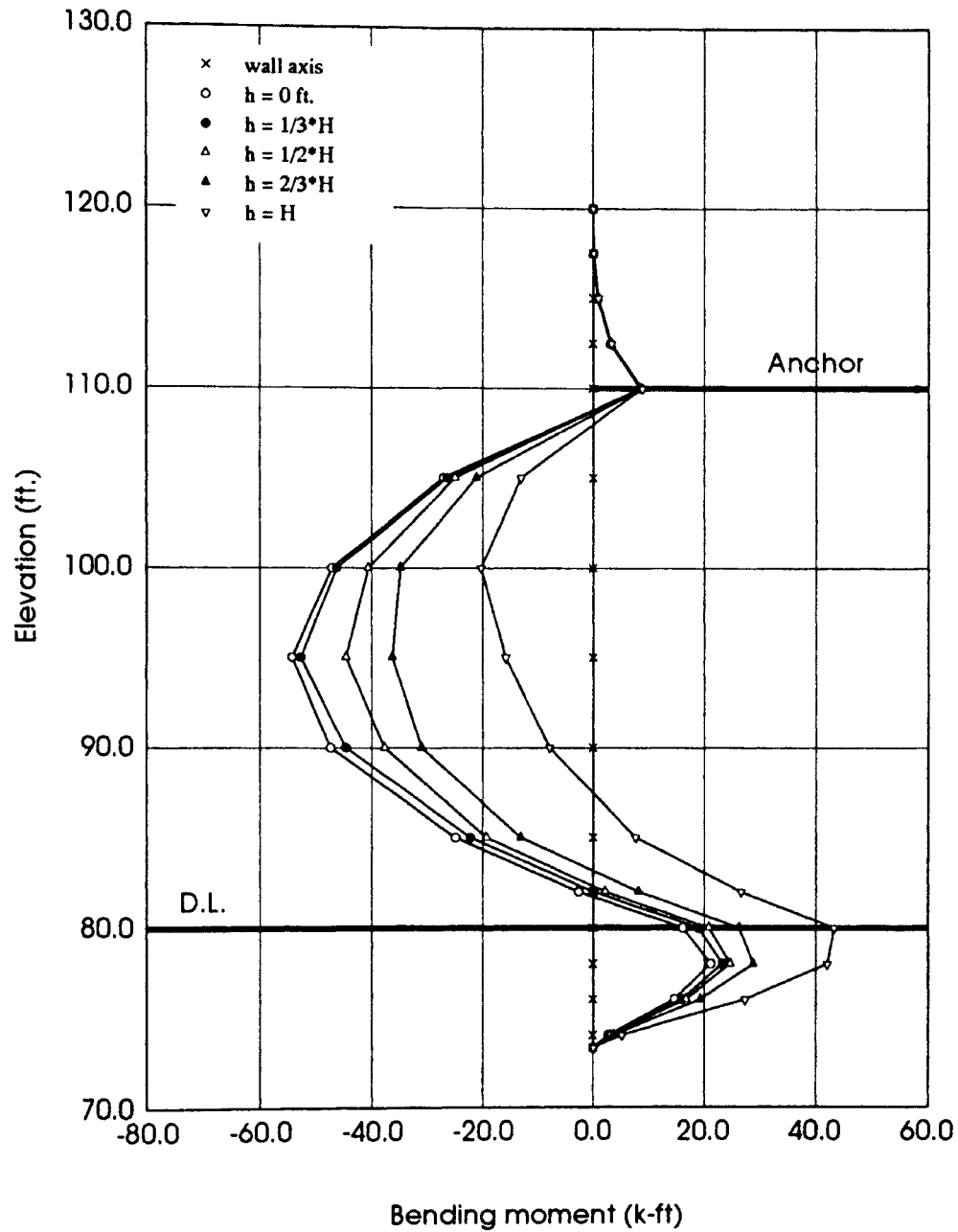


Figure 4.39. Bending Moments for LM40 Case When the Anchor is Placed at Different Fill Levels

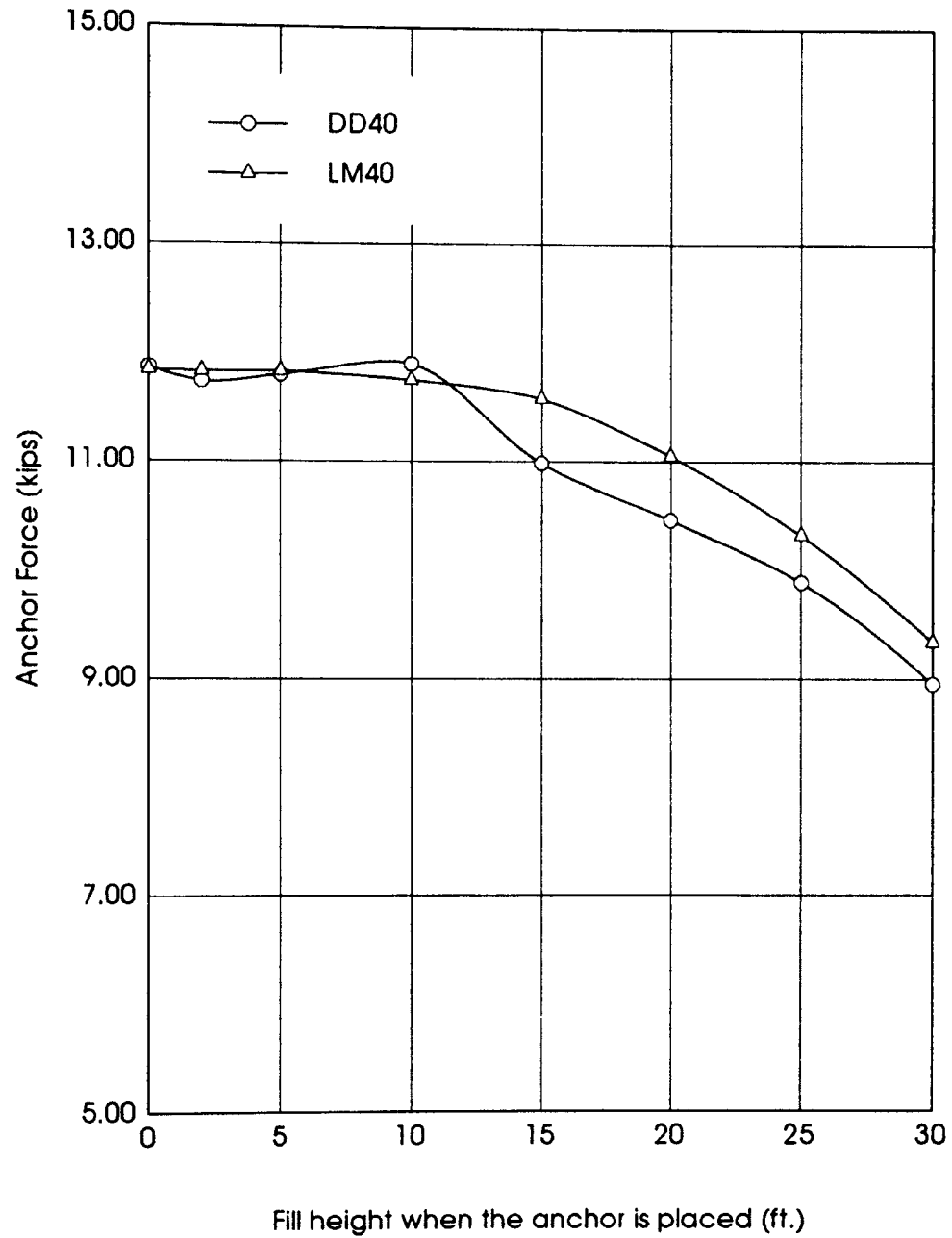


Figure 4.40. Anchor Forces Obtained When the Anchor is Placed at Different Fill Levels

The conclusion reached from the analysis of the results obtained in this section was that if the time for placing the anchor during backfilling was delayed the maximum moments and anchor forces decrease while the deflections increase. For example, if the anchor is placed when the 1/4 of the fill was placed, instead of at the beginning, the maximum bending moment was reduced by 8%, the anchor force remained almost same and the maximum deflection increased by 9%. If the anchor was placed when the 40% of the fill was placed, the maximum bending moment was reduced by 21%, the anchor force was reduced by 5% and the maximum deflection increased by 17%.

This analysis shows that, in engineering problems, the engineer can make a decision on the time of anchor placement according to the priority of the variables of the project at hand. For example, if deflection was the governing criterion then the anchor must be placed at the beginning of the filling. If moment was the governing criterion then the anchor can be placed after some amount of filling was completed.

If an anchored sheet pile wall is constructed by the excavation method, then the anchor may be placed when the excavation reaches the anchor level. Considering this reality, the analyses were repeated for the DD40 and LM40 cases by placing the anchor when excavation reached the anchor level instead of the beginning as it was done in the original analyses. In these cases, the maximum wall deflections increased by about 18%, the maximum moments increased by about 7% and the anchor forces decreased by about 25% by delaying anchor placement until the excavation reached the anchor level.

CHAPTER V

CONCLUSIONS

Twelve anchored sheet pile walls were analyzed by the finite element method for comparing walls constructed by excavation and backfilling. The deformation, stresses and the degree of mobilization in the soil were investigated for comparing the behavior of the soil in wall systems constructed by the two methods. The behavior of the structure was also studied; the deformation and bending moments in the wall and the anchor forces were compared. The conclusions obtained from these comparisons are as follows:

1. The stresses in the soil at large distances from the wall were not affected significantly by the construction method. The differences were localized around the wall, approximately within 10 feet in most cases.
2. In all cases, the soil in front of the wall moved upwards while the soil behind the wall settled, resulting in an overall rotational deformation. The foundation soil in front of the wall heaved considerably in excavation cases because of the reduction in the overburden due to the excavation. In the backfill cases, the settlement due to the weight of the fill behind the wall was more dominant.
3. There was a larger lateral stress in the soil elements in front of the wall near the ground surface as compared with the conventional passive pressures because of the deflection of wall and the soil-wall friction.

4. The maximum deflection of the wall in backfilled cases was larger than for the same wall constructed by excavation (by 43% on the average).
5. The maximum bending moment in backfilled walls was larger than an excavated wall (by 41% on the average).
6. The anchor force was larger in a wall constructed by excavation, as opposed to backfilling, if the foundation soil was an undrained clay. Otherwise, the anchor forces in backfilled cases were larger than those in excavation cases.

The delay in anchor rod installation during a backfilled wall was investigated by a series of special runs. Significant effects of anchor installation time were found:

1. If the time for placing the anchor was delayed, the maximum moments and the anchor forces decreased while the deflections increased. Typical results are such that if the anchor was placed when 40% of the fill was placed, instead of at the beginning of filling, the maximum bending moment was reduced by 21%, the anchor force was reduced by 5% and the maximum deflection increased by 17%. Therefore, if wall deflections were not critical in an application, it may be advantageous to install the anchors at a later stage during backfilling.
2. In an excavated anchored sheet pile wall, the anchor may be placed when the excavation reaches the anchor level. Considering this reality, the analyses were repeated for the DD40 and LM40 cases by placing the anchor when excavation reached the anchor level instead of the beginning. In these cases, the maximum wall deflections increased by about 18%, the maximum moments increased by about 7% and the anchor forces decreased by about 25% by delaying anchor

placement until the excavation reached the anchor level.

These somewhat unexpected and interesting results are certainly very important from a practical point of view. These show that the behavior of an anchored sheet pile wall and the soil mass around the wall are not the same in walls constructed by excavation and backfilling as it is generally assumed. Since the bending moments in the wall are larger in the backfilled cases, the reduction made in the bending moments for free earth support calculations (Rowe 1952, 1957) has to be carefully considered if the wall is constructed by backfilling.

Due to the practical significance of the results of this study it is recommended to perform an experimental counterpart of the investigation for verification. Although a full-scale physical modeling or small-scale centrifuge modeling would be expensive for experimental study, other alternatives may be considered. For example, a few walls that are being constructed may be instrumented for observing their behavior. Small scale laboratory models can also be very useful to compare excavation and backfilling.

BIBLIOGRAPHY

- Bilgin, O., and Oner, M., "Computer Program GENEREF: A User's Guide," Oklahoma State University, Stillwater, 1993.
- Craig, R. F., "Soil Mechanics," Van Nostrand Reinhold, 1989.
- Dawkins, W.P., "Computer Program WALSH: A User's Guide," USAE Waterways Experiment Station, Vicksburg, MS, 1985.
- Duncan, J.M., and Chang, C.Y., "Nonlinear Analysis of Stress and Strain in Soils," Journal of Soil Mechanics and Foundations Division, American Society of Civil Engineers, Vol. 56, 1970, pp. 1625-1653.
- Hallal, I.S., "Analysis of the Nonlinear Behavior of Floodwall Structures," Ph.D. Dissertation, Oklahoma State University, Stillwater, July, 1988.
- Janbu, N., "Soil Model in Offshore Engineering," Geotechnique, Vol. 35, No. 3, 1985, pp. 241-281.
- Kovacs, W.D., Martin, J.H., and Gerig, F.A., "Sheet Pile Design With Variable Soil Parameters," Journal of Soil Mechanics and Foundations Division, American Society of Civil Engineers, Vol. 100, No. 2, Feb., 1974, pp. 200-205.
- Ladd, C.C., Foott, R., Ishihara, K., Schlosser, F., and Poulos, H.G., "Stress-Deformation and Strength Characteristics," Proc. 9th Internal Conference on Soil Mechanics and Foundation Engineering, Tokyo, 1977, Vol. 2, pp. 421-494.
- Oner, M., "Shear Ring Method Verification Studies for Anchored Sheet Pile Walls," An Interim Report for Waterways Experiment Station U.S. Army Corps of Engineers, Oklahoma State University, Stillwater, Mar., 1992.
- Oner, M., "Theoretical Manual for Sheet Pile Walls," (Initial, Partial Draft), Oklahoma State University, Aug., 1989.
- Oner, M., "Computer Program FEMSSI: Finite Element Analysis Method for Soil-Structure Interaction," Oklahoma State University, Stillwater, 1993.

- Rowe, P.W., "Anchored Sheet-Pile Walls," Proceedings, Institution of Civil Engineers, Vol. 4, Part 1, 1952, pp. 27-70.
- Rowe, P.W., "A Theoretical and Experimental Analysis of Sheet-Pile Walls," Proceedings, Institution of Civil Engineers, Vol. 4, Part 1, 1955, pp. 32-69.
- Rowe, P.W., "Sheet-Pile Walls Encastre at the Anchorage," Proceedings, Institution of Civil Engineers, Vol. 4, Part 1, 1955, pp. 70-87.
- Rowe, P.W., "Sheet-Pile Walls At Failure," Proceedings, Institution of Civil Engineers, Vol. 5, Part 1, 1956, pp. 276-315.
- Rowe, P.W., "Sheet-Pile Walls in Clay," Proceedings, Institution of Civil Engineers, Vol. 7, 1957, pp. 629-654.
- Sowers, B.G., and Sowers, G.F., "Failures of Bulkheads and Excavation Bracing," Civil Engineering, American Society of Civil Engineers, Vol. 37, No. 1, 1967, pp. 72-77.

APPENDIXES

APPENDIX A

INPUT AND OUTPUT FILES USED IN
THE FINITE ELEMENT ANALYSES

Example of the GEN file:

DD40 CASE DENSE SAND BACKFILL AND FOUNDATION

'---May 15th 1993

'---nodes in x & y directions & number of layers to excavate

10,23,11

'---extra nodes in the middle (# beams + 1)

17

'---xi (from left to right)

0,2,5,10,20,35,55,80,110,160

'---yi (from bottom to top node)

0,22,40,55,65,70,71.5,72.5,74,76,78,80

82,85,90,95,100,105,110,112.5,115,117.5,120

'---Beam & link data

PZ35

'---Links

DEFAULT

'---Soil props

3

'Number of element layers of each soil type (LayersOfSoilType)

4, 7, 11

'---friction - adhesion

.44523, 0

.44523, 0

.44523, 0

'---Soil props: c, phi, gamma, Ko, nui, nuf, m, n

0.0, 36.0, 110.0, 0.412, 0.25, 0.49, 200, 0.5

0.0, 36.0, 68.5, 0.412, 0.25, 0.49, 200, 0.5

0.0, 36.0, 68.5, 0.412, 0.25, 0.49, 200, 0.5

'---Number of points (depths) in Cu table

0

'---Node from the top where anchor should be placed & AnchorStiff

5, 200000

'---Boundary condition codes (side, corner, bottom)

1, 3, 3

The Input data file for Finite Element Program :

DD40 CASE DENSE SAND BACKFILL AND FOUNDATION

GENERAL

471,446,12,2000

COORDINATES

1,-160,120

2,-110,120

3,-80,120

4,-55,120

.

.

469,80,0

470,110,0

471,160,0

CONNECTIVITY

1 ,1,22,23,2

2 ,2,23,24,3

3 ,3,24,25,4

.

444 ,305,306,-1,0

445 ,326,327,-1,0

446 ,347,348,-1,0

SOIL PROPERTIES FOR 3 TYPE(S)

1 ,0.0, 36.0, 110.0, 0.412, 0.25, 0.49, 200, 0.5

2 ,0.0, 36.0, 68.5, 0.412, 0.25, 0.49, 200, 0.5

3 ,0.0, 36.0, 68.5, 0.412, 0.25, 0.49, 200, 0.5

TYPE NUMBERS 396

1,72,1,1

73,198,1,2

199,396,1,3

BEAM 16

397,412,1,1,4.176E+09,.1,.01742

LINK 34

413,416,1,1,2,1E+09,100000,.44523,0,0,0

430,433,1,1,1,1E+09,100000,.44523,0,0,0

417,423,1,1,2,1E+09,100000,.44523,0,0,0

434,440,1,1,1,1E+09,100000,.44523,0,0,0

424,429,1,1,2,1E+09,100000,.44523,0,0,0

441,446,1,1,1,1E+09,100000,.44523,0,0,0

TO BE EXCAVATED LATER 99

1,9,1

19,27,1

37,45,1

55,63,1
 73,81,1
 91,99,1
 109,117,1
 127,135,1
 145,153,1
 163,171,1
 181,189,1
BOUNDARY NODES 63
 1,337,21,1
 21,357,21,1
 358,434,19,1
 376,452,19,1
 453,471,18,3
 454,470,1,3

STEP 1
GRAVITATE 396 ELEMENTS
 1,396,1
 1.0

STEP 2 : EX LAYER 1
ANCHOR 1
 95,95,1,200000,0
SUBSTEPS 4
EXCAVATE
NODE 10
 1,10,1
SOIL 9
 1,9,1
LINK 1
 413,413,1

STEP 12 : EX LAYER 11
SUBSTEPS 4
EXCAVATE
NODE 10
 211,220,1
SOIL 9
 181,189,1
LINK 1
 423,423,1

The Output File of Finite Element Program :

[DD40 CASE DENSE SAND BACKFILL AND FOUNDATION,

NODAL POINTS = 471
 # ELEMENTS = 446
 # OPERATION STEPS = 12
 ATMOSPHERIC PRES.= 2000.0

NODE COORDINATES

NODE	X	Y
1	-160.00	120.00
2	-110.00	120.00
...		
...		
471	160.00	.00

ELEMENT CORNER NODES

1	1	22	23	2
2	2	23	24	3
...				
...				
446	347	348	-1	0

SOIL MODEL PARAMETERS...

TYPE	C	FI	GAMMA	KO	NUI	NUF	M	N
1	.00	36.00	110.00	.412	.250	.490	200.0	.500
2	.00	36.00	68.50	.412	.250	.490	200.0	.500
3	.00	36.00	68.50	.412	.250	.490	200.0	.500

SOIL TYPE NUMBERS FOR 396 ELEMENTS

FROM	TO	STEPS	TYPE
1	72	1	1
73	198	1	2
199	396	1	3

BEAM ELEMENTS: 16

FROM	TO	STEPS	INIT	E	A	I
397	412	1	1	.4176E+10	.1000E+00	.1742E-01

LINK ELEMENTS: 34

FROM	TO	STEP	INIT	R/L	SN	ST	MU	ADHSN	FN-INIT	FT-INIT
413	416	1	1	2	1.00E+09	1.00E+05	.45	.00	.00	.00
430	433	1	1	1	1.00E+09	1.00E+05	.45	.00	.00	.00
417	423	1	1	2	1.00E+09	1.00E+05	.45	.00	.00	.00
434	440	1	1	1	1.00E+09	1.00E+05	.45	.00	.00	.00
424	429	1	1	2	1.00E+09	1.00E+05	.45	.00	.00	.00
441	446	1	1	1	1.00E+09	1.00E+05	.45	.00	.00	.00

ELEMENTS TO BE EXCAVATED LATER: 99

FROM	TO	STEPS
1	9	1
19	27	1
37	45	1
55	63	1
73	81	1
91	99	1
109	117	1
127	135	1
145	153	1
163	171	1
181	189	1

BOUNDARY CONDITIONS AT 63 NODES

FROM	TO	STEP	X-DIR	Y-DIR	ROTN
1	337	21	FIXED	FREE	FREE
21	357	21	FIXED	FREE	FREE
358	434	19	FIXED	FREE	FREE
376	452	19	FIXED	FREE	FREE
453	471	18	FIXED	FIXED	FREE

454 470 1 FIXED FIXED FREE

HALF BAND WIDTH= 46
ROTATIONAL D.O.F.: 17

```

+-----+
| OPERATION STEP 1 OF 12 |
+-----+

```

[STEP 1

TURN GRAVITY ON 396 ELEMENTS
FROM TO STEPS
1 396 1
FRACTION OF K0 STRESS: 1.00

=== SUBSTEP 1 OF 1 ===

WARNING: BEAM NOT ASSEMBLED DURING GRAVITY TURN-ON.

FORCES IN THE LINK ELEMENTS

ELT.	LINK	FN	FT
413	1	9.4547E+01	1.1102E-11
414	2	3.7818E+02	3.3307E-11
...			
...			
445	33	2.5105E+03	0.0000E+00
446	34	2.5807E+03	1.6653E-11

STRESSES AT THE END OF STEP 1, SUBSTEP 1 OF 1

ELEMENT	X-STRESS	Y-STRESS	XY-STRESS	P.PRES.	G-MOD.	M-MOD.	F
1	75.63	137.50	.00	.00	5.6046E+04	2.4909E+05	.418
2	75.62	137.50	.00	.00	5.6046E+04	2.4909E+05	.418
...							
...							
395	4334.82	7881.50	.00	.00	4.2432E+05	1.8859E+06	.418
396	4334.82	7881.50	.00	.00	4.2432E+05	1.8859E+06	.418

```

+-----+
| OPERATION STEP 2 OF 12 |
+-----+

```

{ STEP 2 : EX LAYER 1

NEW ANCHORS: 1
FROM TO STEPS X-SPRING Y-SPRING
95 95 1 2.0000E+05 0.0000E+00

NUMBER OF SUBSTEPS: 4

REMOVED NODES: 10
FROM TO STEPS
1 10 1

REMOVED SOIL ELEMENTS: 9
FROM TO STEPS
1 9 1

REMOVED LINKS: 1
GENERATED NODAL LOADS
LINK NODE FX FY NODE FX FY

=== SUBSTEP 4 OF 4 ===

...

...

```

+-----+

```

| OPERATION STEP 12 OF 12 |
+-----+

[STEP 12 : EX LAYER 11

NUMBER OF SUBSTEPS: 4

REMOVED NODES: 10
FROM TO STEPS
211 220 1

REMOVED SOIL ELEMENTS: 9
FROM TO STEPS
181 189 1

REMOVED LINKS: 1
GENERATED NODAL LOADS
LINK NODE FX FY NODE FX FY

=== SUBSTEP 4 OF 4 ===

DISPLACEMENTS

NODE NUM	STEP X-DISP.	STEP Y-DISP.	TOTAL X-DISP.	TOTAL Y-DISP.
...				
11	.3102E-03	-.6059E-03	-.8728E-02	.5796E-01
12	.3102E-03	-.5691E-03	-.8728E-02	.4606E-01
...				
470	.0000E+00	.0000E+00	.0000E+00	.0000E+00
471	.0000E+00	.0000E+00	.0000E+00	.0000E+00

DISPLACEMENT OF BEAM ELEMENTS

ELT	NODE	X-DISP.	Y-DISP.	ROTATION	NODE	X-DISP.	Y-DISP.	ROTATION
397	11	-8.728E-03	5.796E-02	-4.064E-03	32	-1.890E-02	5.796E-02	-4.080E-03
398	32	-1.890E-02	5.796E-02	-4.080E-03	53	-2.919E-02	5.796E-02	-4.170E-03
...								
411	305	-8.733E-02	5.816E-02	4.439E-03	326	-8.065E-02	5.816E-02	4.460E-03
412	326	-8.065E-02	5.816E-02	4.460E-03	347	-7.619E-02	5.816E-02	4.464E-03

FORCES IN THE BEAM ELEMENTS

ELT.	NODE	FX	FY	MOMENT	NODE	FX	FY	MOMENT
397	11	-3.704E+02	3.660E+01	1.635E-10	32	3.704E+02	-3.660E+01	-9.260E+02
398	32	-1.356E+03	-8.588E+01	9.260E+02	53	1.356E+03	8.588E+01	-4.315E+03
...								
411	305	-6.815E+02	-1.310E+03	-1.544E+03	326	6.815E+02	1.310E+03	5.218E+02
412	326	-5.218E+02	-7.988E+02	-5.218E+02	347	5.218E+02	7.988E+02	-8.061E-10

FORCES IN THE LINK ELEMENTS

ELT.	LINK	FN	FT
424	23	3.1821E+03	1.4168E+03
...			
445	33	1.3834E+03	-4.1227E+02
446	34	1.5145E+03	-3.9901E+01

ANCHOR FORCES

ANCH.	NODE	X-FORCE	Y-FORCE
1	95	-1.033E+04	0.000E+00

STRESSES AT THE END OF STEP 12, SUBSTEP 4 OF 4

ELEMENT	X-STRESS	Y-STRESS	XY-STRESS	P.PRES.	G-MOD.	M-MOD.	F
10	308.20	162.19	16.51	.00	3.7857E+04	1.6965E+05	.462
...							
395	4124.67	7746.41	206.18	.00	3.9442E+05	1.7587E+06	.444
396	4189.33	7795.94	72.05	.00	4.0476E+05	1.8005E+06	.435

APPENDIX B

POST-PROCESSING PLOTS

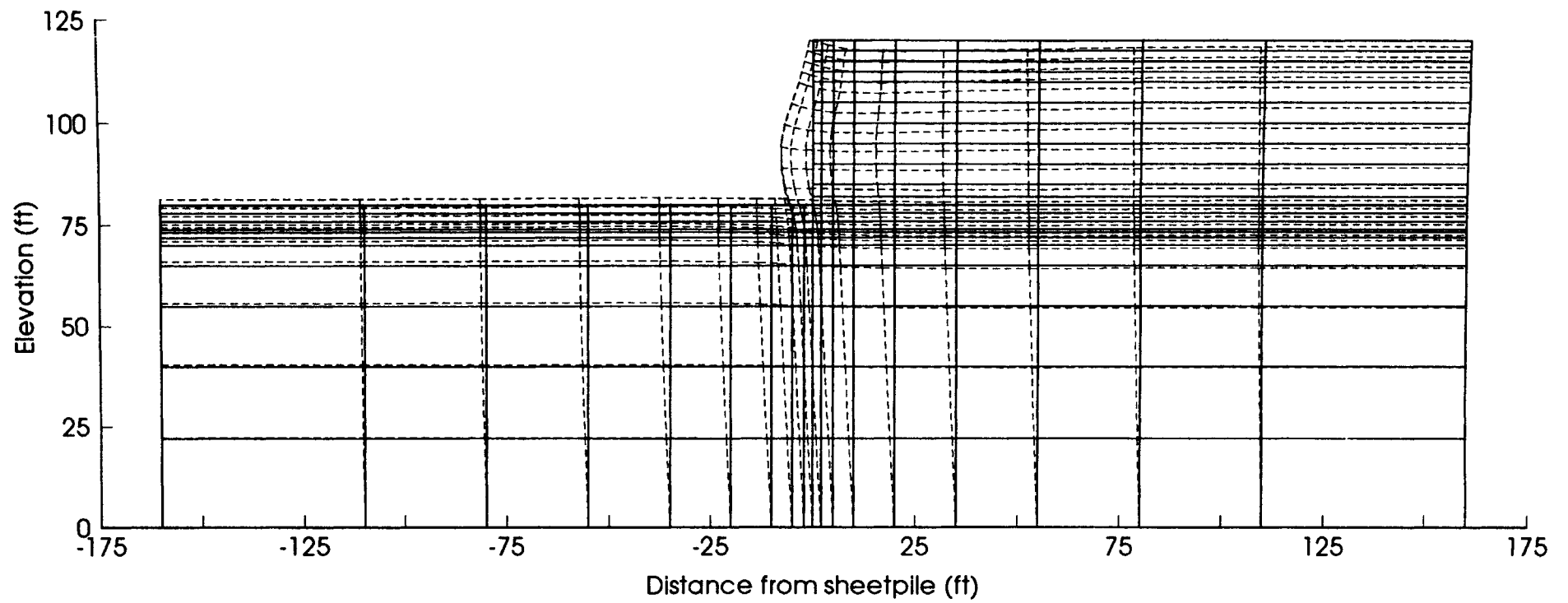


Figure B.1. LM40 Case - Excavation: Deformed Shape (x50)

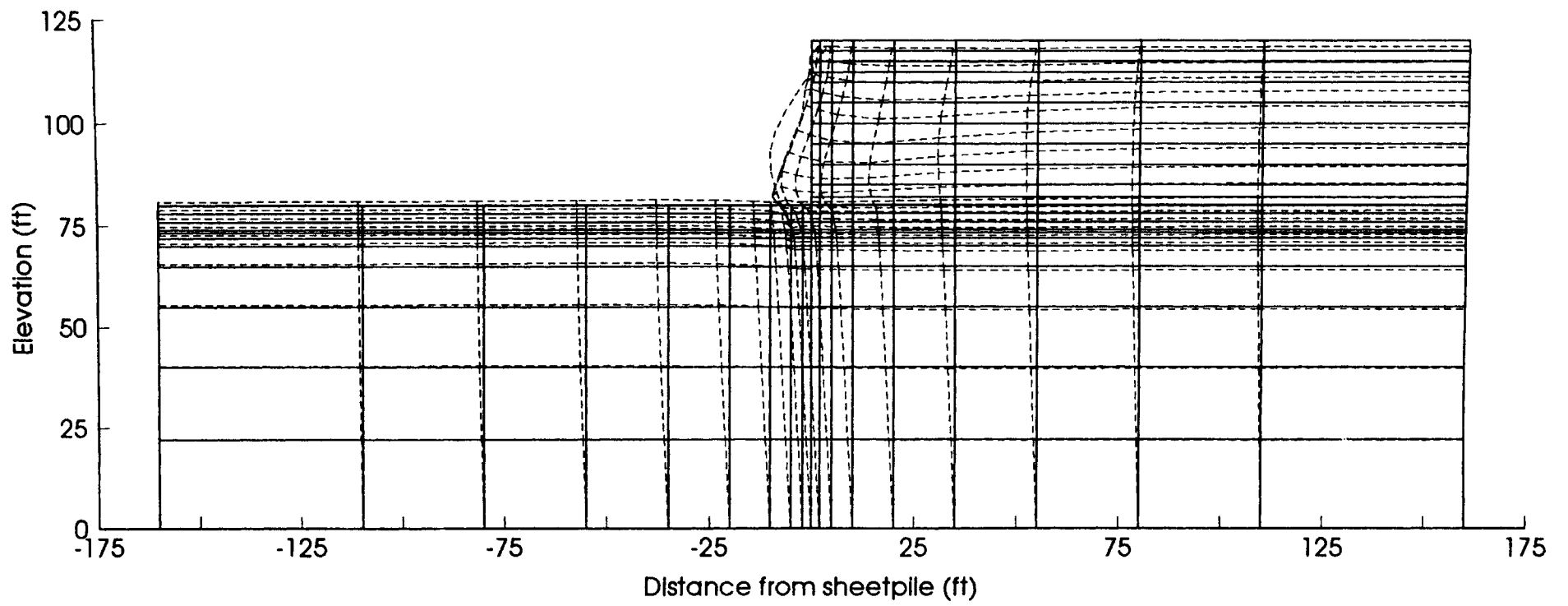


Figure B.2. LM40 Case - Backfill: Deformed Shape (x50)

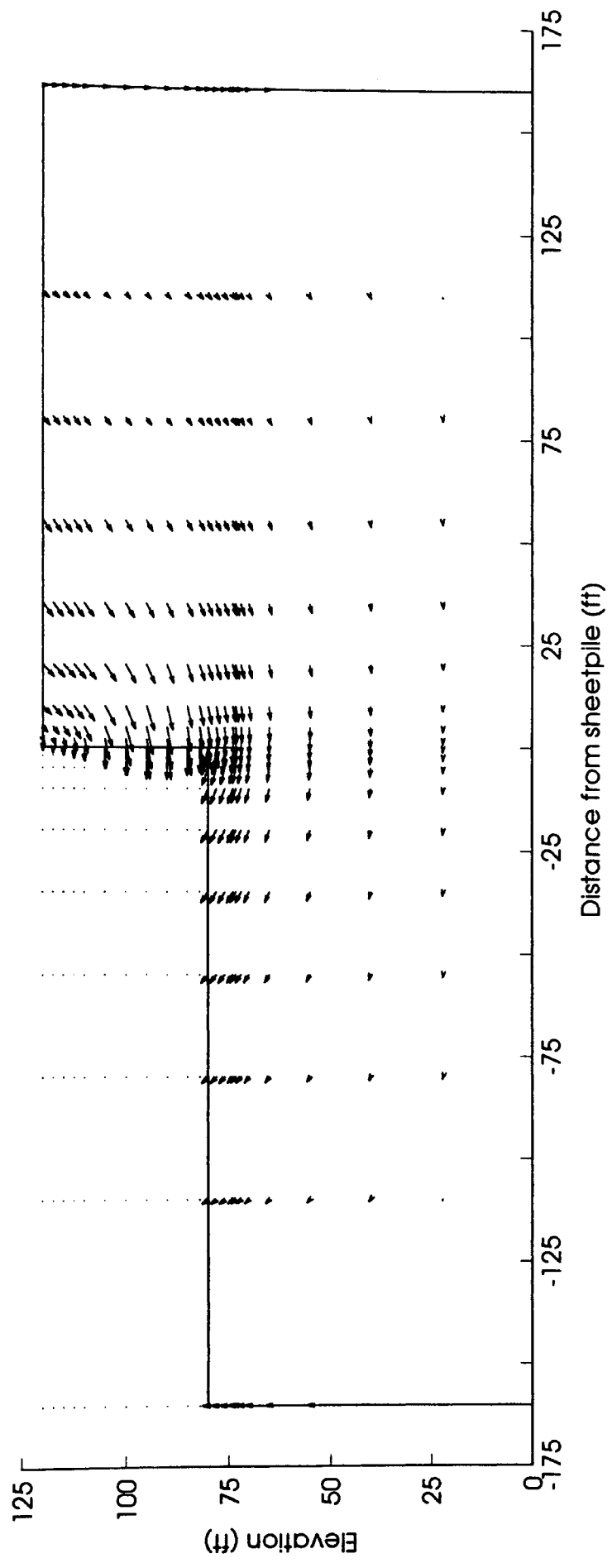


Figure B.3. LM40 Case - Excavation: Displacement Vectors (x50)

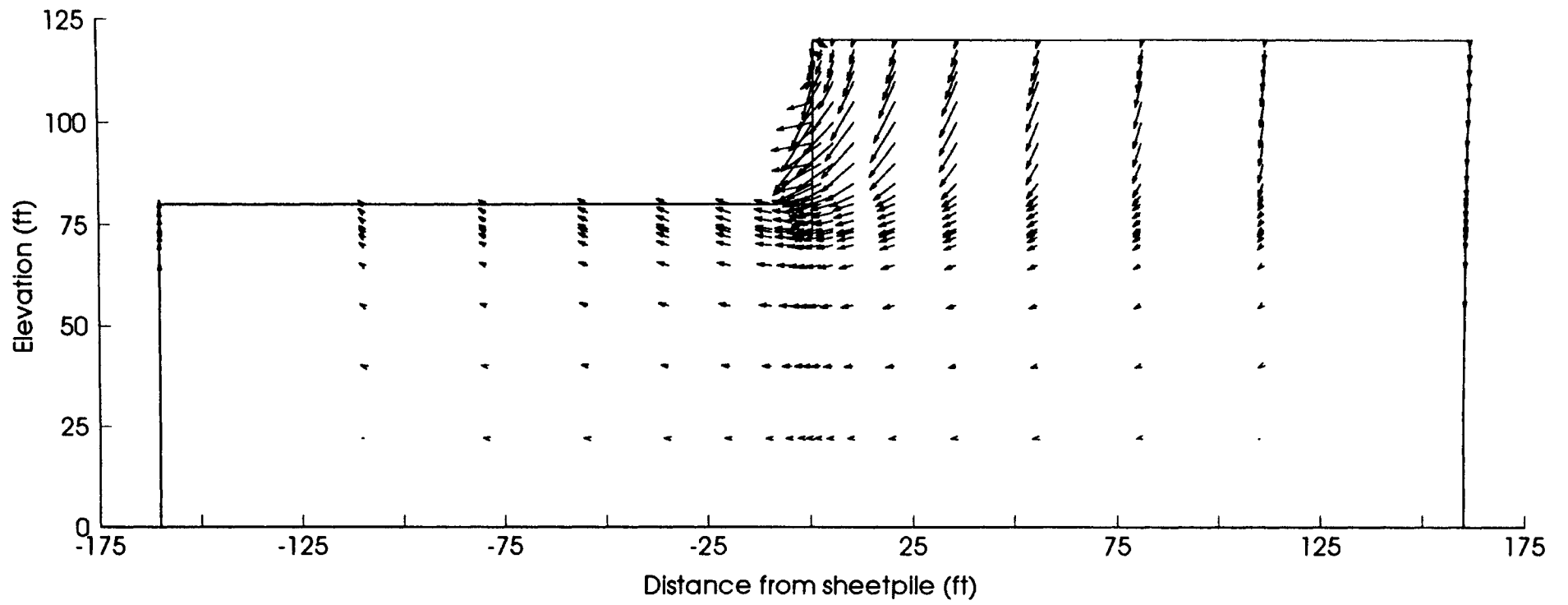


Figure B.4. LM40 Case - Backfill: Displacement Vectors (x50)

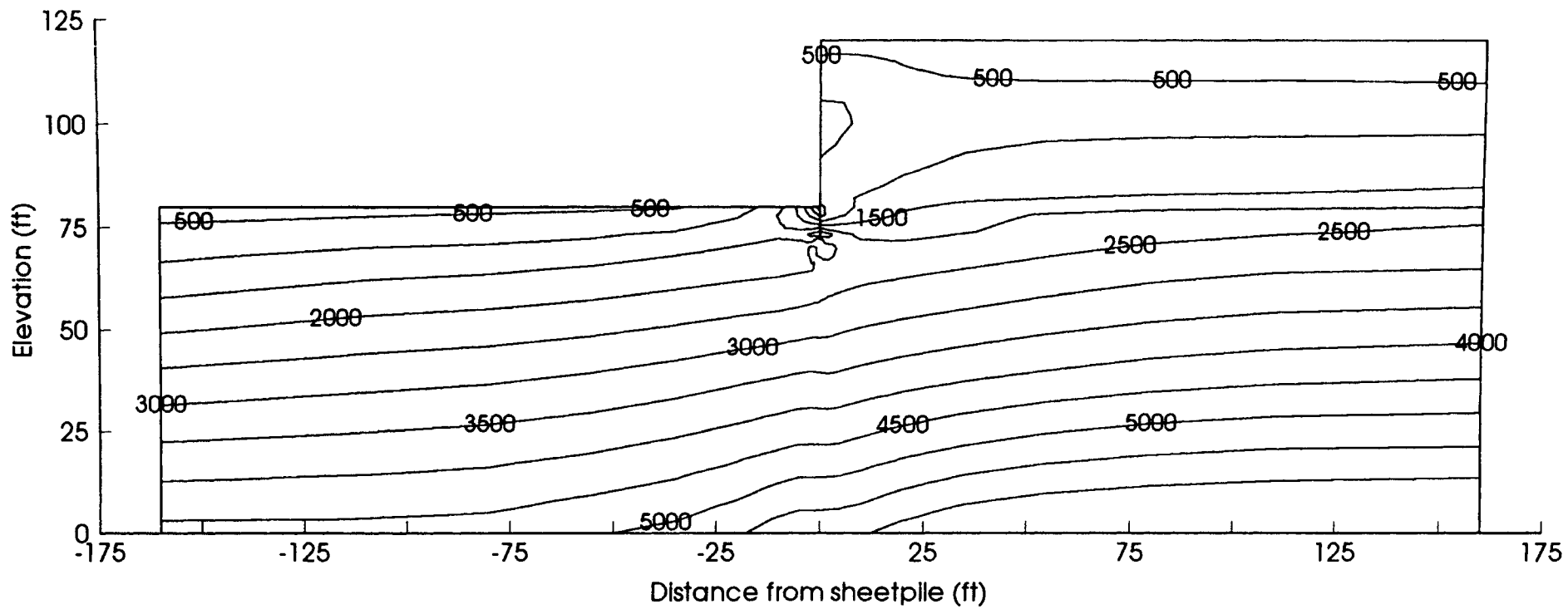


Figure B.5. LM40 Case - Excavation: Horizontal Stress - σ_x (psf)

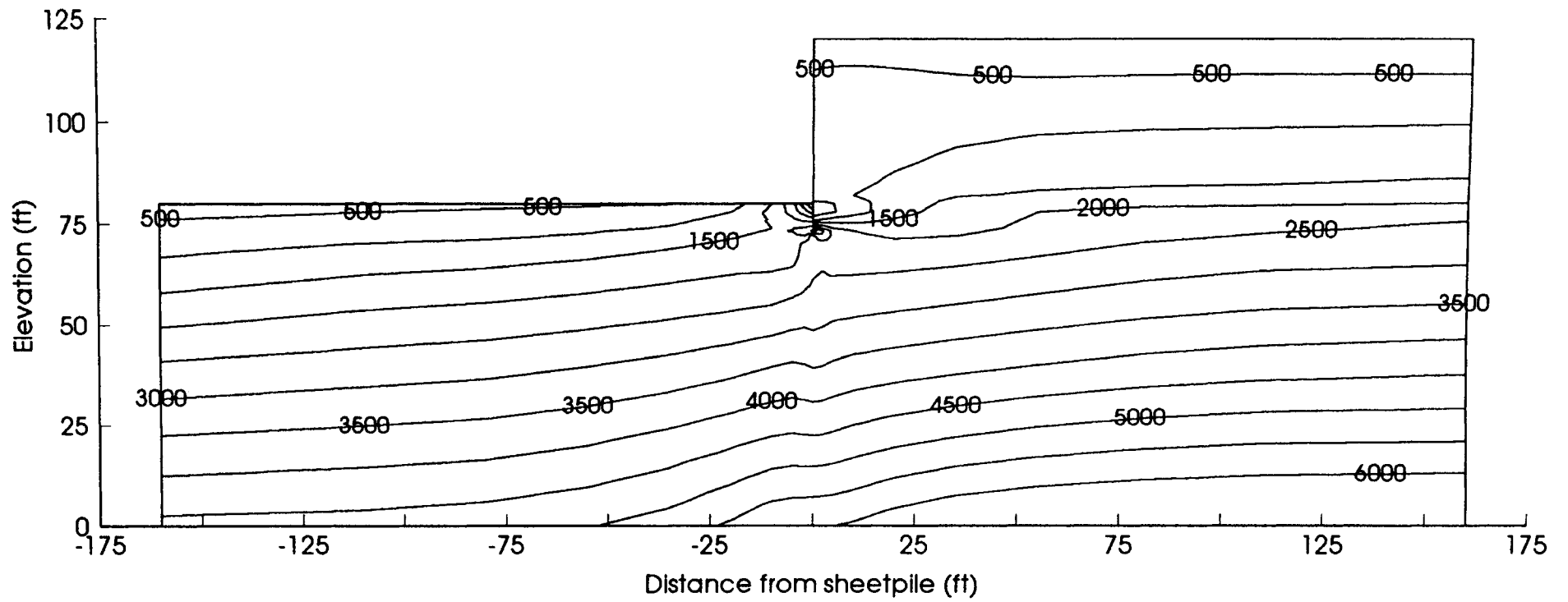


Figure B.6. LM40 Case - Backfill: Horizontal Stress - σ_x (psf)

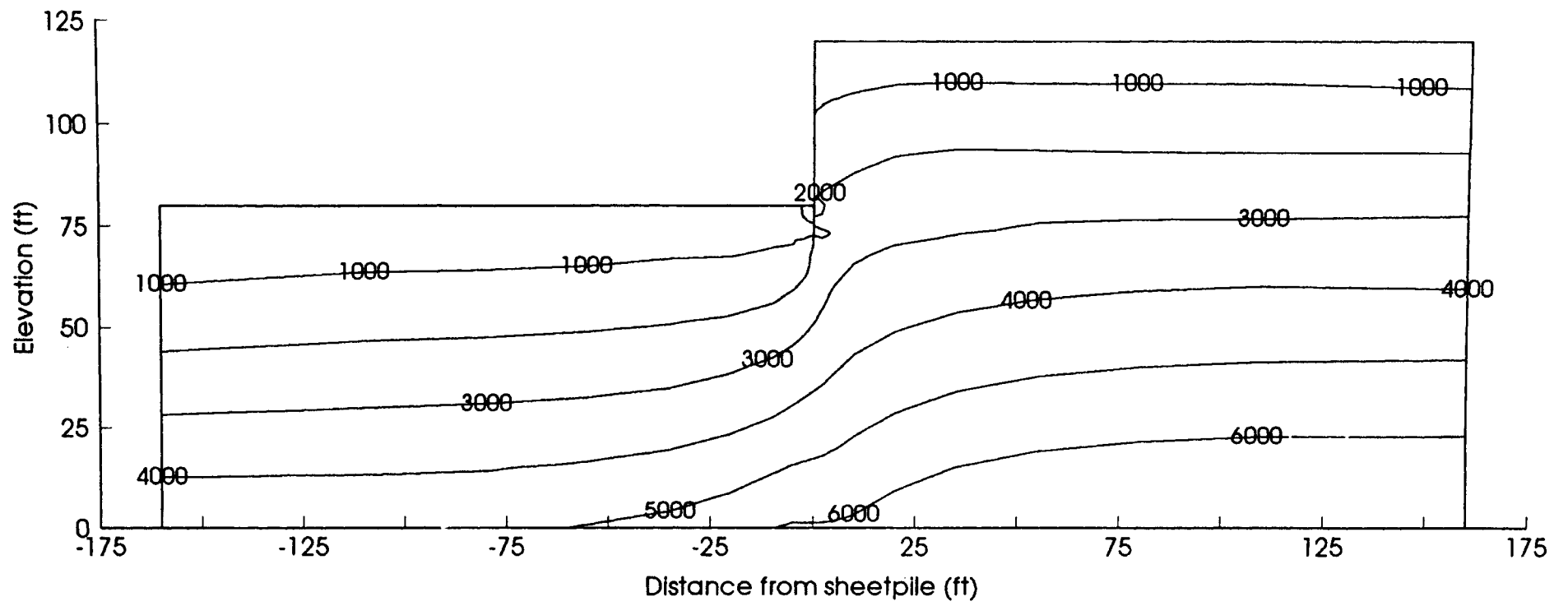


Figure B.7. LM40 Case - Excavation: Vertical Stress - σ , (psf)

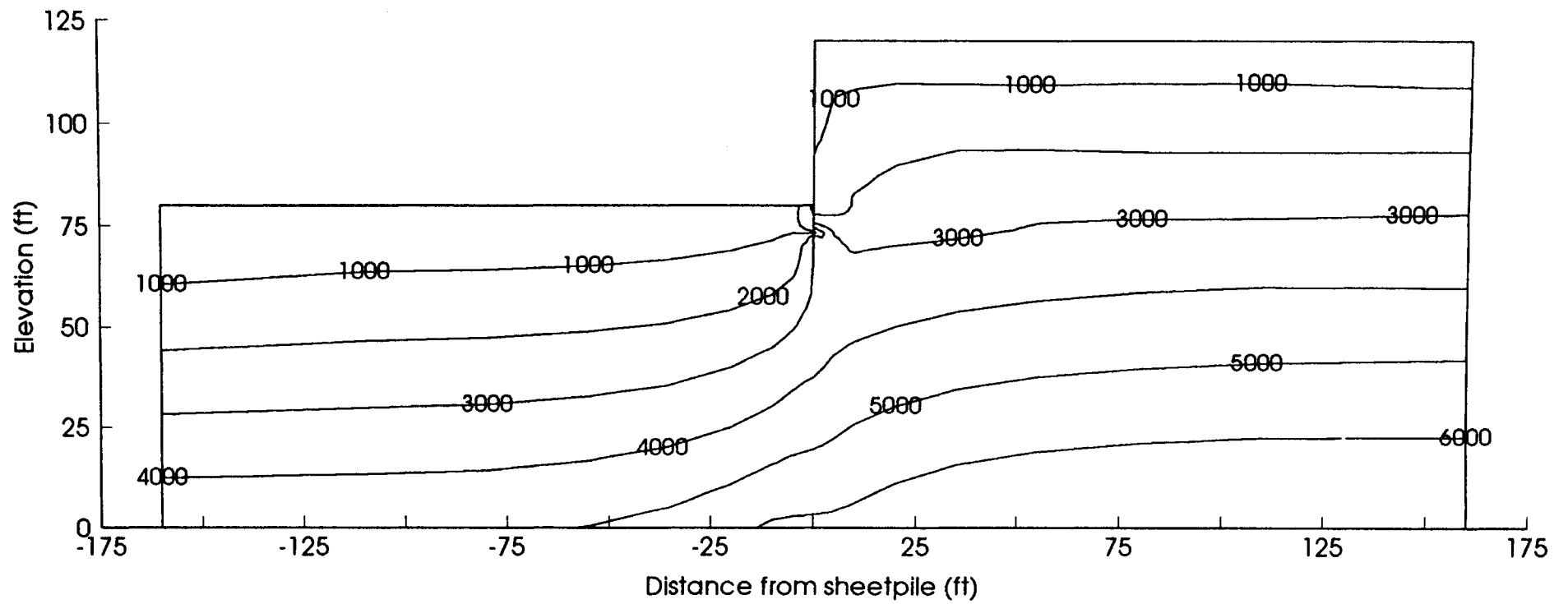


Figure B.8. LM40 Case - Backfill: Vertical Stress - σ , (psf)

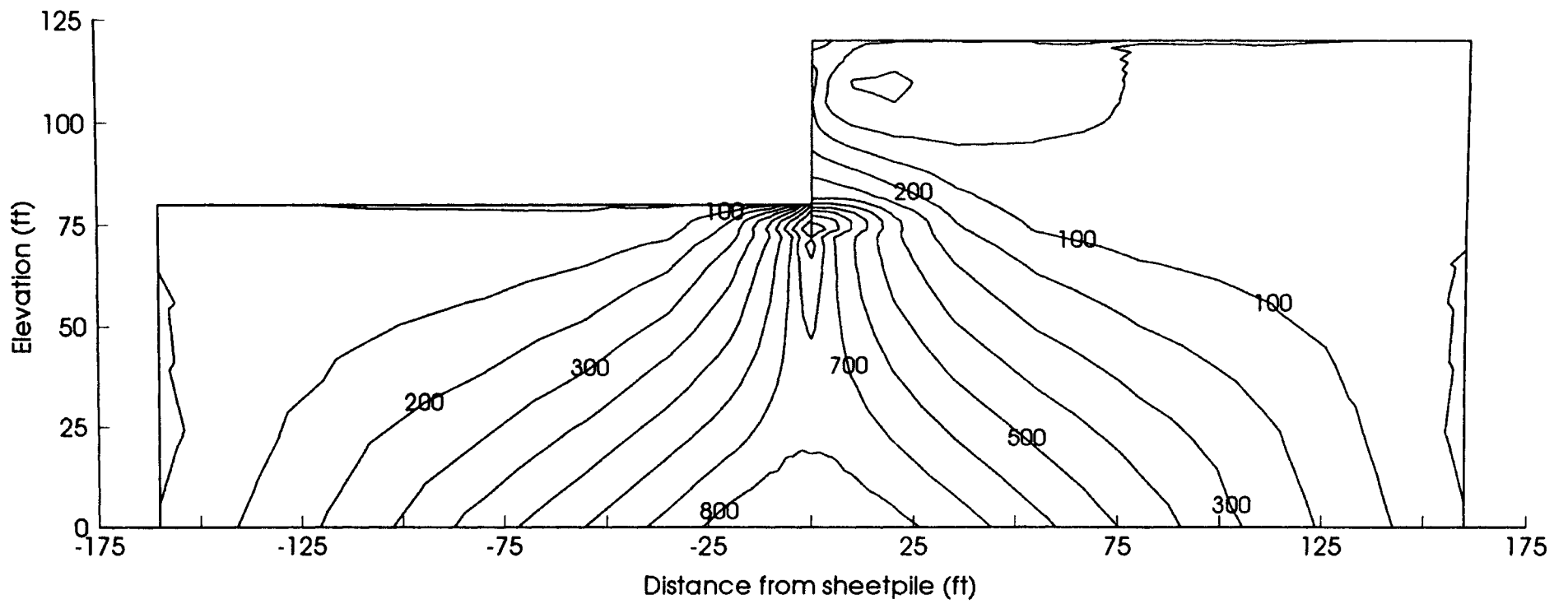


Figure B.9. LM40 Case - Excavation: Shear Stress - τ_v (psf)

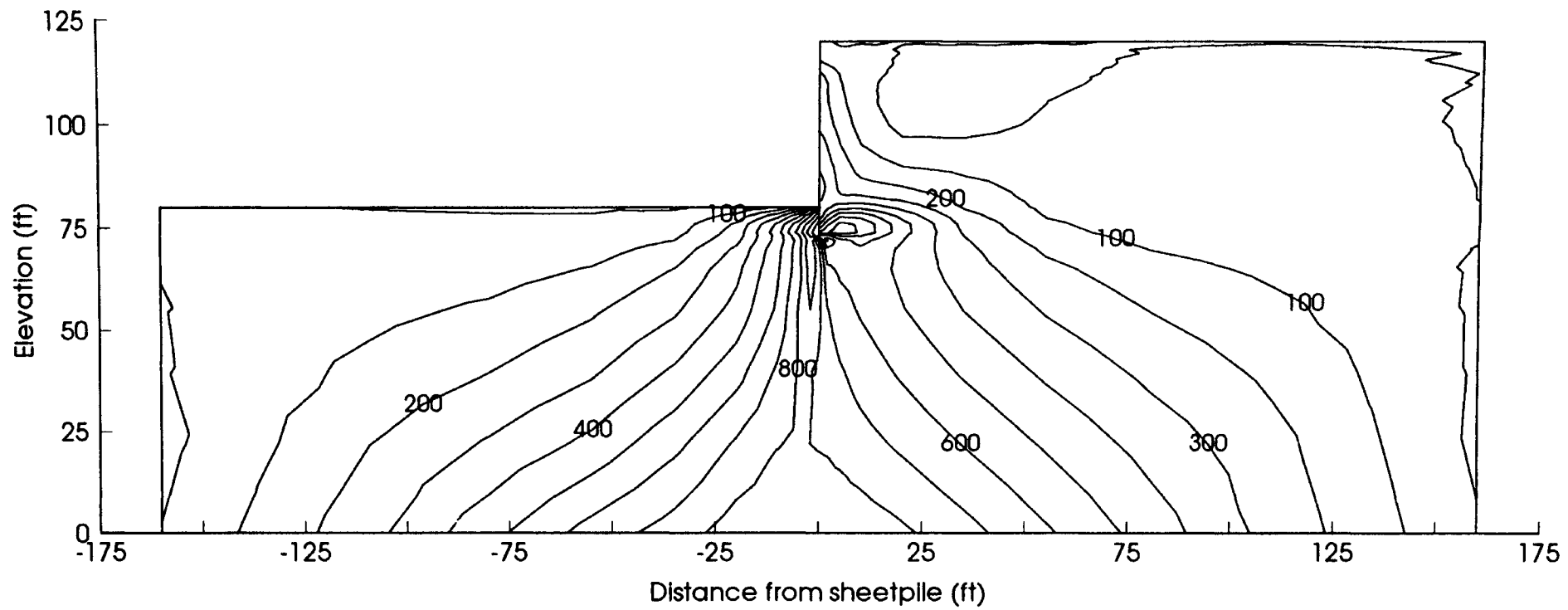


Figure B.10. LM40 Case - Backfill: Shear Stress - τ_v (psf)

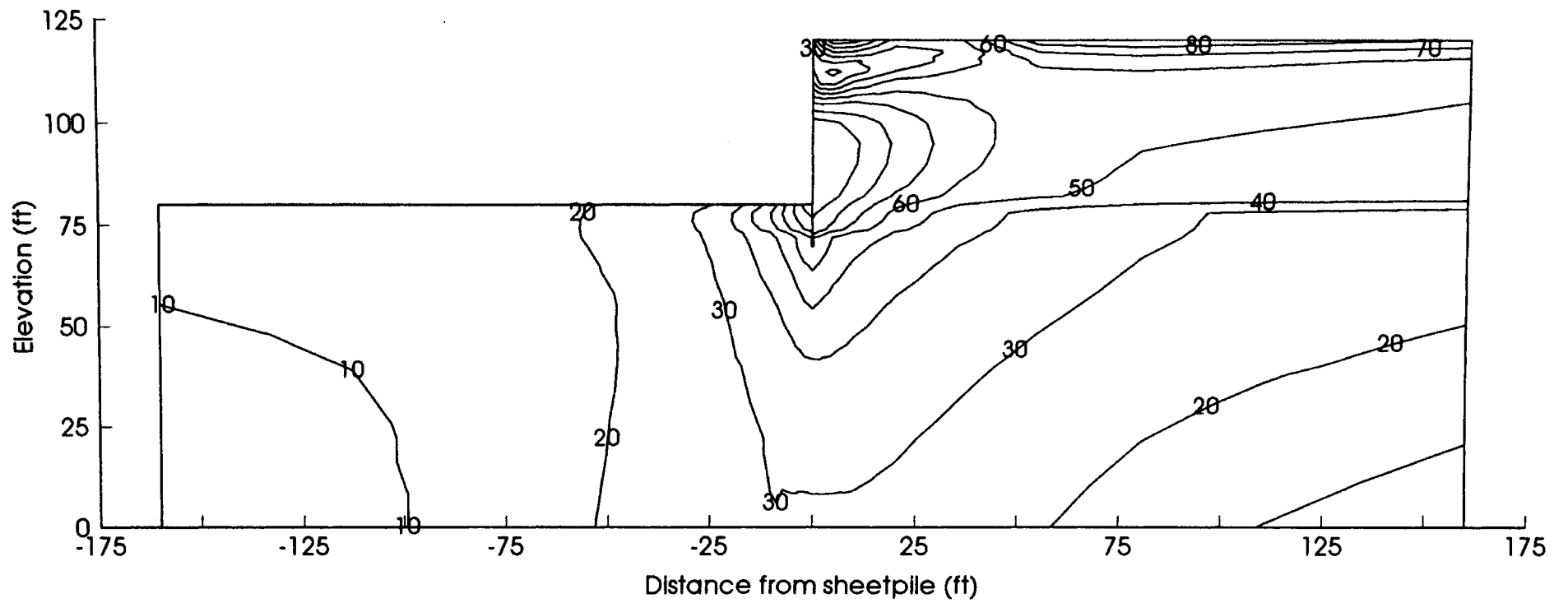


Figure B.11. LM40 Case - Excavation: Degree of Mobilization - f (%)

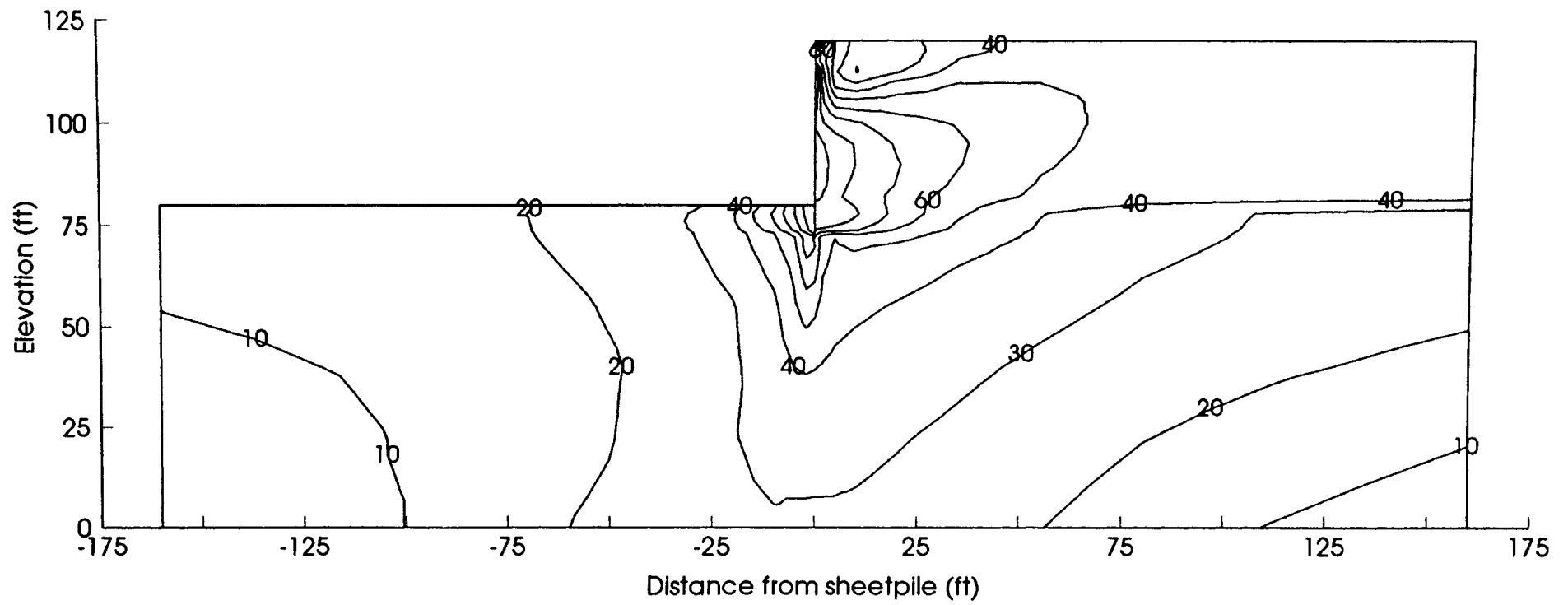


Figure B.12. LM40 Case - Backfill: Degree of Mobilization - f (%)

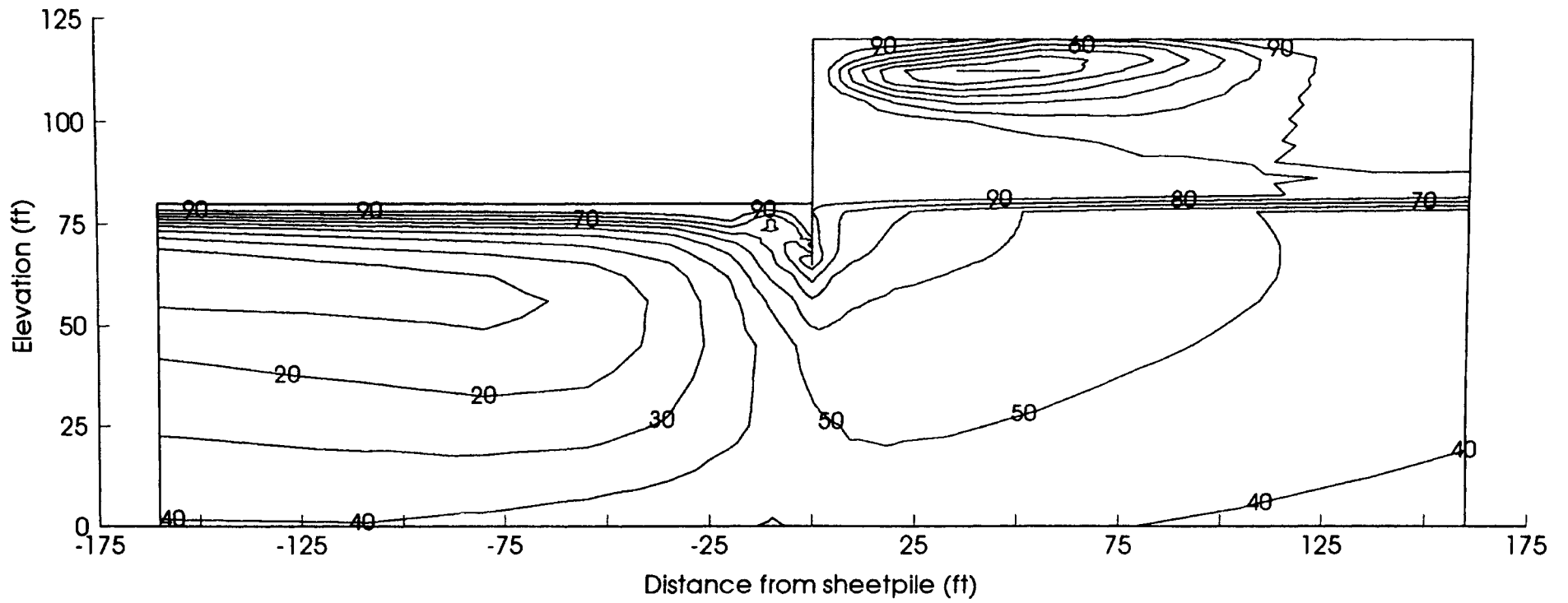


Figure B.13. DN40 Case - Excavation: Degree of Mobilization - f (%)

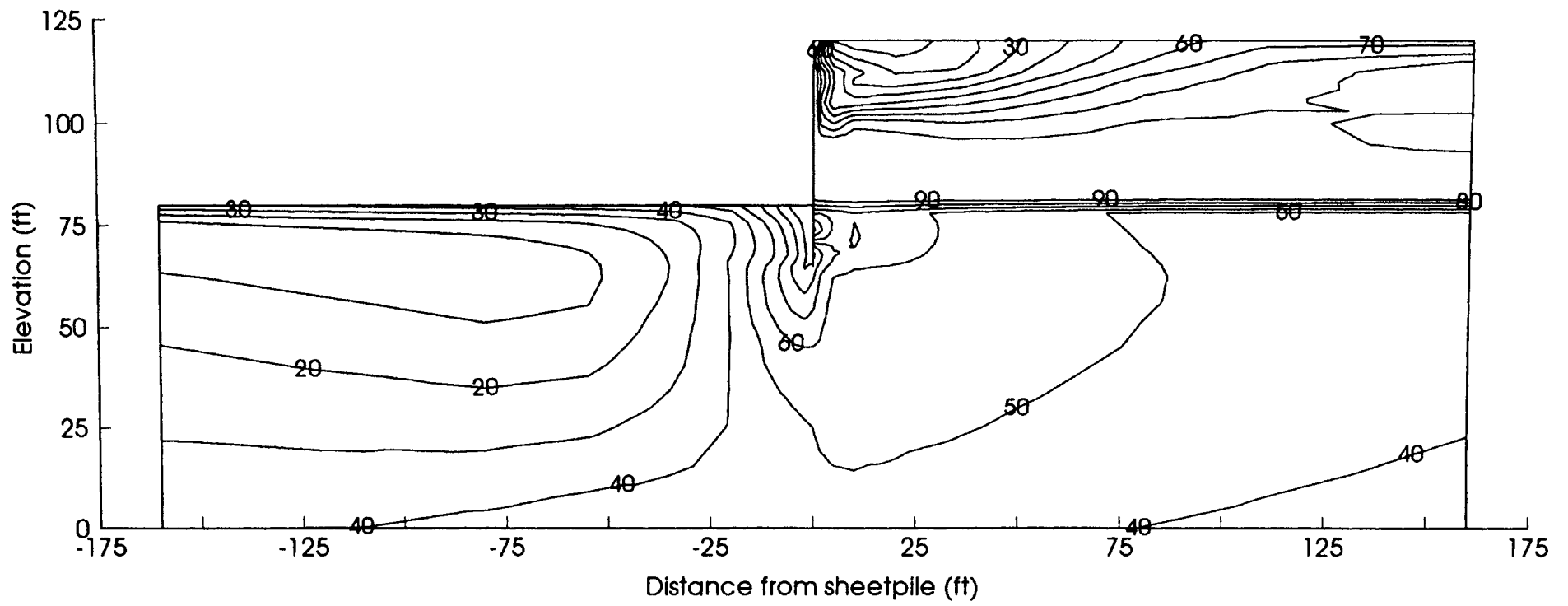


Figure B.14. DN40 Case - Backfill: Degree of Mobilization - f (%)

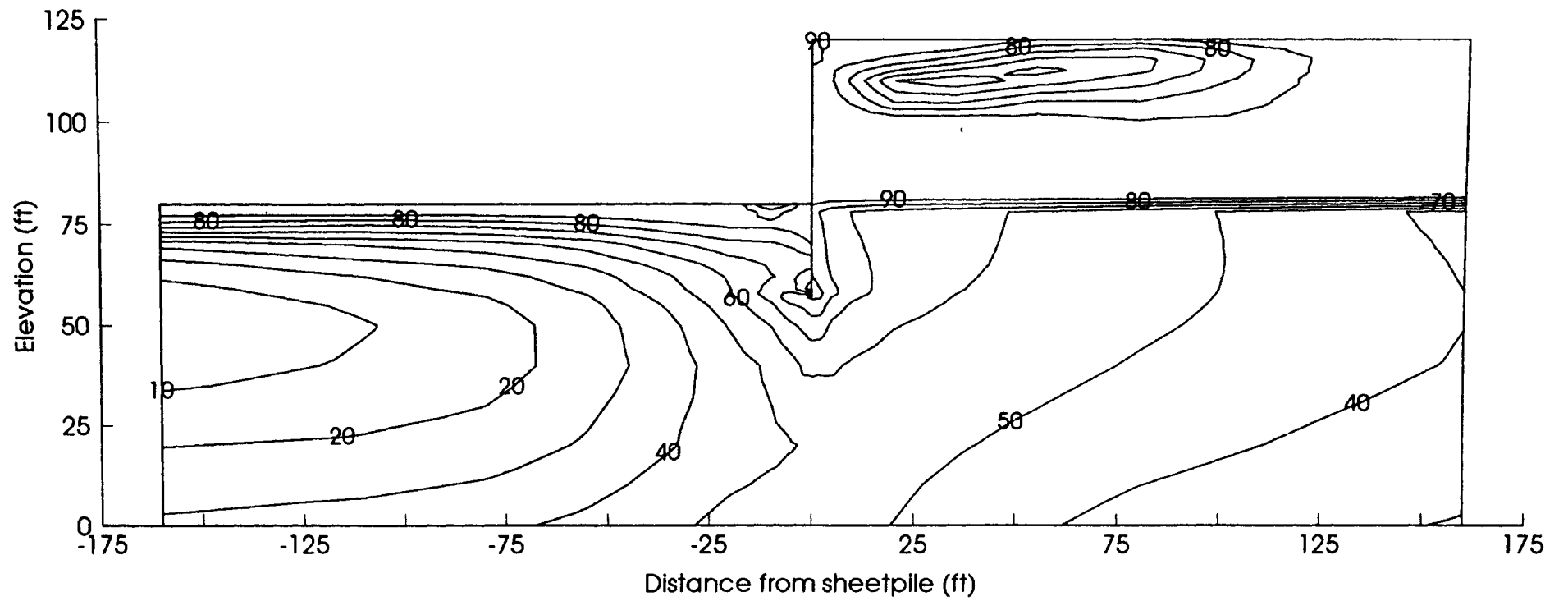


Figure B.15. DT40 Case - Excavation: Degree of Mobilization - f (%)

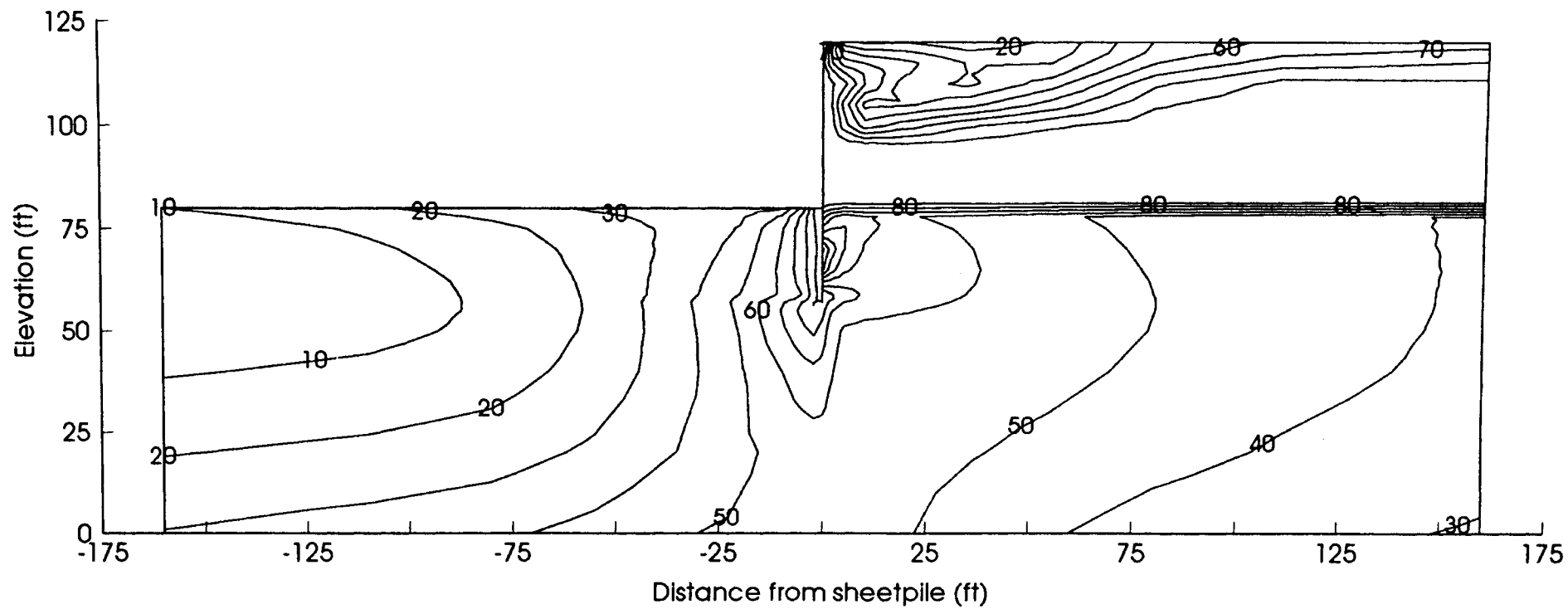


Figure B.16. DT40 Case - Backfill: Degree of Mobilization - f (%)

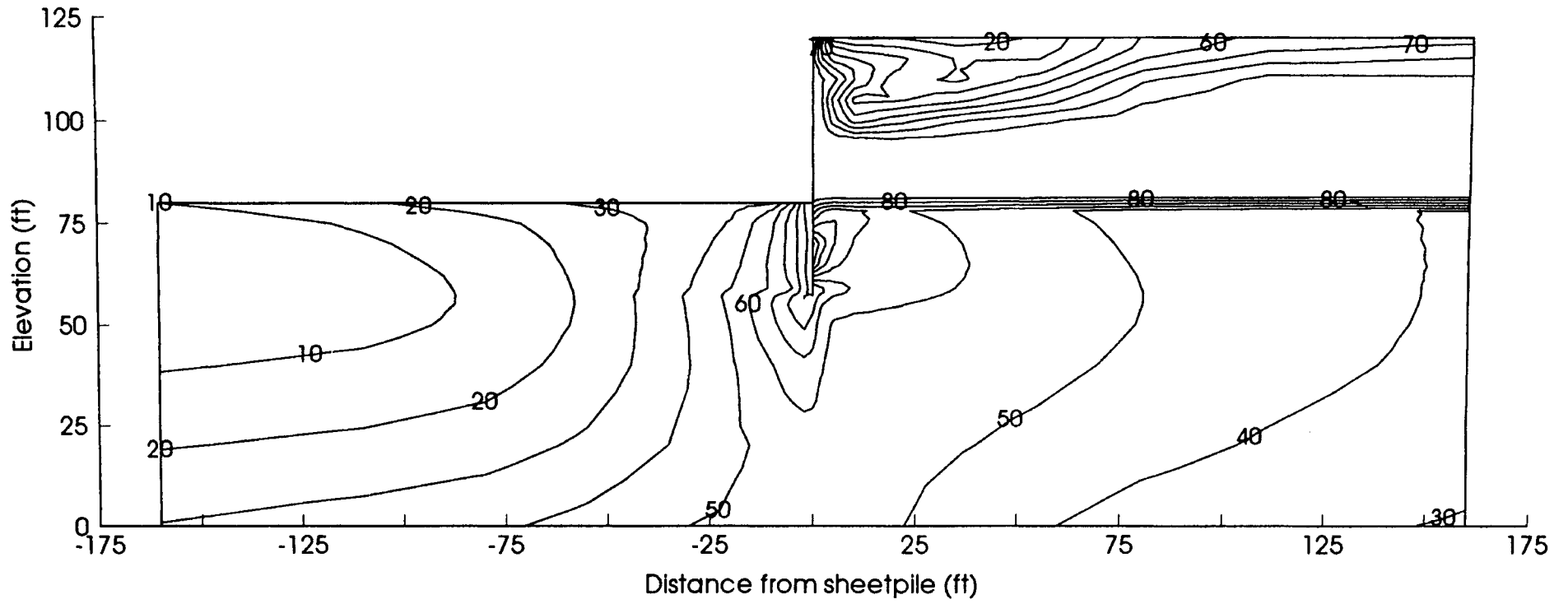


Figure B.16. DT40 Case - Backfill: Degree of Mobilization - f (%)

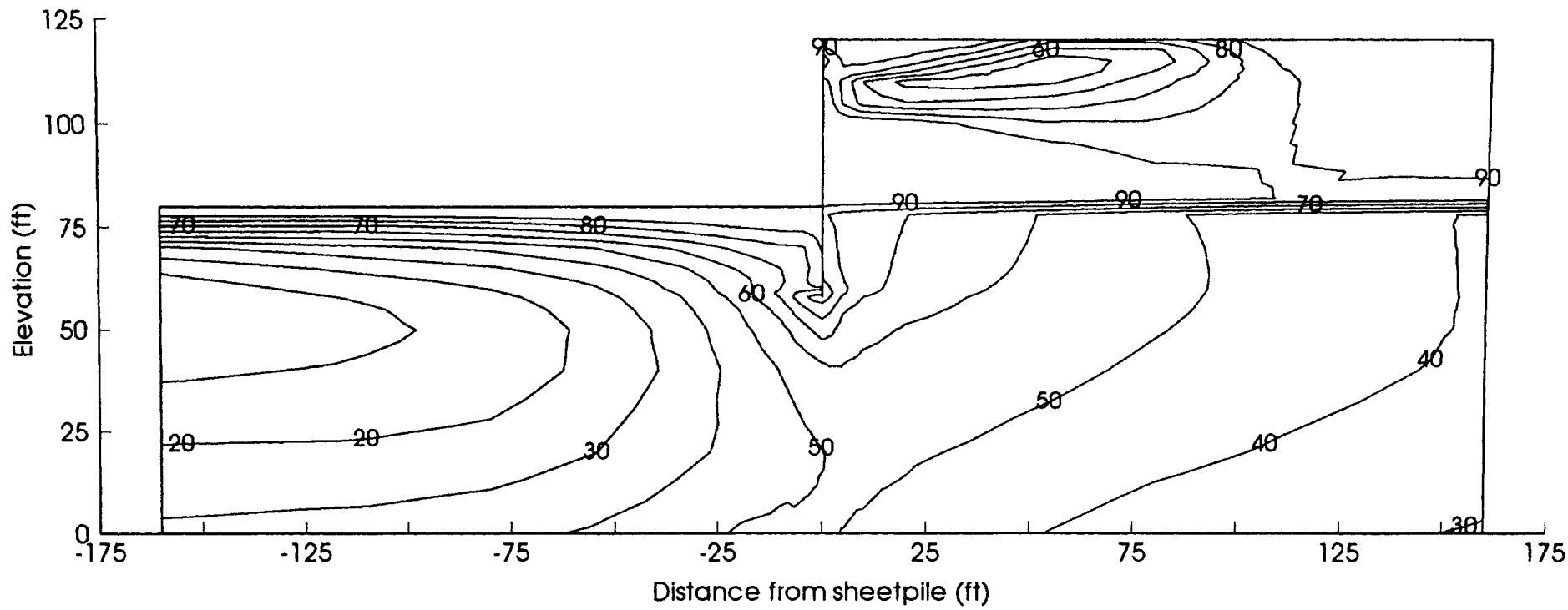


Figure B.17. LT40 Case - Excavation: Degree of Mobilization - f (%)

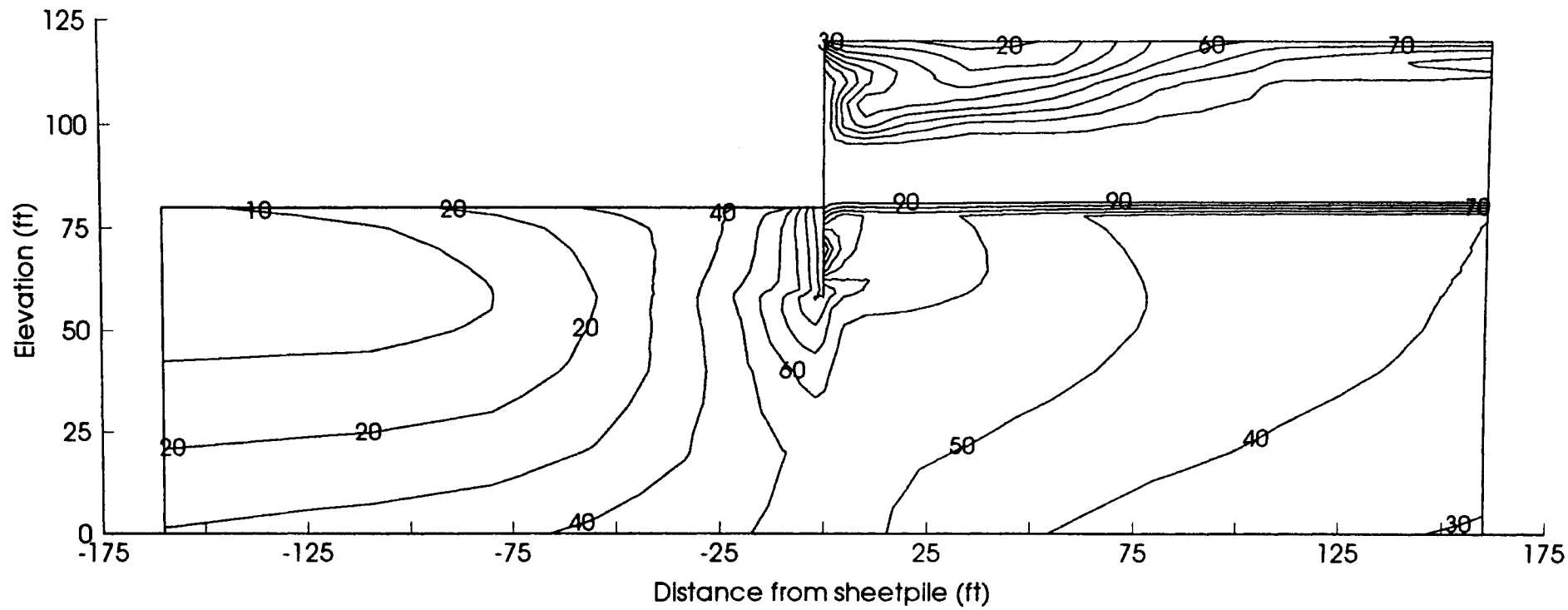


Figure B.18. LT40 Case - Backfill: Degree of Mobilization - f (%)

²
VITA

Omer Bilgin

Candidate for the Degree of

Master of Science

Thesis: THE BEHAVIOR OF ANCHORED SHEET PILE WALLS
CONSTRUCTED BY EXCAVATION AND BACKFILLING

Major Field: Civil Engineering

Biographical:

Personal Data: Born in Sarikamis, Turkey, May 11, 1969, the son of Sefer and Muserref Bilgin.

Education: Graduated from Ankara Ataturk High School, Ankara, Turkey in June 1986; received Bachelor of Science degree in Civil Engineering from Middle East Technical University, Ankara, Turkey in July 1991. Completed the requirements for the Master of Science degree with a major in Civil Engineering at Oklahoma State University in December 1994.

Professional Experience: Civil Engineer, BOTAS Petroleum Pipeline Corporation, Ankara, Turkey, November 1991, to August 1993; Research Assistant, Department of Civil Engineering, Oklahoma State University, August 1993, to present.

Professional Membership: American Society of Civil Engineers (ASCE), Earthquake Engineering Research Institute (EERI), Board of Civil Engineers, Ankara, Turkey.

Professional Registration: Registered Professional Engineer in Turkey.